

# microwaves&rf

JANUARY 2015

TRUSTED ENGINEERING RESOURCE FOR OVER 50 YEARS

[www.mwrf.com](http://www.mwrf.com)

## TECHNOLOGY FORECAST 2015

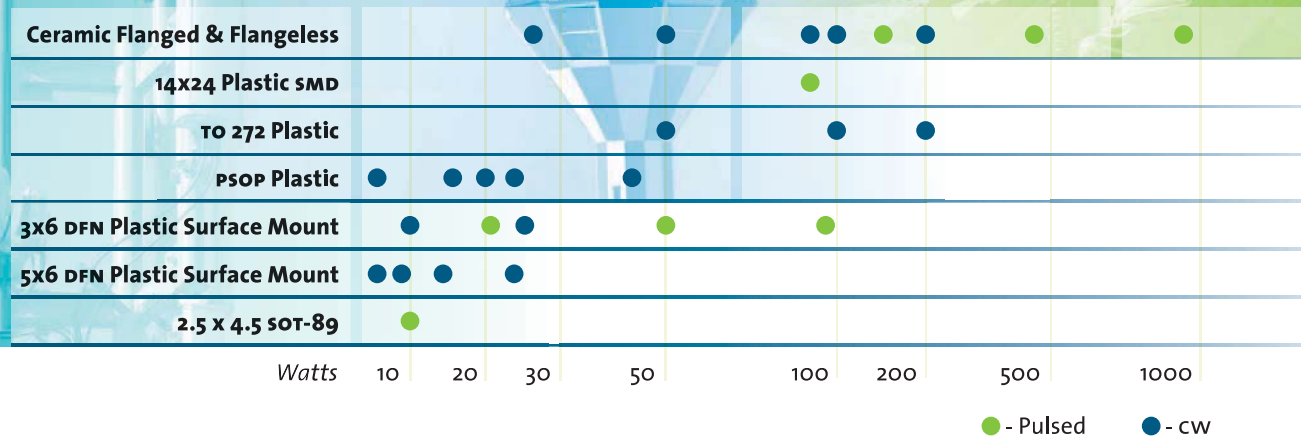


Confidence  
on the Cutting Edge

In the Lab | On the Manufacturing Floor | In the Field

Anritsu

Vector Network Analysis



## Shattering the Barriers to Mainstream GaN Adoption

### MACOM revolutionizes RF applications by securing the supply of the industry's only proven, performance-driven GaN portfolio

MACOM GaN transistors improve upon the high-power handling and voltage operation of LDMOS with the high-frequency performance of GaAs. Improved bandwidth, efficiency and power density give your applications greater power in a variety of packages.

Leveraging deep experience in RF, MACOM engineers are expanding our power transistor family to fuel the future of military and commercial radar as well as other commercial applications. These rugged devices deliver greater flexibility and multi-function capability in your radar communications.

Our growing pulsed power GaN portfolio includes 5W-90W Pk transistors in DFN and SOT-89 plastic packaging, up to 1000W ceramic packages and L-, S-band fully matched modules. Our new CW GaN portfolio includes ceramic package transistors up to 200W, DFN packages from 5W to 25W and TO-272 plastic packages from 50W to 200W.

Only MACOM shatters the final barriers to mainstream GaN adoption by offering dual sourcing for surety of supply.

**MACOM**<sup>™</sup>  
Partners from RF to Light

Get Samples & Learn How MACOM is Shattering the Barriers to Mainstream GaN Adoption at [www.macom.com/gan](http://www.macom.com/gan)





# Planar Monolithics Industries, Inc.

Offering State-Of-The-Art RF and Microwave Components  
& Integrated Assemblies From DC to 40GHz

## ANOTHER PMI BREAKTHROUGH IN HYBRID MIC/MMIC UP & DOWN CONVERTERS

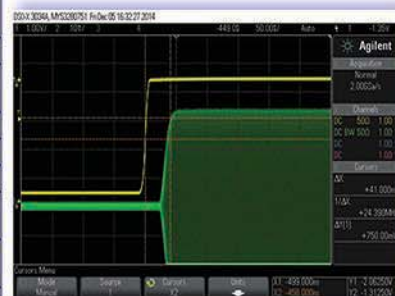
### PMI Model No. PUC-4G18G-CD-1

#### KEY FEATURES:

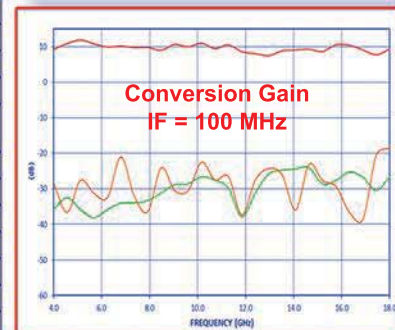
- 4.0 to 18.0 GHz RF Range
- Selectable Side Bands
- 10 to 100 MHz IF Range
- 10dB Conversion Gain
- 25dBc Typical Suppression



Frequency Range	4.0 to 18.0GHz
Conversion Gain	10dB, $\pm 3$ dB max (RF + 0dBm, IF Modulation = +14dBm)
Max Input Power	20dBm max
VSWR	2.0:1 max (RF + 0dBm, IF Modulation = +14dBm)
Carrier Suppression	20dBc min, 25dBc typ
Side Band Suppression	15dBc min, 20dBc typ
IF Frequency Range	10MHz to 100MHz
Power Supply	+15V @ 400mA max -15V @ 100mA max
RF Output 1dB Compression	12dBm typ (RF = 2dBm, IF Modulation = +14dBm)
RF Input 1dB Compression	5dBm typ (IF Modulation = +14dBm, >5dB Attenuation)
Sideband Switching Speed	150ns max
RF Connectors	SMA(F) Inputs and Outputs
Data Control Input	True Binary
Logic Levels	TTL & LVTTTL Compatible
Latch	Logic "1" = Data Transparent Logic "0" = Data Locked
Size	6.5" x 2.5" x 0.5"
Finish	Painted Blue
<b>Attenuator</b>	
Attenuation Range	0 to 31.96dB
Number of Attenuation Bits	10-Bits (1024 Steps)
Max Attenuation Step Size	0.03dB
Switching Speed	500ns max

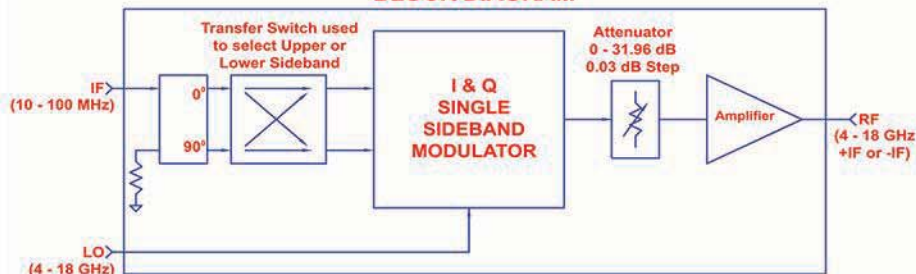


Sideband Switching Speed  
45ns Measured



Conversion Gain  
IF = 100 MHz

#### BLOCK DIAGRAM



#### West Coast Operation:

4921 Robert J. Mathews Pkwy, Suite 1  
El Dorado Hills, CA 95762 USA  
Tel: 916-542-1401 Fax: 916-265-2597

ISO9001:2008 REGISTERED

Email: [sales@pmi-rf.com](mailto:sales@pmi-rf.com)

#### East Coast Operation:

7311-F Grove Road  
Frederick, MD 21704 USA  
Tel: 301-662-5019 Fax: 301-662-1731

ISO9001:2008 REGISTERED

Website: [www.pmi-rf.com](http://www.pmi-rf.com)

Hermetic Sealing, High Reliability to Mil-Std-883, Small Quantity Requirements accepted & we offer Custom Designs too

Amplifiers

Attenuators - Variable

DLVA & ERLVA &  
SDLVA's

DTO's & Frequency  
Synthesizers

Filters

Form, Fit & Function  
Products

IFM's & Frequency  
Discriminators

Integrated MIC/MMIC  
Modules

I/Q Vector Modulators

Limiters & Detectors

Log Amplifiers

Pulse & Bi-Phase  
Modulators

Phase Shifters

Rack & Chassis Mount  
Products

Receiver Front Ends &  
Transceivers

Single Sideband  
Modulators

SMT & QFN Products

Solid-State Switches

Switch Matrices

Switch Filter Banks

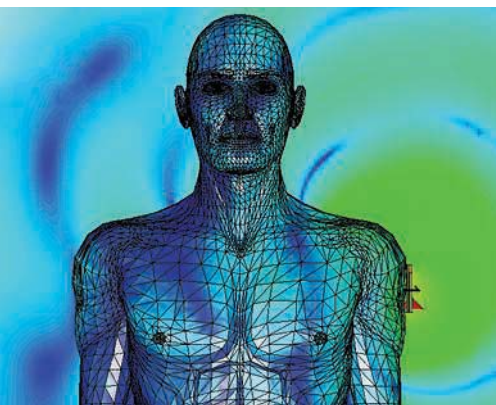
Threshold Detectors

USB Products



# Make the Connection

Find the simple way through complex  
EM systems with CST STUDIO SUITE



Components don't exist in electromagnetic isolation. They influence their neighbors' performance. They are affected by the enclosure or structure around them. They are susceptible to outside influences. With System Assembly and Modeling, CST STUDIO SUITE helps optimize component and system performance.

Involved in antenna development? You can read about how CST technology is used to simulate antenna performance at [www.cst.com/antenna](http://www.cst.com/antenna).

If you're more interested in filters, couplers, planar and multilayer structures, we've a wide variety of worked application examples live on our website at [www.cst.com/apps](http://www.cst.com/apps).

Get the big picture of what's really going on. Ensure your product and components perform in the toughest of environments.

**Choose CST STUDIO SUITE –  
Complete Technology for 3D EM.**





# NARDA

## Celebrating 60 Years!



**Narda started in 1954** as a small group of engineers on Long Island offering new and innovative technology to a growing RF and microwave industry. Sixty years later, Narda has become the global standard for quality and durability by continually producing the industry's most reliable RF and microwave components. ***We thank you for sixty years of loyalty to Narda Microwave, and look forward to serving you in the years to come.***

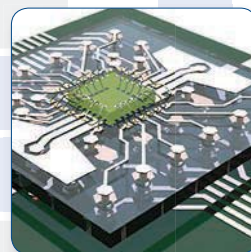
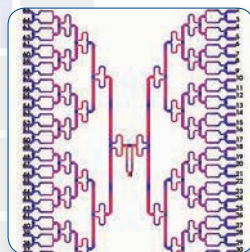
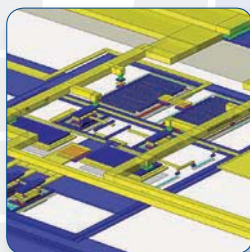
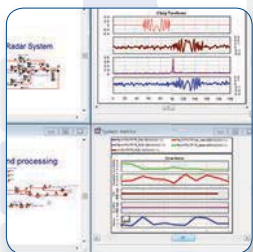
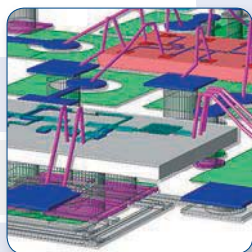
# narda

an **L3** company

**www.nardamicrowave.com • 631.231.1700**

**Six decades of technological innovation**

# Try NI AWR Design Environment Today!



Microwave Office | Visual System Simulator | Analog Office | AXIEM | Analyst

NI AWR Design Environment consists of a comprehensive software product portfolio that offers a variety of high-frequency design tools that embrace system simulation, circuit simulation, and electromagnetic analysis.

- Microwave Office for MMIC, module, and RF PCB design
- Visual System Simulator for RF/comms. systems design
- Analog Office for analog and RFIC design
- AXIEM for 3D planar electromagnetic analysis
- Analyst for 3D FEM EM simulation and analysis

## Try NI AWR Design Environment

today and see for yourself how easy and effective it is to streamline your design process, improve end product performance, and accelerate time to market for MMICs, RFICs, RF PCBs, microwave modules, 3D/planar passive interconnects, antennas, communication systems, and more.

**>> Learn more at [ni.com/awr](http://ni.com/awr)**



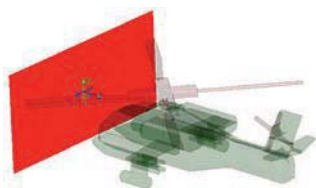
Visit [awrcorp.com/whatsnew](http://awrcorp.com/whatsnew) for a complete list of features found in the current version of NI AWR Design Environment.



# In This Issue

## FEATURES

- 87 SPECIAL FEATURE:**  
SPECTRUM ANALYZER IS TRULY PORTABLE PAST 6 GHz  
Fitting into a tiny housing, this very modern spectrum analyzer teams with a computer to accurately scrutinize spectrum past 6 GHz.
- 40 MAN AND MACHINE: BONDED TOGETHER WITH RF GLUE**  
By embracing cost-sensitive and integrated approaches, unmanned systems, COTS, DASs/small cells, and test are opening new technological frontiers.
- 56 LIMITERS PROTECT ADCs WITHOUT ADDING HARMONICS**  
This experiment seeks to find a diode limiter that can protect high-speed ADCs from high-level overload signals.
- 62 MODEL DEPICTS EM FROM ROUGH SURFACES**  
Predicting the scattering of EM radiation from rough surfaces can provide invaluable data for systems that must process such target information.
- 68 ANALYZE QUASI-TEM RECTANGULAR COAX COUPLERS**  
Digging into the even- and odd-mode electromagnetic parameters of quasi-TEM rectangular coaxial couplers can boost performance.
- 74 FILTERS BUILD UPON MCSRRs**  
Several different types of bandpass filters are constructed using MCSRRs, series capacitive gaps, and grounded stubs on low-cost circuit material.
- 80 ANTENNA TACKLES WI-FI AND WIMAX**  
This slotted microstrip antenna provides efficient service for both Wi-Fi and WiMAX wireless communications applications.



## INDUSTRY TRENDS & ANALYSIS

- 48 RF ESSENTIALS**  
EM simulation
- 52 INDUSTRY INSIGHT**  
Plastic packaging

## PRODUCT TECHNOLOGY

- 91 PRODUCT TRENDS**  
EMI/EMC testing
- 94 PRODUCT FEATURE**  
Portable oscilloscopes
- 96 PRODUCT FEATURE**  
Software-simplified testing

## NEWS & COLUMNS

- 11 EXCLUSIVELY ON MWRF.COM**
- 13 EDITORIAL**
- 18 FEEDBACK**
- 22 NEWS**
- 32 COMPANY NEWS**
- 34 INSIDE TRACK**  
with SiTime's Aaron Partridge 
- 36 R&D ROUNDUP**
- 38 MICROWAVES IN EUROPE**
- 84 APPLICATION NOTES**
- 100 ADVERTISERS INDEX**
- 102 NEW PRODUCTS**

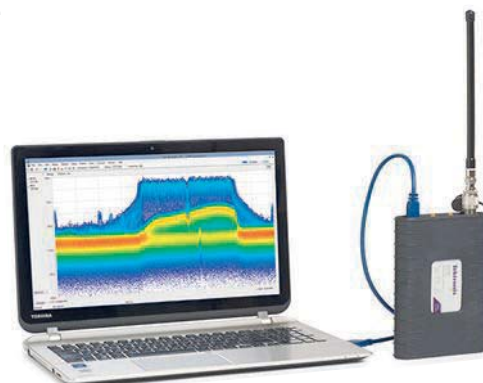
### JOIN US ONLINE



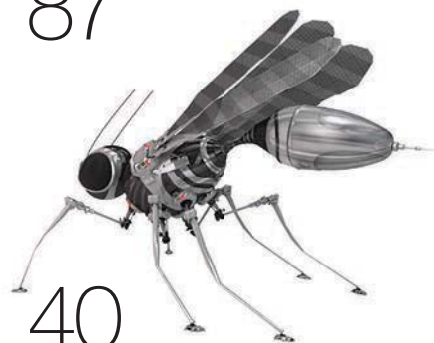
follow us @MicrowavesRF



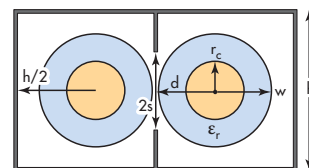
become a fan at  
facebook.com/microwavesRF



87



40

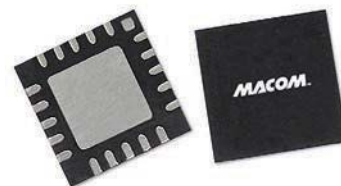


(a)

68



74



102



# Keeping Pace with Your Life

## Innovative Solutions for

Fitness Bands • Smart Watches • Smart Scales

► [www.skyworksinc.com](http://www.skyworksinc.com)





# Wearable Technology Solutions



Fitness Trackers



Smart Watches



Smart Scales

## High Performance Front-end Modules and Low Noise Amplifiers

### | Low Power Bluetooth® Low Energy (BLE) Front-end Modules: SKY66110-11, SKY66111-11

- For fitness trackers, sport and smart watches
- Operating range: 2.4 to 2.485 GHz
- Low power consumption: 10 mA in transmit mode
- Output power: 10 dBm
- Supply operation: 1.8 to 5 V
- Low sleep current: 1  $\mu$ A maximum
- Low Rx bypass insertion loss
- Package: MCM 20L 3.3 x 3.0 x 0.8 mm

### | 2 GHz 256 QAM Low-Noise Amplifier (LNA): SKY65971-11

- For 256 QAM 802.11g/n WLANs, access points, routers, gateways, wireless video systems, 2 GHz ISM radios, smartphones, notebooks, netbooks, tablets, and smart scales
- Ultra-low noise figure
- Operating range: 2.4 to 2.5 GHz
- Enable/disable/bypass modes
- High IIP3
- High gain
- Single-supply operation: 2.8 V to 3.6 V
- Package: QFN 6-pin 1.5 x 1.5 x 0.5 mm

### | 2.4 GHz ZigBee® / Connected Home Front-end Module: SKY66109-11

- For smart meters, in-home appliances, smart thermostats, and fitness trackers
- Integrated PA with up to 22.5 dBm output power
- Integrated LNA with programmable bypass
- Integrated antenna switching with transmit and receive diversity function
- Low noise figure: 2 dB typical
- Differential transmit/receive interface with integrated baluns
- Fast switch on/off time: <800 ns
- Supply range: 2 V to 3.6 V
- Sleep mode current: 0.05  $\mu$ A typical
- Package: MCM 20-pin 3 x 4 x 0.9 mm

Learn More



[www.skyworksinc.com](http://www.skyworksinc.com)



Scan to join our customer email program today!



INTRODUCING  
**TOKYO KEIKI**

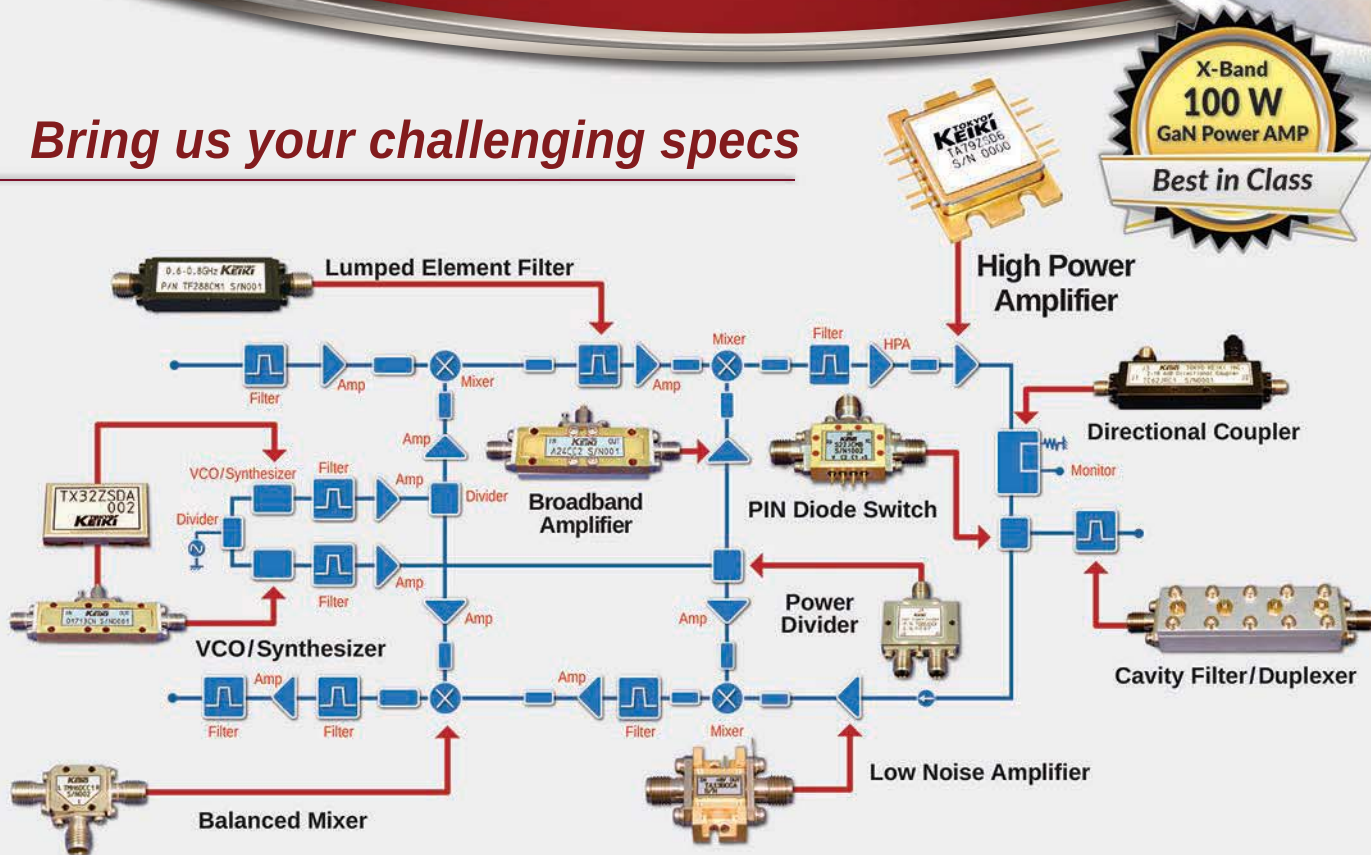


# CUSTOM RF PRODUCTS

Delivering High Quality & Performance

**5** CLEANROOMS  
JIS-Q9100 CERTIFIED FACTORY  
**AS9100** U.S. EQUIVALENT

*Bring us your challenging specs*



**TOKYO  
KEIKI**

Scan code to learn more or visit:  
[www.cel.com/TK-MWRF](http://www.cel.com/TK-MWRF)







#### V-Line Power Divider/Combiners

Increased power rating and extended frequency range! 2-way thru 16-way, 40 watt and available in N, SMA, BNC, TNC, QMA & RP-TNC connectors from 0.698 – 2.7 GHz and their rugged construction makes them ideal for both base station and in-building wireless systems.

**1 to 500 Watt Terminations**  
MECA offers a wide selection of terminations from stock ready for your just-in-time shipments. With power ratings from 1 to 500 watts and frequency ranges up to 40 GHz, our terminations are designed to exceed commercial specifications.



#### Attenuators

MECA offers a wide selection of attenuators designed to exceed commercial specifications. Standard attenuation values of 3, 6, 10, 20, 30 and 40 dB are available from STOCK! Need a special value? Many of our attenuators are available in all values from 0 - 20 dB in 1 dB increments.

#### Circulators & Isolators

MECA offers Circulators and Isolators in N, SMA, and 2.92mm Female connectors with average power ratings from 2 - 250 watts. The most "popular" frequency bands between 0.698 - 40.0 GHz are readily available and can ship from STOCK. IP 67 compliant isolators available.



## BETTER BUILDINGS / BETTER NETWORKS

### Dr. D.A.S. © Prescribes: MECA Low PIM Products & Equipments

Since 1961 MECA Electronics (Microwave Equipment & Components of America) has served the RF/Microwave industry with equipment and passive components covering Hz to 40 GHz. MECA is a privately held ISO9001:2008 Certified, global designer and manufacturer for the communications industry with all products manufactured in the **United States of America**.



*DR. D.A.S. prescribes...*

#### Directional & 3 dB Hybrid Couplers

MECA offers a wide selection of directional couplers designed to exceed commercial specifications. Standard coupling values of 6, 10, 20 and 30 dB in frequency bands from 0.400 to 18.0 GHz, in N, SMA, 2.92mm and 7/16 DIN.

3 dB, 90° hybrid couplers and 0°/180° hybrid divider/combiner with power ratings up to 500 watts available in N, SMA and 7/16 DIN in frequency bands from 0.400 to 18.0 GHz.



MECA Electronics designs and manufactures an extensive line of RF/Microwave Equipment and Components with industry leading performance including DAS Racks/Equipment, Low PIM Products, Power Dividers & Combiners, Directional & Hybrid Couplers, Fixed & Variable Attenuators, RF Terminations, Circulators/Isolators, DC Blocks & Bias Tees, Adapters & Jumpers. Models available in industry common connector styles: N, SMA, TNC, BNC, 7/16 & 4.1/9.5 DIN as well as QMA, Reverse Polarity SMA, TNC and various mounting solutions.

#### 4.1/9.5 (Mini-DIN) 1 & 10 Watt Terminations

MECA offers low power, 4.1/9.5 (Mini-DIN) Male & Female 50 ohm loads efficiently designed for high performance, cost effective solutions. Rated for 1 & 10 watts average power (2 kW peak). Available from stock to 3 wks. Made in USA - 36 month warranty.



#### Integrated D.A.S. Equipment

Let MECA create an integrated assembly with any of our RF/Microwave products on 19" panels, shelves or NEMA enclosures.



e-MECA.com

### MECA Electronics, Inc.

Microwave Equipment & Components of America

The Professional's Choice for RF/Microwave Passive Components

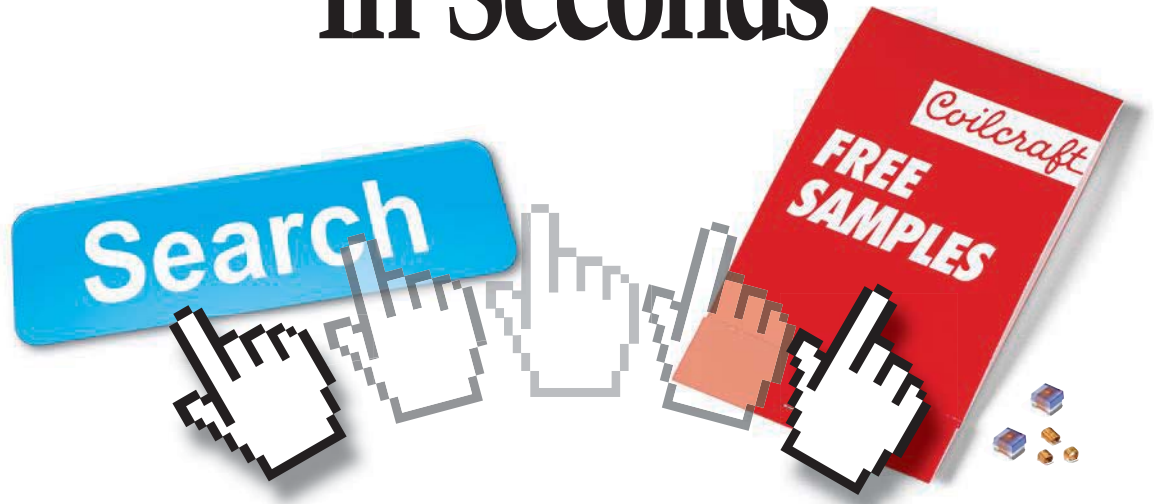
459 E. Main St., Denville, NJ 07834

Tel: 973-625-0661 Fax: 973-625-9277 Sales@e-MECA.com



**iBwave**  
Founding Member

# From Search to Samples in Seconds

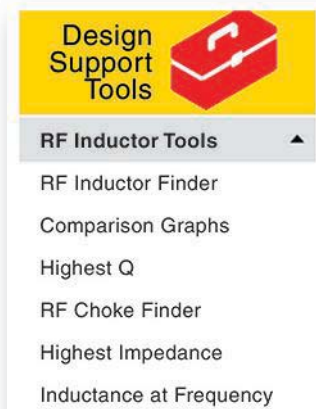


**Our web tools help you quickly pick the perfect inductor.  
Then get free samples overnight!**

We make picking inductors fast, easy, and almost fun!

Start with a quick parametric search for parts that meet your specs. (We even show you volume pricing.) Click to instantly compare Q, L, Z and ESR for multiple inductors.

Looking for inductors with the highest impedance



Visit us at the IMS Show Booth #708

or Q factors? There are tools for that! All based on real data, not theoretical models.

When you've picked your inductors, just click to get free samples. Do it by 5:00 p.m. CST and they'll ship to you the same day!

See how fast *you* can go from search to samples. Visit [coilcraft.com/tools](http://coilcraft.com/tools).



WWW.COILCRAFT.COM







## THE MISSING INGREDIENT THAT COULD SAVE ENGINEERING

<http://mwrf.com/blog/missing-ingredient-could-save-engineering>

It is impossible to deny that certain technology fields are missing a critical ingredient—an ingredient that has the potential to revitalize engineering fields in desperate need of qualified engineers and to introduce a valuable perspective that could speed up technological development. Surprisingly, this ingredient is abundantly available, though it has remained largely untapped by the engineering universe—the ingredient is women.



## IMPEDANCE TUNING 101

<http://mwrf.com/test-measurement/impedance-tuning-101>

Non-50ohm measurements have become a hot topic over the past few years, with techniques being used for amplifier design, model extraction, model validation, performance and ruggedness testing, and more. For a beginner, so much information might seem overwhelming. You've asked, we've answered...introducing a beginner's guide to all things "load pull."

join us online



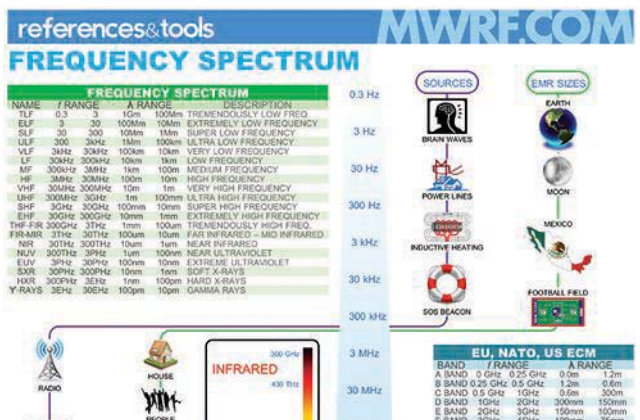
twitter.com/MicrowavesRF facebook.com/microwavesrf



## TOP PRODUCTS OF 2014

<http://mwrf.com/systems/top-products-2014>

2014 saw a number of solid RF/microwave engineering and technical advances, with the industry continuing to find practical ways of generating, sending, and receiving electromagnetic (EM) energy across wider bandwidths and at higher frequencies. As 2015 gets underway, take a look back at the previous 12 months' most notable offerings.



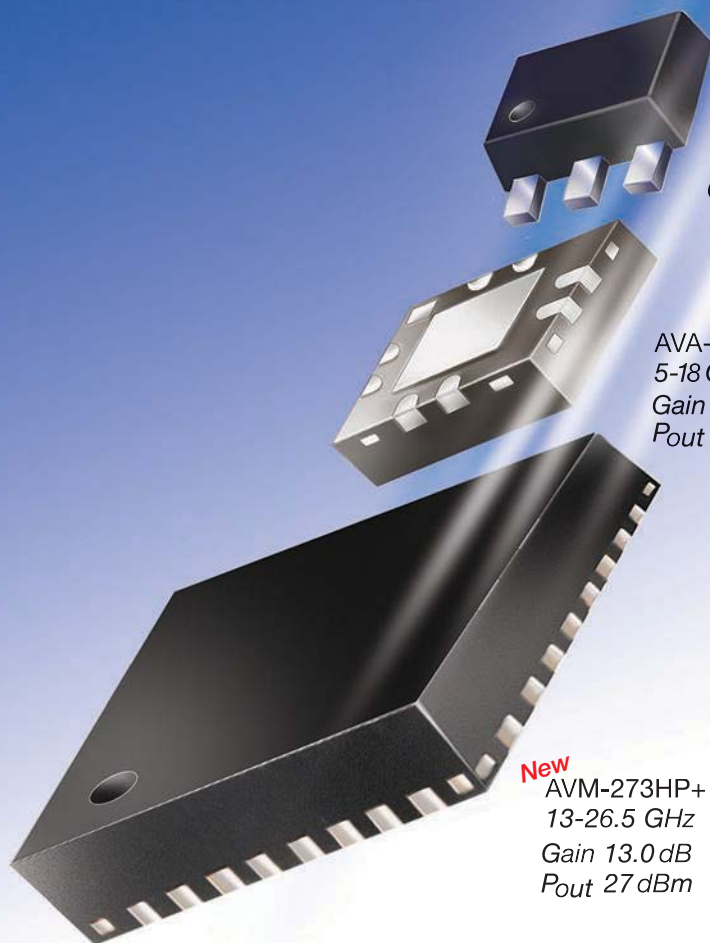
## REFERENCES & TOOLS

<http://mwrf.com/references-tools>

Visit our online References & Tools section to quickly and easily download tables covering topics such as Connector Frequency, which include Coaxial and Waveguide; Frequency Nomenclature: KiloHertz to TeraHertz; Frequency Spectrum & Allocations; and Wireless Coexistence: From 300 MHz to 6 GHz.

# 50 MHz to 26.5 GHz

## THREE AMPLIFIERS COVER IT ALL!



PHA-1+ \$**1**99  
0.05-6 GHz ea. (qty. 20)  
Gain 13.5 dB  
P<sub>out</sub> 22 dBm

AVA-183A+ \$**6**95  
5-18 GHz ea. (qty. 10)  
Gain 14.0 dB  
P<sub>out</sub> 19 dBm

**New**  
AVM-273HP+ \$**27**95  
13-26.5 GHz ea. (qty. 10)  
Gain 13.0 dB  
P<sub>out</sub> 27 dBm

Mini-Circuits' **New** AVM-273HP+ wideband, 13 dB gain, unconditionally stable microwave amplifier supports applications from 13 to 26.5 GHz with 0.5W power handling! Gain flatness of  $\pm 1.0$  dB and 58 dB isolation make this tiny unit an outstanding buffer amplifier in P2P radios, military EW and radar, DBS, VSAT, and more! Its integrated application circuit provides reverse voltage protection, voltage sequencing, and current stabilization, all in one tiny package!

The AVA-183A+ delivers 14 dB Gain with excellent gain flatness ( $\pm 1.0$  dB) from 5 to 18 GHz, 38 dB isolation, and 19 dBm power handling. It is unconditionally stable and an ideal LO driver amplifier. Internal DC blocks, bias tee, and

microwave coupling capacitor simplify external circuits, minimizing your design time.

The PHA-1+ uses E-PHEMT technology to offer ultra-high dynamic range, low noise, and excellent IP3 performance, making it ideal for LTE and TD-SCDMA. Good input and output return loss across almost 7 octaves extend its use to CATV, wireless LANs, and base station infrastructure.

**We've got you covered!** Visit [minicircuits.com](http://minicircuits.com) for full specs, performance curves, and free data! These models are in stock and ready to ship today!



FREE X-Parameters-Based  
Non-Linear Simulation Models for ADS



<http://www.modelithics.com/mvp/Mini-Circuits.asp>





## Editorial

NANCY K. FRIEDRICH

Content Director

nancy.friedrich@penton.com



# Before Embracing the Future, Secure Today

**E**very new year is brimming with possibilities—especially this one. We are on the brink of the “Internet of Things” or “Internet of Everything,” which will connect us to each other, our homes, our vehicles, and more. Much of this innovation aims to keep us from harm’s way—for example, advanced driver assistance systems (ADASs), which many believe will put an end to fatalities suffered in car accidents. Other applications, such as those serving the connected home, should help us manage our households more easily while conserving energy. In the midst of this excitement, however, many experts, skeptics, and doomsayers warn us that being more connected will expose us to severe risks.

On Jan. 7, an article in *The New York Times* (“CES: Security Risks From the Smart Home”) quoted Edith Ramirez, chairwoman of the Federal Trade Commission, as saying, “Any device that is connected to the Internet is at risk of being hijacked.” The quote was taken from her prepared remarks at the 2015 Consumer Electronics Show (CES), where she added: “Moreover, the risks that unauthorized access create intensify as we adopt more and more devices linked to our physical safety, such as our cars, medical care, and homes.”

In U.S. society, there already is a high level of concern over keeping one’s personal information safe—especially financial information. Yet the steps taken by concerned consumers to safeguard their information will likely be insignificant or outdated in the face of so much connectivity. And the concerns will extend beyond personal and financial information to the remote control of home and other systems. Imagine, for example, someone remotely unlocking a home or being able to see inside it.

These concerns bring me back to when consumers first started using IEEE 802.11b Wi-Fi networks in their homes. Those initial Wi-Fi access points had security features built-in, although they were very basic. Even more problematic, they had to be activated by the consumers themselves, who were largely unaware of this extra step. Judging from the new wave of connected devices that are already available in the market, it seems like they will follow the Wi-Fi path by building in only minimal security. We’ve come such a long way to this state of almost-connected everything, but we still haven’t learned to build in better security from the get-go. **mw**

## DETECTORS FOR VERY LOW SIGNALS

**Direct Measurement of Microwave  
Signals at -80 dBm or lower  
over 1 to 40 GHz**



MODEL	FREQ RANGE (GHz)	MIN VOLTAGE SENSITIVITY K (mV/μW)	TYP TSS (dBm)
DTA1-1860A DTA1-1870A DTA1-1880A	1-18	10 100 1000	-80 -70 -80
DTA182660A DTA182670A DTA182680A	18-26	10 100 1000	-80 -70 -80
DTA264060A DTA264070A DTA264080A	26-40	10 100 1000	-80 -70 -80
DTA184060A DTA184070A DTA184080A	18-40	10 100 1000	-80 -70 -80

- > Octave Band or Wide Band
- > Options for TSS to -60 dBm, -70 dBm, -80 dBm
- > Very High Sensitivity
- > Stable and Quiet Low 1/f Noise Operation
- > Extremely Fast Pulse Response (1 nsec rise time typical)
- > Matched Input for Low VSWR
- > Flat Frequency Response
- > Hermetically sealed package
- > Removable connectors

Narrow Band models are also available

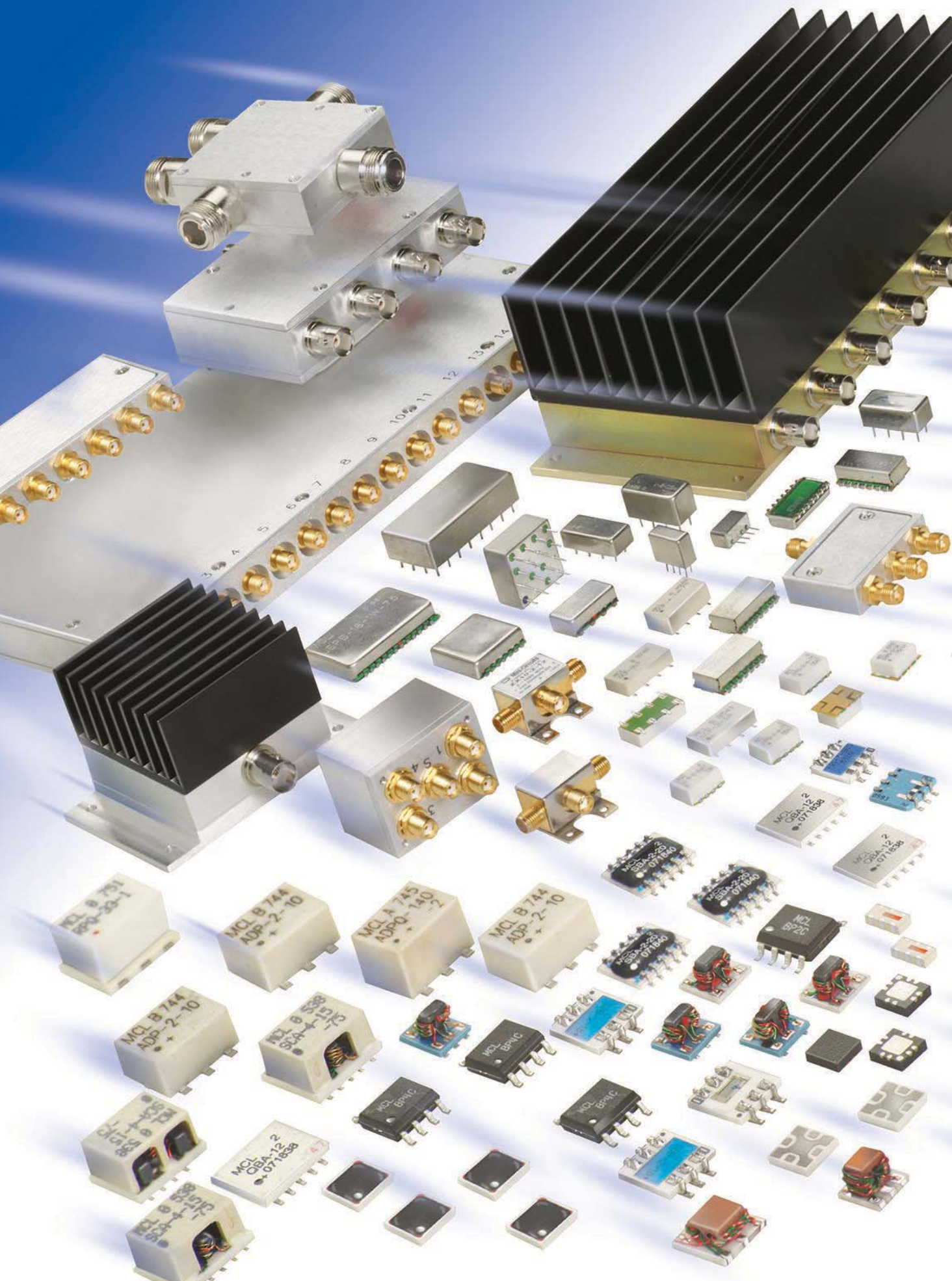
**Other Products: Amplifiers, Comb Generators, Limiters, Switches, Impulse Generators, Integrated Subsystems**

Please call for Detailed Brochures



155 Baytech Dr. San Jose, CA. 95134  
PH: 408-941-8399 . FAX: 408-941-8388  
E-Mail: [info@herotek.com](mailto:info@herotek.com)  
Web Site: <http://www.herotek.com>  
Visa/MasterCard Accepted









# POWER SPLITTERS/ COMBINERS

**NOW!** from **2 kHz to 18 GHz** as low as **79¢**

*The Industry's Largest Selection includes THOUSANDS of models, from 2 kHz to 18 GHz, at up to 300 watts power, in coaxial, flat-pack, surface-mount and rack-mount housings for 50 and 75  $\Omega$  systems.*

*From 2-way through 48-way designs, with 0°, 90°, or 180° phase configurations, Mini-Circuits power splitters/combiners offer outstanding performance for insertion loss, isolation, and VSWR. Decades of experience with multiple technologies make it all possible, from core & wire, microstrip, and stripline, to semiconductors and LTCC ceramics.*

*Get easy-to-find, detailed data and performance curves, S-parameters, outline drawings, PCB layouts, and everything else you need to make a decision quickly, at [minicircuits.com](http://minicircuits.com). Just enter your requirements, and our patented search engine, Yoni2, searches *actual test data* to find the models that meet your needs.*

*All Mini-Circuits catalog models are in stock, continuously replenished, and backed by our 1-year guarantee. We even list *current stock quantities and real-time availability*, as well as pricing, to help our customers plan ahead and make quick decisions.*

*So why wait? Take a look at [minicircuits.com](http://minicircuits.com) today!*

 **RoHS Compliant**  
Product availability is listed on our website.



# WE SUPPORT THE DESIGN PROCESS FROM INTENT TO ACTION

*Defense Electronics* serves electronic design engineers working in defense and aerospace markets with the latest technology-based news, design, and product information. It reviews the latest advances in electronics technologies related to military and aerospace electronic systems, from the device and component levels through the system level, also covering the latest developments in the software needed to simulate those defense/aerospace systems and the test equipment needed to analyze and maintain them. It is the industry's most trusted source of technical information for electronic engineers involved in military/aerospace circuit and system design.



## defense electronics

A Special Section to  
PENTON'S DESIGN ENGINEERING & SOURCING GROUP

**Penton**  
inform • engage • advance



WHERE ENGINEERING COMES FIRST

JANUARY | 2015

**microwaves&rf**

A Penton® Publication

### EDITORIAL

CONTENT DIRECTOR: **NANCY K. FRIEDRICH** nancy.friedrich@penton.com  
TECHNICAL CONTRIBUTOR: **JACK BROWNE** jack.browne@penton.com  
TECHNICAL ENGINEERING EDITOR: **JEAN-JACQUES DELISLE** jean-jacques.delisle@penton.com  
CONTENT PRODUCTION DIRECTOR: **MICHAEL BROWNE** michael.browne@penton.com  
PRODUCTION EDITOR: **JEREMY COHEN** jeremy.cohen@penton.com  
CONTENT PRODUCTION SPECIALIST: **ROGER ENGELKE** roger.engelke@penton.com  
ASSOCIATE CONTENT PRODUCER: **ILIZA SOKOL** iliza.sokol@penton.com  
EUROPEAN EDITOR: **PAUL WHYTOCK** p.whytoc@btinternet.com

### ART DEPARTMENT

GROUP DESIGN DIRECTOR: **ANTHONY VITOLO** tony.vitolo@penton.com  
SENIOR ARTIST: **JIM MILLER** jim.miller@penton.com  
CONTRIBUTING ART DIRECTOR: **RANDALL L. RUBENKING** randall.rubenking@penton.com

### PRODUCTION

GROUP PRODUCTION MANAGER: **CAREY SWEETEN** carey.sweeten@penton.com  
PRODUCTION MANAGER: **VICKI MCCARTY** vicki.mccarty@penton.com  
CLASSIFIED PRODUCTION COORDINATOR: **LINDA SARGENT** linda.sargent@penton.com

### AUDIENCE MARKETING

USER MARKETING DIRECTOR: **BRENDA ROODE** brenda.roode@penton.com  
USER MARKETING MANAGER: **DEBBIE BRADY** debbie.brady@penton.com  
FREE SUBSCRIPTION/STATUS OF SUBSCRIPTION/ADDRESS CHANGE/MISSING BACK ISSUES  
T | 866.505.7173 microwaves&rf@halldata.com F | 847.763.9673

### SALES & MARKETING

AL, AR, CT, DE, FL, GA, IA, IL, IN, KS, KY, LA, MA, MD, ME, MI, MN, MO, MS, NC, NE, NH, NJ, NY, OH, OK, RI, SC, TN, TX, PA, VA, VT, WV, E/CANADA:

MANAGING DIRECTOR: **TRACY SMITH** T | 913.967.1324 F | 913.514.6881 tracy.smith@penton.com

### REGIONAL SALES REPRESENTATIVES

AZ, NM, TX: **BILL YARBOROUGH** T | 713.636.3809 F | 913.514.7251 bill.yarborough@penton.com  
AK, CA, CO, ID, MT, ND, NV, OR, SD, UT, WA, WI, WY, W/CANADA: **JAMIE ALLEN** T | 415.608.1959  
F | 913.514.3667 jamie.allen@penton.com

PLEASE SEND INSERTION ORDERS TO: orders@penton.com

PENTON REPRINTS: **WRIGHT'S MEDIA** T | 877.652.5295 penton@wrightsmedia.com

CIRCULATION: **CUSTOMER SERVICE** T | 866.505.7173 F | 847.763.9673 microwaves&rf@halldata.com

### INTERNATIONAL SALES

EUROPE: **TRACY SMITH** T | 913.967.1324 F | 913.514.6881 tracy.smith@penton.com

PAN-ASIA: **HELEN LAI** T | 886 2-727 7799 helen@twoway.com

LIST RENTALS, CUSTOMER SERVICE-SUBSCRIPTIONS:

ONLINE MARKETING MANAGER: **SARAH NOWOWIEJSKI** T | (212) 204 4295

sarah.nowowiejski@penton.com

### ONLINE

PRODUCT DEVELOPMENT DIRECTOR: **RYAN MALEC** ryan.malec@penton.com

### DESIGN ENGINEERING & SOURCING GROUP

VICE PRESIDENT & MARKET LEADER: **BILL BAUMANN**

EXECUTIVE DIRECTOR OF CONTENT AND USER ENGAGEMENT: **NANCY K. FRIEDRICH**

GROUP DIRECTOR OF OPERATIONS: **CHRISTINA CAVANO**

GROUP DIRECTOR OF MARKETING: **JANE COOPER**

### PENTON MEDIA INC.

CHIEF EXECUTIVE OFFICER: **DAVID KIESELSTEIN** david.kieselstein@penton.com

CHIEF FINANCIAL OFFICER: **NICOLA ALLAIS** nicola.allais@penton.com

SENIOR VP, DESIGN ENGINEERING GROUP: **BOB MACARTHUR** bob.macarthur@penton.com

1166 AVENUE OF THE AMERICAS, 10TH FLOOR NEW YORK, NY 10036 T | 212.204.4200

**Penton**

Electronic Design | Machine Design | Microwaves & RF | Medical Design | Source ESB | Hydraulics & Pneumatics | Global Purchasing | Distribution Resource | Power Electronics | Defense Electronics | Electronic Design Europe | Engineering TV



# RF Amplifiers and Sub-Assemblies for Every Application

Delivery from Stock to 2 Weeks ARO from the catalog or built to your specifications!

- Competitive Pricing & Fast Delivery
- Military Reliability & Qualification
- Various Options: Temperature Compensation, Input Limiter Protection, Detectors/TTL & More
- Unconditionally Stable (100% tested)

ISO 9001:2000  
and AS9100B  
CERTIFIED



## OCTAVE BAND LOW NOISE AMPLIFIERS

Model No.	Freq (GHz)	Gain (dB) MIN	Noise Figure (dB)	Power-out @ P1-dB	3rd Order ICP	VSWR
CA01-2110	0.5-1.0	28	1.0 MAX, 0.7 TYP	+10 MIN	+20 dBm	2.0:1
CA12-2110	1.0-2.0	30	1.0 MAX, 0.7 TYP	+10 MIN	+20 dBm	2.0:1
CA24-2111	2.0-4.0	29	1.1 MAX, 0.95 TYP	+10 MIN	+20 dBm	2.0:1
CA48-2111	4.0-8.0	29	1.3 MAX, 1.0 TYP	+10 MIN	+20 dBm	2.0:1
CA812-3111	8.0-12.0	27	1.6 MAX, 1.4 TYP	+10 MIN	+20 dBm	2.0:1
CA1218-4111	12.0-18.0	25	1.9 MAX, 1.7 TYP	+10 MIN	+20 dBm	2.0:1
CA1826-2110	18.0-26.5	32	3.0 MAX, 2.5 TYP	+10 MIN	+20 dBm	2.0:1

## NARROW BAND LOW NOISE AND MEDIUM POWER AMPLIFIERS

CA01-2111	0.4-0.5	28	0.6 MAX, 0.4 TYP	+10 MIN	+20 dBm	2.0:1
CA01-2113	0.8-1.0	28	0.6 MAX, 0.4 TYP	+10 MIN	+20 dBm	2.0:1
CA12-3117	1.2-1.6	25	0.6 MAX, 0.4 TYP	+10 MIN	+20 dBm	2.0:1
CA23-3111	2.2-2.4	30	0.6 MAX, 0.45 TYP	+10 MIN	+20 dBm	2.0:1
CA23-3116	2.7-2.9	29	0.7 MAX, 0.5 TYP	+10 MIN	+20 dBm	2.0:1
CA34-2110	3.7-4.2	28	1.0 MAX, 0.5 TYP	+10 MIN	+20 dBm	2.0:1
CA56-3110	5.4-5.9	40	1.0 MAX, 0.5 TYP	+10 MIN	+20 dBm	2.0:1
CA78-4110	7.25-7.75	32	1.2 MAX, 1.0 TYP	+10 MIN	+20 dBm	2.0:1
CA910-3110	9.0-10.6	25	1.4 MAX, 1.2 TYP	+10 MIN	+20 dBm	2.0:1
CA1315-3110	13.75-15.4	25	1.6 MAX, 1.4 TYP	+10 MIN	+20 dBm	2.0:1
CA12-3114	1.35-1.85	30	4.0 MAX, 3.0 TYP	+33 MIN	+41 dBm	2.0:1
CA34-6116	3.1-3.5	40	4.5 MAX, 3.5 TYP	+35 MIN	+43 dBm	2.0:1
CA56-5114	5.9-6.4	30	5.0 MAX, 4.0 TYP	+30 MIN	+40 dBm	2.0:1
CA812-6115	8.0-12.0	30	4.5 MAX, 3.5 TYP	+30 MIN	+40 dBm	2.0:1
CA812-6116	8.0-12.0	30	5.0 MAX, 4.0 TYP	+33 MIN	+41 dBm	2.0:1
CA1213-7110	12.2-13.25	28	6.0 MAX, 5.5 TYP	+33 MIN	+42 dBm	2.0:1
CA1415-7110	14.0-15.0	30	5.0 MAX, 4.0 TYP	+30 MIN	+40 dBm	2.0:1
CA1722-4110	17.0-22.0	25	3.5 MAX, 2.8 TYP	+21 MIN	+31 dBm	2.0:1

## ULTRA-BROADBAND & MULTI-OCTAVE BAND AMPLIFIERS

Model No.	Freq (GHz)	Gain (dB) MIN	Noise Figure (dB)	Power-out @ P1-dB	3rd Order ICP	VSWR
CA0102-3111	0.1-2.0	28	1.6 MAX, 1.2 TYP	+10 MIN	+20 dBm	2.0:1
CA0106-3111	0.1-6.0	28	1.9 MAX, 1.5 TYP	+10 MIN	+20 dBm	2.0:1
CA0108-3110	0.1-8.0	26	2.2 MAX, 1.8 TYP	+10 MIN	+20 dBm	2.0:1
CA0108-4112	0.1-8.0	32	3.0 MAX, 1.8 TYP	+22 MIN	+32 dBm	2.0:1
CA02-3112	0.5-2.0	36	4.5 MAX, 2.5 TYP	+30 MIN	+40 dBm	2.0:1
CA26-3110	2.0-6.0	26	2.0 MAX, 1.5 TYP	+10 MIN	+20 dBm	2.0:1
CA26-4114	2.0-6.0	22	5.0 MAX, 3.5 TYP	+30 MIN	+40 dBm	2.0:1
CA618-4112	6.0-18.0	25	5.0 MAX, 3.5 TYP	+23 MIN	+33 dBm	2.0:1
CA618-6114	6.0-18.0	35	5.0 MAX, 3.5 TYP	+30 MIN	+40 dBm	2.0:1
CA218-4116	2.0-18.0	30	3.5 MAX, 2.8 TYP	+10 MIN	+20 dBm	2.0:1
CA218-4110	2.0-18.0	30	5.0 MAX, 3.5 TYP	+20 MIN	+30 dBm	2.0:1
CA218-4112	2.0-18.0	29	5.0 MAX, 3.5 TYP	+24 MIN	+34 dBm	2.0:1

## LIMITING AMPLIFIERS

Model No.	Freq (GHz)	Input Dynamic Range	Output Power Range Psat	Power Flatness dB	VSWR
CLA24-4001	2.0-4.0	-28 to +10 dBm	+7 to +11 dBm	+/- 1.5 MAX	2.0:1
CLA26-8001	2.0-6.0	-50 to +20 dBm	+14 to +18 dBm	+/- 1.5 MAX	2.0:1
CLA712-5001	7.0-12.4	-21 to +10 dBm	+14 to +19 dBm	+/- 1.5 MAX	2.0:1
CLA618-1201	6.0-18.0	-50 to +20 dBm	+14 to +19 dBm	+/- 1.5 MAX	2.0:1

## AMPLIFIERS WITH INTEGRATED GAIN ATTENUATION

Model No.	Freq (GHz)	Gain (dB) MIN	Noise Figure (dB)	Power-out @ P1-dB	Gain Attenuation Range	VSWR
CA001-2511A	0.025-0.150	21	5.0 MAX, 3.5 TYP	+12 MIN	30 dB MIN	2.0:1
CA05-3110A	0.5-5.5	23	2.5 MAX, 1.5 TYP	+18 MIN	20 dB MIN	2.0:1
CA56-3110A	5.85-6.425	28	2.5 MAX, 1.5 TYP	+16 MIN	22 dB MIN	1.8:1
CA612-4110A	6.0-12.0	24	2.5 MAX, 1.5 TYP	+12 MIN	15 dB MIN	1.9:1
CA1315-4110A	13.75-15.4	25	2.2 MAX, 1.6 TYP	+16 MIN	20 dB MIN	1.8:1
CA1518-4110A	15.0-18.0	30	3.0 MAX, 2.0 TYP	+18 MIN	20 dB MIN	1.85:1

## LOW FREQUENCY AMPLIFIERS

Model No.	Freq (GHz)	Gain (dB) MIN	Noise Figure (dB)	Power-out @ P1-dB	3rd Order ICP	VSWR
CA001-2110	0.01-0.10	18	4.0 MAX, 2.2 TYP	+10 MIN	+20 dBm	2.0:1
CA001-2211	0.04-0.15	24	3.5 MAX, 2.2 TYP	+13 MIN	+23 dBm	2.0:1
CA001-2215	0.04-0.15	23	4.0 MAX, 2.2 TYP	+23 MIN	+33 dBm	2.0:1
CA001-3113	0.01-1.0	28	4.0 MAX, 2.8 TYP	+17 MIN	+27 dBm	2.0:1
CA002-3114	0.01-2.0	27	4.0 MAX, 2.8 TYP	+20 MIN	+30 dBm	2.0:1
CA003-3116	0.01-3.0	18	4.0 MAX, 2.8 TYP	+25 MIN	+35 dBm	2.0:1
CA004-3112	0.01-4.0	32	4.0 MAX, 2.8 TYP	+15 MIN	+25 dBm	2.0:1

CIAO Wireless can easily modify any of its standard models to meet your "exact" requirements at the Catalog Pricing.

Visit our web site at [www.ciaowireless.com](http://www.ciaowireless.com) for our complete product offering.

Ciao Wireless, Inc. 4000 Via Pescador, Camarillo, CA 93012

Tel (805) 389-3224 Fax (805) 389-3629 [sales@ciaowireless.com](mailto:sales@ciaowireless.com)





## TESTING THE GROWTH OF DIGITAL TECHNOLOGY

As an older RF/microwave design engineer well versed in analog technologies, I have been intrigued by the growing number of articles on digital technologies appearing within your magazine.

Your December 2014 issue serves as a prime example. The announcement of an arbitrary waveform generator (AWG) on the front cover certainly reveals the interest of your editors in the growing use of digital technologies for RF and microwave applications. In this case, this

product feature on the model M8195A AWG explores impressive performance levels for this digital electronic product from Keysight Technologies.

This is a test instrument that, quite simply, would not have been possible several years ago. It achieves a frequency bandwidth as wide as 20 GHz using 8-b, 65 GSamples/s digital-to-analog converters (DACs). As digital technology has established itself and expanded into a plethora of markets, few would now question the capabilities of such high-performance digital components in microwave signal generators, a technical area once dominated by analog components and signal synthesis techniques.

This AWG actually integrates four of these high-speed DACs per modular instrument to provide the capability of generating four high-speed signal channels. The amplitude and phase of each channel can be precisely controlled to achieve the type of multiple-channel signals needed for sensitive defense-related applications.

As this story clearly emphasizes, the world is going digital. For many applications, this may be a good thing. But it should not be a signal that it is time to abandon analog electronic technologies, notably in the area of high-frequency signal generation. Progress continues in the design of low-noise clock oscillators and in the refinement of low-noise, stable, RF/microwave analog signal sources with outstanding performance.

In applications including airborne and in-field use, such analog high-frequency sources have long proven their value, and should not be abandoned or dismissed because of the advances of digital RF/microwave signal sources. Both analog and digital RF/microwave signal-generation technologies have their merits and weaknesses and I feel it is a responsibility of your publication to serve your readers by continuing to cover both analog and digital RF/microwave technologies.

DR. MITCHELL FENSTER

## Microwave Multi-Octave Directional Couplers Up to 60 GHz



Frequency Range	I.L. (dB) min.	Coupling Flatness max.	Directivity (dB) min.	VSWR max.	Model Number
0.5-2.0 GHz	0.35	± 0.75 dB	23	1.20:1	CS*-02
1.0-4.0 GHz	0.35	± 0.50 dB	23	1.20:1	CS*-04
0.5-6.0 GHz	1.00	± 0.80 dB	15	1.50:1	CS10-24
2.0-8.0 GHz	0.35	± 0.40 dB	20	1.25:1	CS*-09
0.5-12.0 GHz	1.00	± 0.80 dB	15	1.50:1	CS*-19
1.0-18.0 GHz	0.90	± 0.50 dB	15 12	1.50:1	CS*-18
2.0-18.0 GHz	0.80	± 0.50 dB	15 12	1.50:1	CS*-15
4.0-18.0 GHz	0.60	± 0.50 dB	15 12	1.40:1	CS*-16
8.0-20.0 GHz	1.00	± 0.80 dB	15 12	1.50:1	CS*-21
6.0-26.5 GHz	0.70	± 0.80 dB	13	1.55:1	CS20-50
1.0-40.0 GHz	1.60	± 1.50 dB	10	1.80:1	CS20-53
2.0-40.0 GHz	1.60	± 1.00 dB	10	1.80:1	CS20-52
6.0-40.0 GHz	1.20	± 1.00 dB	10	1.70:1	CS10-51
6.0-50.0 GHz	1.60	± 1.00 dB	10	2.00:1	CS20-54
6.0-60.0 GHz	1.80	± 1.00 dB	07	2.00:1	CS20-55

10 to 500 watts power handling depending on coupling and model number..

SMA and Type N connectors available to 18 GHz.

\* Coupling Value: 3, 6, 8, 10, 13, 16, 20 dB.

**PULSAR**

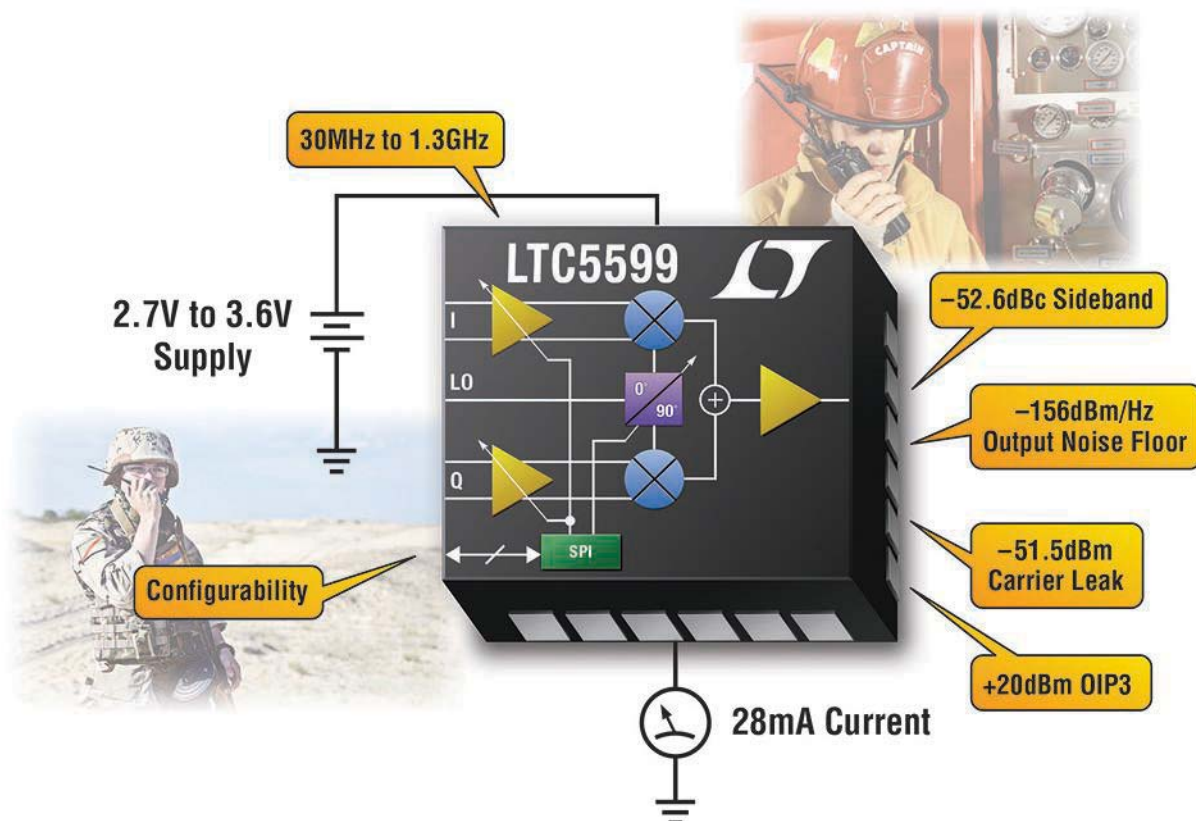
MICROWAVE CORPORATION

▶ [www.pulsarmicrowave.com](http://www.pulsarmicrowave.com)

48 Industrial West, Clifton, NJ 07012 | Tel: 973-779-6262 · Fax: 973-779-2727 | sales@pulsarmicrowave.com



# 90mW I/Q Modulator



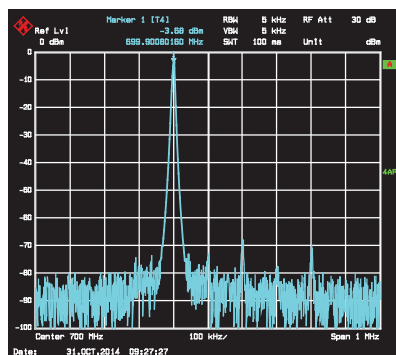
Powered from a single supply from 2.7V to 3.6V, the LTC<sup>®</sup>5599's 28mA supply current extends battery run time. The modulator offers superb -52.6dBc sideband and -51.5dBm carrier suppression—without the need of calibration. Its low noise floor of -156dBm/Hz and 20dBm OIP3 capability ensure outstanding transmitter performance. The LTC5599's built-in configurability allows users to optimize performance from 30MHz to 1.3GHz, minimizing external components and saving costs.

## ▼ Features

Built-in Configurability Features:

- Gain Adjustable from 0dB to -19dB, with Supply Current Change from 35mA to 8mA
- Improves Sideband Suppression from -52.6dBc to -60dBc
- Reduces Carrier Leakage from -51.5dBm to -60dBm

## Output Spectra (Optimized)



## ▼ Info & Free Samples

[www.linear.com/product/LTC5599](http://www.linear.com/product/LTC5599)

1-800-4-LINEAR



[www.linear.com/solutions/5429](http://www.linear.com/solutions/5429)

LT, LT, LTC, LTM, Linear Technology and the Linear logo are registered trademarks of Linear Technology Corporation. All other trademarks are the property of their respective owners.

# Eureka!

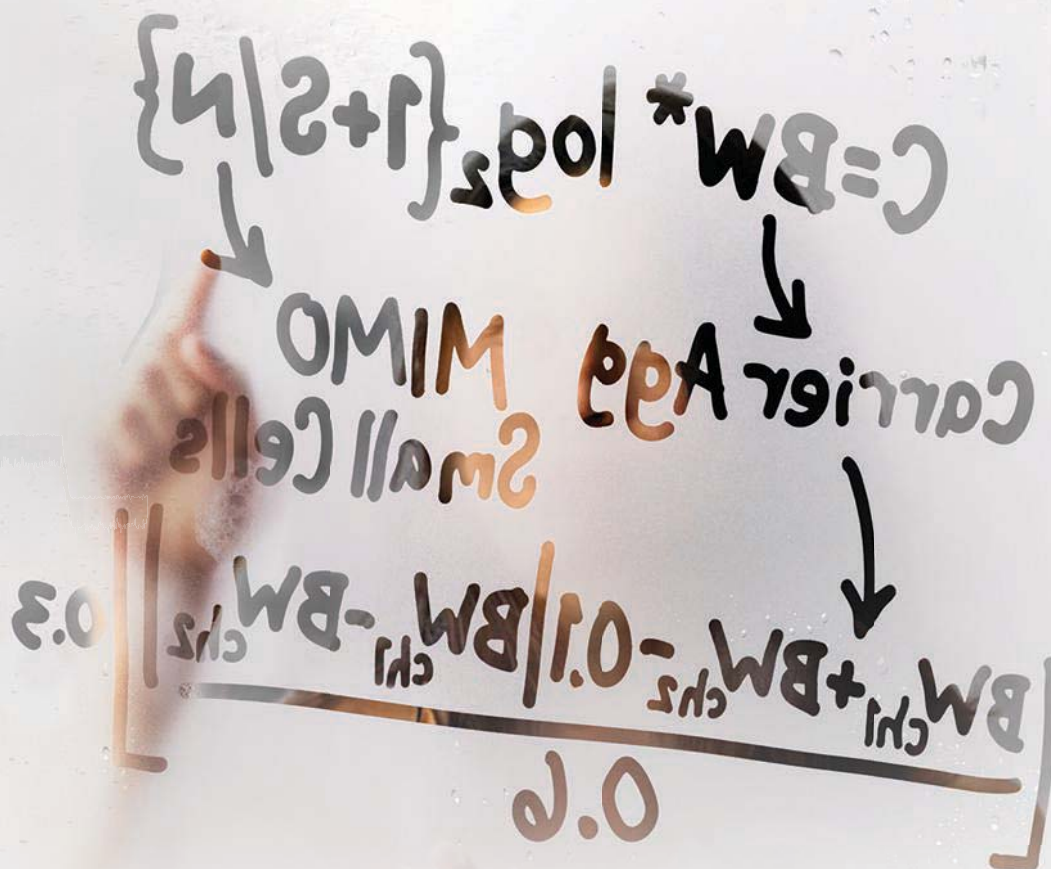
## We'll help you get there.

Insight. It comes upon you in a flash. And you know at once you have something special. At Keysight Technologies, we think precise measurements can act as a catalyst to breakthrough insight. That's why we offer the most advanced electronic measurement tools for LTE-A technology. We also offer sophisticated, future-friendly software. In addition, we can give you expert testing advice to help you design custom solutions for your particular needs.



Keysight 89600 VSA software

**HARDWARE + SOFTWARE + PEOPLE = LTE-A INSIGHTS**



Download new **LTE-A Technology and Test Challenge – 3GPP Releases 10,11,12 and Beyond**  
[www.keysight.com/find/LTE-A-Insight](http://www.keysight.com/find/LTE-A-Insight)



USA: 800 829 4444 CAN: 877 894 4414

© Keysight Technologies, Inc. 2014



Keysight W1715EP SystemVue  
MIMO channel builder



Keysight Infiniium S-Series  
high-definition oscilloscope  
with N8807A MIPI DigRF v4 (M-PHY)  
protocol decode software

Keysight N9040B UXA signal analyzer  
with 89600 VSA software



Keysight MIMO PXI test solution  
with N7624/25B Signal Studio software  
for LTE-Advanced/LTE FDD/TDD and  
89600 VSA software



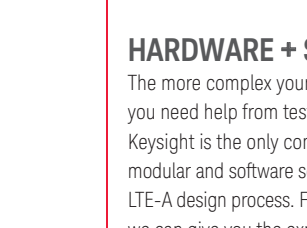
Keysight E7515A UXM wireless test set  
with E7530A/E7630A LTE-Advanced/LTE test/  
lab application software



Keysight N5182B MXG X-Series  
RF vector signal generator  
with N7624/25B Signal Studio software for  
LTE-Advanced/LTE FDD/TDD



Keysight E6640B EXM wireless test set  
with V9080/82B LTE FDD/TDD measurement  
applications and N7624/25B Signal Studio  
software for LTE-Advanced/LTE FDD/TDD



## HARDWARE + SOFTWARE

The more complex your LTE-A design, the more you need help from test and measurement experts. Keysight is the only company that offers benchtop, modular and software solutions for every step of the LTE-A design process. From R&D to manufacturing, we can give you the expertise, instruments and applications you need to succeed.

- Complete LTE-Advanced design and test lifecycle
- Identical software algorithms across platforms
- 300+ software applications for the entire wireless lifecycle

## PEOPLE

We know what it takes for your designs to meet LTE-A standards. After all, Keysight engineers have played major roles in LTE-A and other wireless standards bodies, including 3GPP. Our engineers even co-authored the first book about LTE-A design and test. We also have hundreds of applications engineers. You'll find them all over the world, and their expertise is yours for the asking.

- Representation on every key wireless standards organization globally
- Hundreds of applications engineers in 100 countries around the world
- Thousands of patents issued in Keysight's history



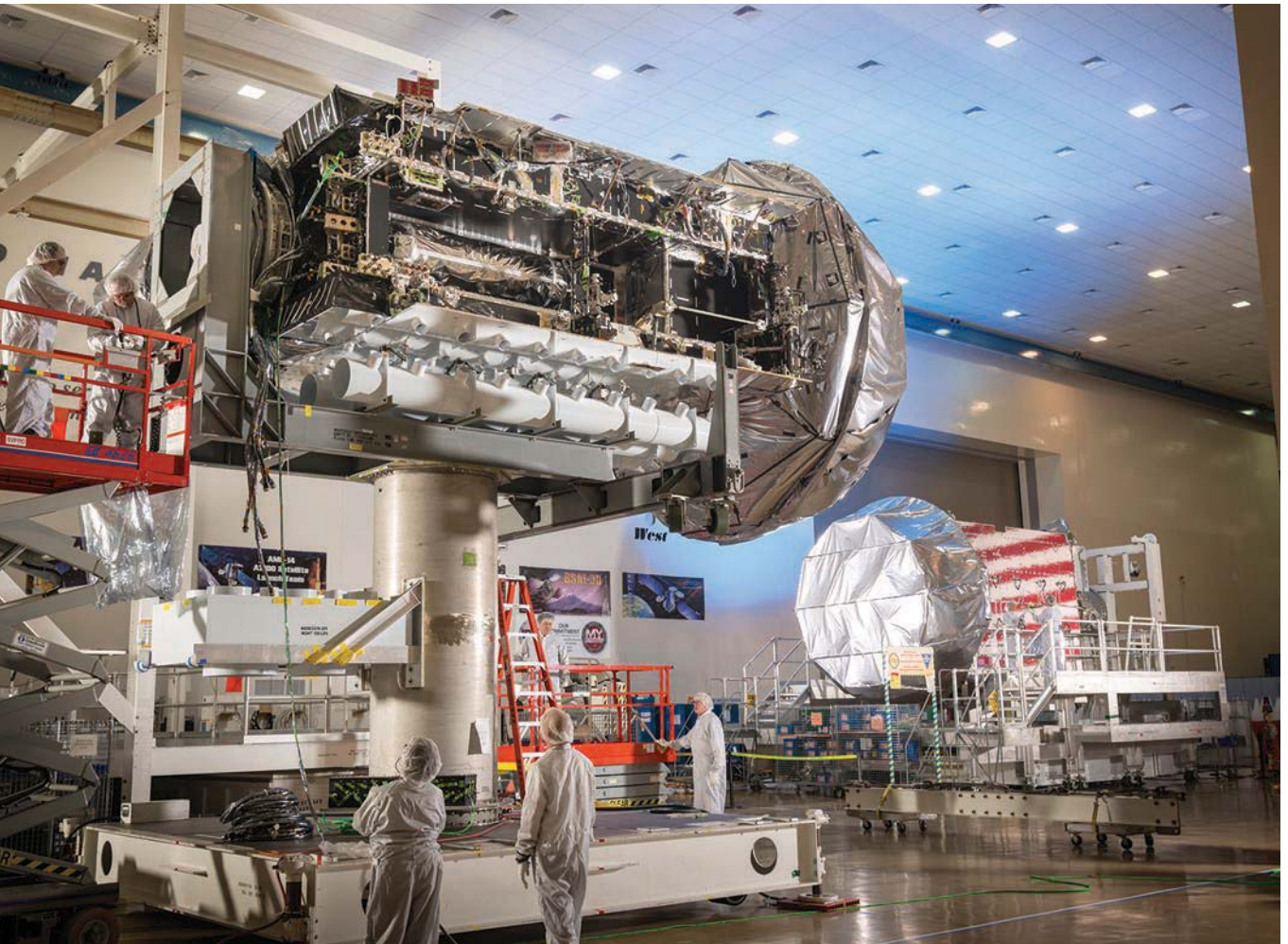
Unlocking Measurement Insights

# News

## THIRD OF FOUR MUOS SATELLITES **Readied for Launch**

**S**atellites continue to be delivered to strengthen the U.S. Navy and Lockheed Martin's Mobile User Objective System (MUOS) fleet. MUOS satellites, which operate in a similar fashion as smartphones, help improve secure mobile

satellite communications for warfighters. The third MUOS spacecraft was recently delivered to Cape Canaveral Air Force Station in Florida, where it was slated to be launched this month aboard a United Launch Alliance Atlas V rocket.



The third Mobile User Objective System (MUOS) satellite, part of a system that leverages smartphone technology for secure satellite communications, has been delivered. (Image courtesy of Lockheed Martin)



The key to MUOS's connectivity is the use of the latest wide-band code-division multiple-access (WCDMA) technology. WCDMA gives users beyond-line-of-sight capabilities to transmit and receive voice and data using an Internet Protocol-based system leveraged from commercial 3G technology. The WCDMA architecture can provide up to 16 times greater capacity than current ultra-high-frequency (UHF) satellites, and offers adaptive power control to provide the necessary quality of service while maximizing system capacity.

The MUOS system will consist of four satellites in geosynchronous earth orbit (GEO), with an on-orbit spare and a fiber-optic terrestrial network to connect four ground stations. It is expected to be fully operational in 2017. MUOS has previously been used to demonstrate the transfer of megabyte data files (see "MUOS Satellites Transfer Huge Data Files in the Arctic" at [www.mwrf.com](http://www.mwrf.com)) and as part of the radio testing laboratories that make up the soldier's network (see "Second MUOS-Satellite Radio Test Lab Begins Operations" at [www.mwrf.com](http://www.mwrf.com)). ■

## EUROPEAN SPACEDATAHIGHWAY Achieves Near-Real-Time Communications

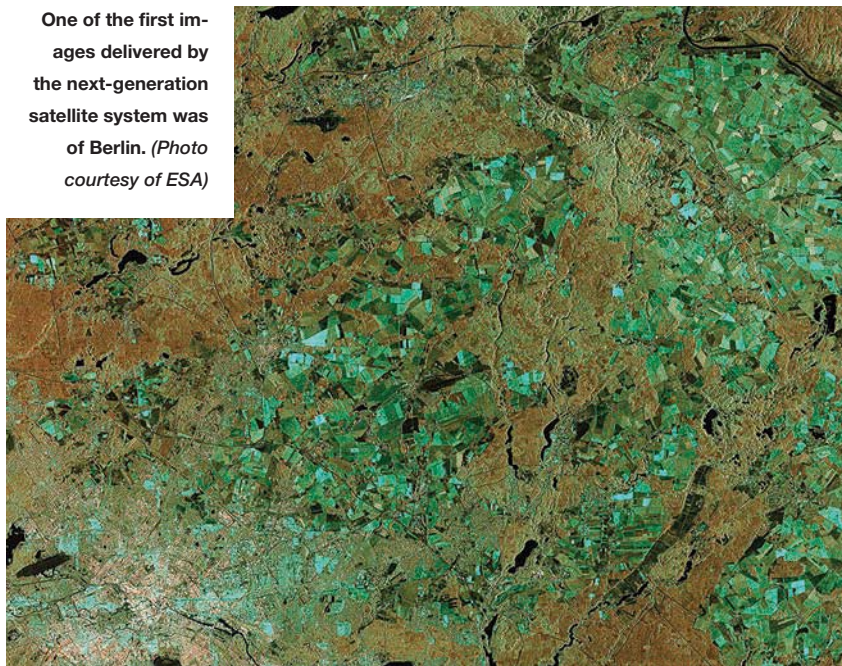
**ANOTHER MILESTONE HAS** been met in the development of the European Space-DataHighway, or European Data Relay Satellite (EDRS), a high-performance alternative for space data transfer. The system of two geostationary satellites relays information between Low Earth Orbit (LEO) satellites, spacecraft, or UAVs, and fixed ground stations. Recently, it achieved a high-volume data connection at a distance of 36,000 km between a LEO satellite and a satellite located in geostationary orbit.

Sentinel-1A, an Earth observation satellite, and Alphasat, a European communication satellite, were used as part of the demonstration. Each was equipped with a laser communication terminal (LCT) containing several optical components and systems. The terminals, developed by Tesat-Spacecom GmbH & Co. KG and Berliner Glas Group, allow high-speed data transfers of up to 1.8 Gbits/s between LEO and geostationary orbit.

During a previous demonstration, the EDRS successfully completed a gigabit transmission via laser of imagery between the radar sensors. The image of the city of Berlin was achieved when the data transfer reached 0.6 Gbits/s of the possible 1.8 Gbits/s over 45,000 km between the LCTs. Such high bandwidths significantly improved data latency and system reactivity.

The EDRS enables satellites to immediately transfer data to the ground, instead of the usual waiting for hours to fly over a fixed ground station—essentially in real-time. The use of optical components allows for increased amounts of data to be made available more quickly. The service provided by EDRS can also be scaled and adapted for users in terms of volume transmission and security requirements. Potential applications include emergency response, open ocean surveillance, weather forecasting, and wide-area monitoring. ■

One of the first images delivered by the next-generation satellite system was of Berlin. (Photo courtesy of ESA)



## CLOUD HELPS CURTAIL CYCLIST, Car Crashes

**A**ccording to the National Highway Traffic Safety Administration (NHTSA), nearly 50,000 cyclist fatalities and injuries occur in the U.S. every year. Looking for ways to curb those numbers, a new collaboration aims to alert drivers and cyclists about impending accidents. A joint effort between Volvo, POC, and Ericsson uses a connected car and bicycle helmet prototype to establish communication and offer proximity alerts to avoid collisions.

The cloud-based concept aims to alert users even if they are in a blind spot, in conjunction with Volvo's City Safety system. The helmet uses Bluetooth and a smartphone app (such as Strava) to send out the cyclist's position, which can then be shared through the Volvo cloud and vice versa. If an imminent collision

is determined, both users are warned—the driver will be alerted through a head-up display alert, and the cyclist will be warned via a helmet-mounted alert light and vibrations.

The system is just one part of a development to save lives across the entirety of “unprotected” road users. The cloud technology, which aims to further eliminate all remaining



## Redefining Frequency Synthesizers

With QuickSyn Technology



Design smaller and more efficient instruments with National Instruments QuickSyn synthesizers. The revolutionary phase-refining technology used in QuickSyn synthesizers enables blazing fast switching speeds, very low spurious and phase noise performance, wide frequency range, and small footprint.

### QuickSyn Models

Full-Featured	Lite Version
FSW-0010 10 GHz	FSL-0010 10 GHz
FSW-0020 20 GHz	FSL-0020 20 GHz

[ni-microwavecomponents.com/quicksyn](http://ni-microwavecomponents.com/quicksyn)

408 610 6810



©2014 National Instruments. All rights reserved. National Instruments, NI, and ni.com are trademarks of National Instruments. Other product and company names listed are trademarks or trade names of their respective companies. 17281

**New cloud technology seeks to help reduce the number of bicycle and vehicle accidents by eliminating blind spots.** (Image courtesy of Volvo)

blind spots between cyclists and drivers, was presented at this year’s International Consumer Electronics Show (CES) in Las Vegas. Further innovations seek to reduce the consequences of accidents for other gravity sports athletes and cyclists.

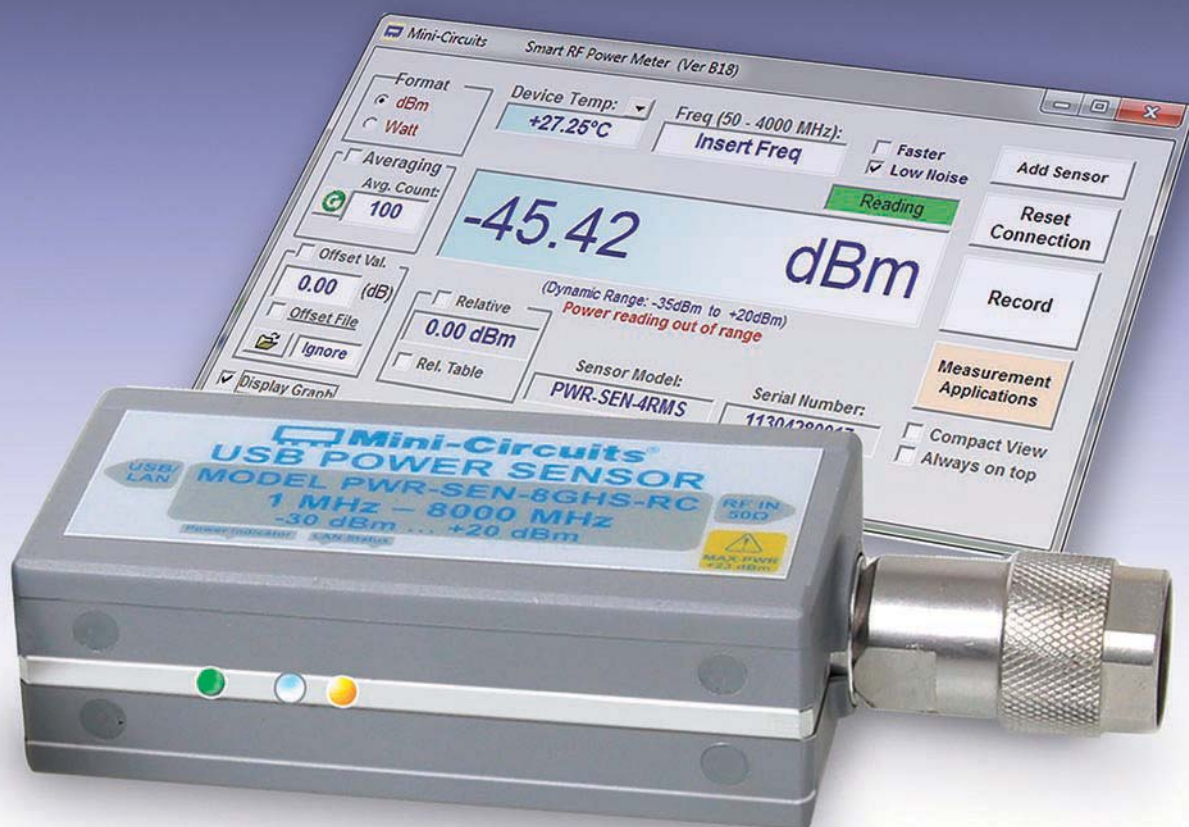
**“If an imminent collision is determined, both users are warned—the driver will be alerted through a head-up display alert, and the cyclist will be warned via a helmet-mounted alert light and vibrations.”**

Volvo’s City Safety system, which now comes standard in the new XC90, includes a variety of other features. Adaptive Cruise Control helps keep distance between other cars, and a 360-deg. camera helps detect obstacles at any angle for easier parking and maneuvering. An active high beam automatically senses other vehicles and people on the road, temporarily switching between low and high beams at night.

Additional radar sensors help provide blind-spot information when switching lanes and Forward Collision Warning scans all objects within 500 feet in front of the vehicle to avoid accidents. A Park Assist Pilot allows users to pull up to a parking space, let go of the wheel, and have the car steer itself into the spot, alerting the user when to brake. ■



# Turn Smart Power Sensors into Low-Cost RF Power Meters!



**USB &  
Ethernet**

## **POWER SENSORS** from **\$695** ea. qty. (1-4)

Mini-Circuits' RF power sensors turn almost any Windows® or Linux® based computer into a low-cost testing platform for all kinds of RF components and applications. To give you even more options, our new PWR-8GHS-RC model allows easy remote signal monitoring and data acquisition with USB and Ethernet control.

With 7 different models in stock offering measurement speeds as fast as 10 ms\*, dynamic range as wide as -35 to +20 dBm†, and measurement capability for continuous wave and modulated signals, chances are, we have a power sensor to meet your needs and fit your budget!

Our user-friendly GUI provides a full range of measurement tools including measurement averaging, time-scheduled measurements, multi-sensor support, and measurement applications supporting RF testing of couplers, filters, amplifiers and more! View data and graphs on-screen or export to Excel® for reporting and data analysis.

All Mini-Circuits power sensors fit in your pocket and come supplied with all the accessories you need for immediate use right out of the box. Visit [minicircuits.com](http://minicircuits.com) and place your order today for delivery as soon as tomorrow!

RoHS compliant

Model	Power Measurement	Frequency MHz	Control Interface	Price \$ ea. (Qty 1-4)
PWR-2.5GHS-75 (75Ω)	Peak	0.1 to 2500	USB	795.00
PWR-4GHS	Peak	0.009 to 4000	USB	795.00
PWR-6GHS	Peak	1 to 6000	USB	695.00
PWR-8GHS	Peak	1 to 8000	USB	869.00
<b>NEW!</b> PWR-8GHS-RC	Peak	1 to 8000	USB & Ethernet	969.00
PWR-8FS	Peak	1 to 8000	USB	969.00
PWR-4RMS	Average	50 to 4000	USB	1169.00

\*Measurement speed as fast as 10 ms for model PWR-8-FS. All other models as fast as 30 ms.

†Dynamic range as wide as -35 to +20 dBm for model PWR-4RMS. All other models as wide as -30 to +20 dBm.

Excel is a registered trademark of Microsoft Corporation in the US and other countries.

Neither Mini-Circuits nor Mini-Circuits Power Sensors are affiliated with or endorsed by the owners of the above-referenced trademarks.



## KUDOS

**KEYSIGHT TECHNOLOGIES**—Was recognized with the 2014 Global Frost & Sullivan Award for Market Leadership in Instrumentation Software for excellence in capturing the highest market revenue within its industry. The award is based on the global growth consulting firm's recent analysis of the instrumentation software market.

**RFMD**—Earned Huawei's Supplier of the Year Award at a ceremony held at Huawei's headquarters in Shenzhen, China. The award recognizes RFMD as Huawei's best supplier of RF components, which are used in Huawei's mobile phones and infrastructure products. This is the second year in a row that RFMD was named Huawei's Supplier of the Year.

# Powerful Multipath/Link Emulator

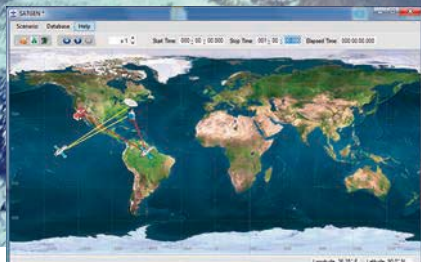
**Multipath Rayleigh & Rician Fading**  
**Unmanned Aerial Vehicle (UAV) testing**  
**Sophisticated Satellite link emulation**  
**Mobile Comm's on the move testing**

**250 MHz  
bandwidth**

Test solutions for ....

**WIN-T** - warfare information networks, tactical  
**MUOS** - mobile user objective system  
**JTRS** - Joint Tactical Radio System  
**IRIS** - Internet routing in space

Software showing mobile link setup



RF Test Equipment for Wireless Communications

**dBm Corp, Inc**

32A Spruce Street ♦ Oakland, NJ 07436  
 Tel (201) 677-0008 ♦ Fax (201) 677-9444

**www.dbmcorp.com**

## CATEGORY 9 LTE-A Successfully Tested at 410-Mb/s Download Speeds

**THE EVOLUTION FROM CATEGORY 6** to Category 9 LTE-Advanced (LTE-A) connectivity is expected to bring faster peak download speeds, swift application response times, and more reliable connectivity. Interoperability testing of LTE Category 9 connectivity was recently completed with 3-carrier downlink aggregation and download speeds up to 410 Mb/s. The demonstration was com-



pleted by Qualcomm Technologies, EE, and Huawei.

Qualcomm supplied its Snapdragon 810 processor with Huawei's commercial infrastructure solution across EE's LTE-A "4G+" network. The Category 9 Carrier Aggregation allowed EE to aggregate 20 MHz of 1800-MHz spectrum with another 20 MHz of 2.6 GHz, and a third carrier of 15 MHz of 2.6 GHz. The test marked what is reportedly the first time LTE Category 9 interoperability testing has been completed with major solutions providers and operators in Europe.

The Snapdragon 810 processor features a fully integrated 64-bit multicore



**You're developing  
a prototype for  
a critical project.**

**You promised  
delivery tomorrow.**

**And, one of the  
components is MIA.**



**Not a problem.**

At Fairview, we realize that having the correct part shipped directly to you the same day can mean the difference between success and failure. That's why you can count on us to stock the components you need, and reliably ship them when you need them. We're RF on demand. When you add Fairview to your team, you can consider it done!

[fairviewmicrowave.com](http://fairviewmicrowave.com)  
1.800.715.4396

 **Fairview Microwave**  
RF COMPONENTS ON DEMAND. *Done!*

CPU and LTE-A multimode modem to support up to three 20-MHz Category 9 Carrier Aggregation, as well as aggregation across frequency-division-duplex (FDD) and time-division-duplex (TDD) carriers. It has separately been demonstrated at download speeds up to 450 Mb/s over three 20-MHz LTE carriers.

According to EE, use of the remaining 15 MHz of 2.6-GHz spectrum enables both faster speeds and an increased capacity across the network. The technology is also backwards-compatible with all major cellular standards and technologies. As part of the next step toward the 5G era, the technology will be demonstrated at Wembley Stadium in London, England in early 2015. ■

#### PEOPLE

**RFMW LTD.**—CHRISTIAN GRIESWELLE was promoted to director of sales for RFMW Europe. Grieswelle has served as RFMW's Germany Country Manager for the past three years, establishing a successful track record of developing RFMW's presence in Germany. In his new position, he will be leading and further developing the European sales team that now reports to him in their entirety. Grieswelle graduated with a degree in electrical engineering from the University of Paderborn, Germany.



GRIESWELLE

**CURTISS-WRIGHT CORP.**—DAVID C. ADAMS has assumed the role of chairman, effective immediately and pursuant to the company's October 2014 announcement, adding to his role as CEO. Former Executive Chairman Martin R. Benante has retired from the company effective Jan. 1, 2015, completing a long legacy as only the 11th leader in Curtiss-Wright's 85-year history. As part of the formal transition plan announced in 2013, Benante will continue as a member of the board of directors until the conclusion of the company's next annual meeting in May 2015, at which time he will retire from the board.



ADAMS

## KINETIC BOOT Generates 1.5 W per Foot for Soldiers

**NOT ONLY ARE** U.S. Marines always on their feet, but they often have to carry more than 15 lbs of batteries on top of their heavy equipment to charge their electronics. To help alleviate this, Lockheed Martin joined forces with STC Footwear to develop a kinetic boot that transforms the motion of footsteps into a functional power source. In its current design, the Kinetic Boot is capable of generating up to 1.5 W of power per foot to charge reusable batteries or connect directly to systems.

Previous solutions, such as solar-power chest panels and helmets, still added significant weight to soldiers' uniforms. On the other hand, the Kinetic Boot only adds 2 to 3 oz. of weight per boot—all while generating more energy. During a demonstration at the Marine Corps' Experimental Forward Operating Base (ExFOB), a pair of Kinetic Boots was able to generate between 2 to 3 average watts of power, or enough to power



U.S. Marines try out a Kinetic Boot prototype at ExFOB 2014. (Photo courtesy of U.S. Marines)

an iPhone 5 three times after a 60-minute walk.

While the concept of harvesting energy from motion is not entirely new, efficiency has remained an ever-present

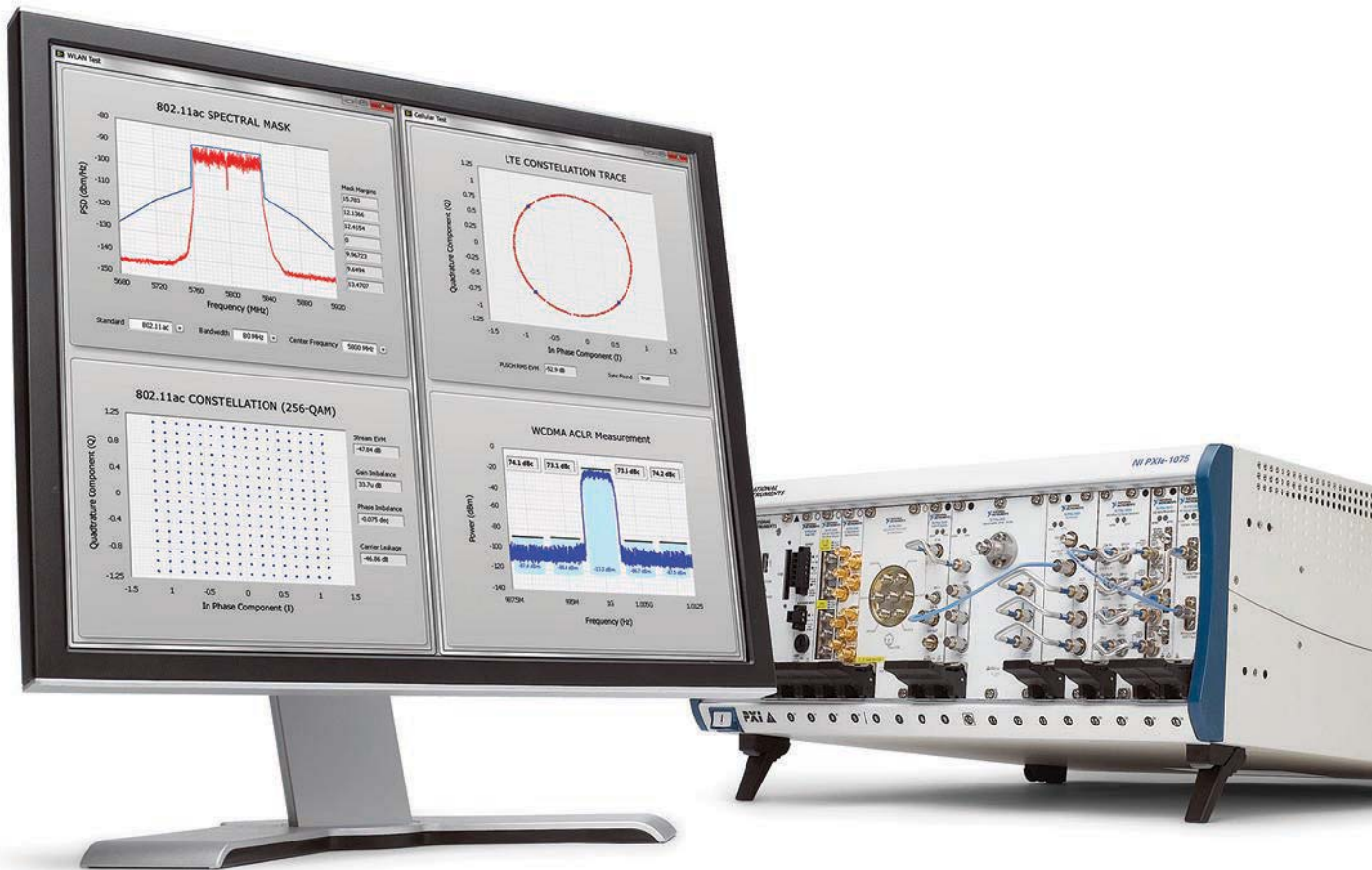
problem. Further optimization of the boots will help achieve maximum power generation while ruggedizing the design for harsh military conditions. Enhanced ruggedized packaging will not

only protect the boots' components from environmental factors, including dust and mud, but will also standardize the components' positioning to increase reliability. ■



# Redefining RF and Microwave Instrumentation

with open software and modular hardware



Achieve speed, accuracy, and flexibility in your RF and microwave test applications by combining National Instruments open software and modular hardware. Unlike rigid traditional instruments that quickly become obsolete by advancing technology, the system design software of NI LabVIEW coupled with NI PXI hardware puts the latest advances in PC buses, processors, and FPGAs at your fingertips.

## WIRELESS TECHNOLOGIES

National Instruments supports a broad range of wireless standards including:

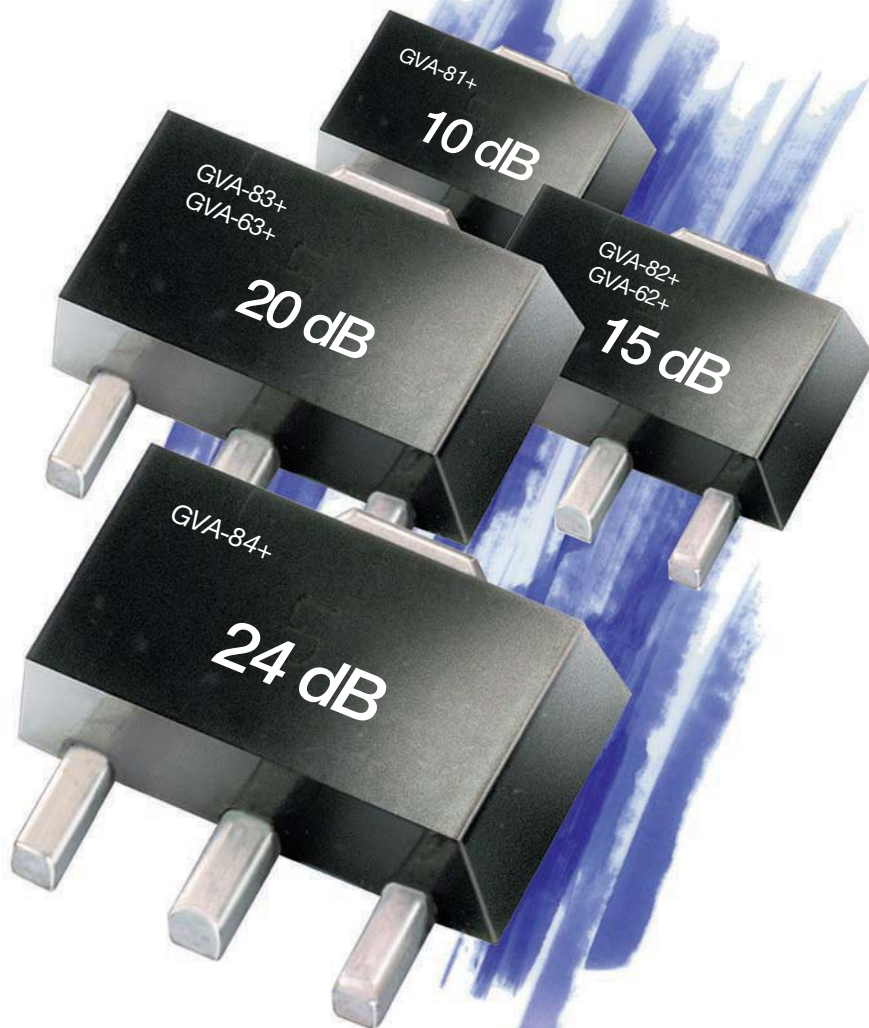
LTE	GSM/EDGE
802.11a/b/g/n/ac	CDMA2000/EV-DO
WCDMA/HSPA/HSPA+	Bluetooth

>> Learn more at [ni.com/redefine](http://ni.com/redefine)

800 813 5078

©2012 National Instruments. All rights reserved. LabVIEW, National Instruments, NI, and ni.com are trademarks of National Instruments. Other product and company names listed are trademarks or trade names of their respective companies. 05532





*+20 dBm Power Amplifiers with a choice of gain*

# GVA AMPLIFIERS

DC\* to 7 GHz from 94¢  
ea. (qty. 1000)

**2 New  
Models!**

The GVA-62+ and -63+ add gain flatness as low as  $\pm 0.7$  dB across the entire 100 MHz to 6 GHz range to our GVA lineup! The GVA series covers DC\* to 7 GHz with various gain options from 10 to 24 dB and wide dynamic range to fit your application. Based on high-performance InGaP HBT technology, these patented amplifiers all provide +19 dBm or better output power

and IP3 performance as high as +41 dBm. GVA amplifiers are unconditionally stable and designed for a single 5V supply. All models are in stock for immediate delivery! Visit [minicircuits.com](http://minicircuits.com) for detailed specs, performance data, export info, **free X-Parameters**, low prices, and everything you need to choose your GVA today!

US patent 6,943,629

\*Low frequency cut-off determined by coupling cap, except for GVA-60+, GVA-62+ and GVA-63+ low cut-off at 10 MHz.

**FREE X-Parameters-Based  
Non-Linear Simulation Models for ADS**



<http://www.modelithics.com/mvp/Mini-Circuits.asp>

**Mini-Circuits®**

[www.minicircuits.com](http://www.minicircuits.com) P.O. Box 350166, Brooklyn, NY 11235-0003 (718) 934-4500 [sales@minicircuits.com](mailto:sales@minicircuits.com)

458 rev N



# SUPER ULTRA WIDEBAND AMPLIFIERS

up to +27 dBm output... **0.1 to 21 GHz**

**Ultra wide coverage and super flat gain** make our ZVA family ideal for ECM, instrumentation, and test systems. With output power up to 0.5 Watts, they're simply some of the most usable amplifiers you'll find, for a wide range of applications and architectures!

All of our ZVA models are unconditionally stable, ruggedly constructed, and able to withstand open or short circuits at full output. For more details, from data sheets to environmental ratings, pricing, and real-time availability, just go to [minicircuits.com](http://minicircuits.com)!

*All models IN STOCK!*

 RoHS compliant



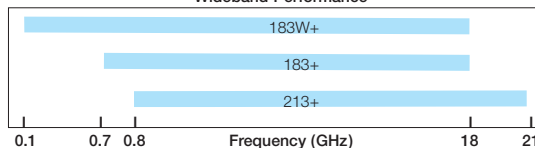
from **\$845** ea.

*Electrical Specifications (-55 to +85°C base plate temperature)*

Model	Frequency (GHz)	Gain (dB)	P1dB (dBm)	IP3 (dBm)	NF (dB)	Price \$ * (Qty. 1-9)
<b>NEW</b> ZVA-183WX+	0.1-18	28±2	27	35	3.0	1345.00
ZVA-183X+	0.7-18	26±1	24	33	3.0	845.00
ZVA-213X+	0.8-21	26±2	24	33	3.0	945.00

\* Heat sink must be provided to limit base plate temperature. To order with heat sink, remove "X" from model number and add \$50 to price.

**Wideband Performance**



 **Mini-Circuits®**

[www.minicircuits.com](http://www.minicircuits.com) P.O. Box 350166, Brooklyn, NY 11235-0003 (718) 934-4500 [sales@minicircuits.com](mailto:sales@minicircuits.com)

### CONTRACTS

**Norsat International Inc.**—Received an order to deliver its recently launched SigmaLink AUTO and Ranger products to a major military contractor that supplies communications solutions to governments and militaries worldwide. This marks the first sale of these next-generation technologies designed to improve ease of use and address industry trends triggered by military customers that increasingly demand very small form factors. The 1.8-m and 2.4-m SigmaLink AUTO series of transportable satellites are designed to provide broadband connectivity for basecamp operations, while the Ranger is a high-performance, self-

**MERCURY**  
Fills  
Defense Order

**NORSAT**  
Marks  
First New  
Tech Sale

contained multiband microsat terminal, offering portability and rapid deployment.

**Mercury Systems Inc.**—Announced that its Mercury Defense Systems subsidiary recently received a \$1.2 million order from a leading international aerospace and defense company for radar environment simulation equipment to support European Fighter Aircraft (EFA). The order was booked in the company's fiscal 2015 second quarter and is expected to ship by its fiscal 2016 third quarter. Mercury is a provider of open-sensor processing systems and services for commercial, defense, and intelligence applications.

### FRESH STARTS

**MACOM**—Successfully completed its previously announced acquisition of BinOptics Corp., a merchant provider of indium-phosphide lasers for data centers, mobile backhaul, silicon photonics, and access networks, in an all-cash transaction valued at \$230 million. The goal of this acquisition is to further extend MACOM's position in the optical space with an even broader platform to benefit from what the company anticipates will be a strong secular growth driver for many years to come. MACOM funded the purchase price of the acquisition from a combination of cash on hand and incurrence of \$100 million of additional indebtedness from its existing revolving credit facility.

**Anritsu**—Announced that the GCF, the certification body for the mobile-phone industry, has validated its LTE eMBMS Band 4 and Band 13 RF conformance test cases. Anritsu is the world's first test-equipment supplier to gain validation for these Band 4 and Band 13 test cases. The enhanced Multimedia Broadcasting Multicast Services (eMBMS) technology is a multicast service for LTE mobile networks that provides for high-capacity data distribution. The eMBMS technology enables network operators to simultaneously broadcast data to unlimited numbers of users on an LTE network, providing for high distribution efficiency. It can also be used during live broadcasts to send multiple video

streams from different angles to crowds at concerts, sports events, etc. Commercial services started in South Korea in 2014, and are expected to start soon in North America.

**Keysight Technologies**—Joined the NYU WIRELESS university research center as a key sponsor of the fundamental groundwork that the center is laying for a new generation of wireless technologies, also known as 5G. The announcement comes as the Federal Communications Commission's Notice of Inquiry explores the potential of mobile radio services in the millimeter-wave radio spectrum—an area in which NYU WIRELESS is developing fundamental science and mathematical channel models needed for 5G equipment.

**Modelithics**—Expanded its partnership with TACTRON ELEKTRONIK GmbH in Martinsried, Germany, as a reseller for Modelithics library sales and services. TACTRON, currently a reseller for Modelithics in Germany, Switzerland, and Austria, will now offer the same representation in Italy and France.

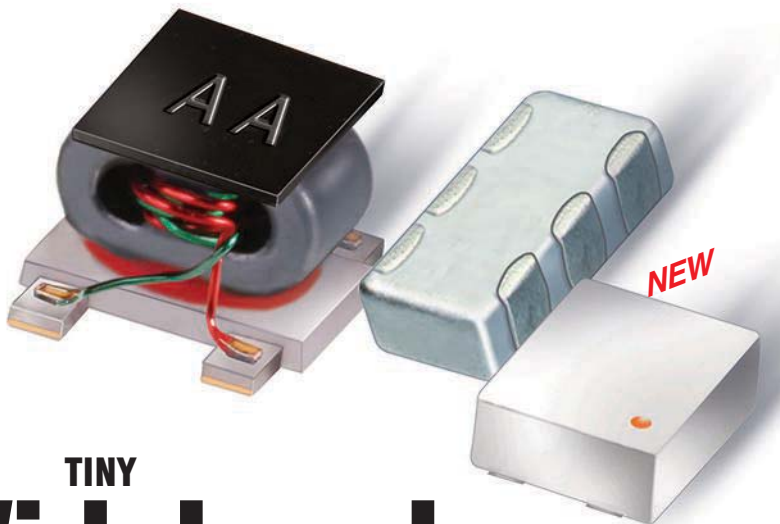
In other Modelithics news, the company, in partnership with TriQuint Semiconductor, released the latest update to the growing library of high-accuracy nonlinear simulation models for TriQuint gallium-nitride (GaN) transistors. The TriQuint GaN library, v1.5.0, now contains precision models for 29 of TriQuint's most popular GaN transis-

tors, including the model T1G2028536-FL, T1G4012036-FS, and T2G4005528-FS package-format transistors, and the model TGF2023-2-01, TGF2023-2-10, and TGF2954 die-format transistors.

**Mouser Electronics**—Expanded its strategic partnership and worldwide distribution agreement with Analog Devices (ADI) to include ADI's recently acquired RF and microwave products from Hittite Microwave, marketed as Hittite Microwave Products from Analog Devices. The Hittite Microwave product line, available now from Mouser Electronics, includes high-performance microwave, RF, and millimeter-wave products and subsystems, capable of operating over frequencies from DC up to 110 GHz. Products include digital, RF, and monolithic microwave ICs.

**Richardson RFPD**—Moved to a larger and recently renovated office space in Geneva, Ill. The new 24,000-sq.-ft. corporate headquarters is sized to accommodate the company's continued growth as a global leader in the RF and wireless communications, power conversion, and renewable energy markets. The new facility features a modern office floorplan designed to enhance internal efficiency and communication, with the goal of offering improved services to customers and suppliers. It also provides room for the company to continue to expand staff and drive global growth and market reach.





# TINY Wideband Transformers & Baluns!

**NOW!**  
**4 kHz - 18 GHz** From **99¢**  
ea. (qty. 20)

To support an even wider range of applications, Mini-Circuits tiny surface-mount transformers and baluns now cover frequencies up to 18 GHz! Our latest designs achieve consistent performance across very wide frequency bands, and our baluns have demonstrated great utility for chipsets. With over 250 trusted models in stock representing a wide selection of circuit topologies and impedance ratios, chances are, we have a solution for your needs!

Our Low Temperature Co-Fired Ceramic (LTCC) models provide reliable performance in tough operating conditions, tiny size – as small as 0805 – and very low cost. All core-and-wire models are available with our exclusive Top Hat™ feature, improving pick-and-place accuracy and throughput. We even manufacture our own transmission wire under rigorous control and use all-welded connections to ensure reliability and repeatability you can count on.

Visit [minicircuits.com](http://minicircuits.com) and use **Yoni2™**, our patented search engine to search our entire model database by performance criteria and find the models that meet your requirements. Order today and have them in hand as soon as tomorrow! Cost-effective custom designs and simulations with fast turnarounds are just a phone call away!



**TC**  
0.15" x 0.15"



**NC**  
0.08 x 0.05"  
Ceramic



**NCR2**  
0.08 x 0.10"  
Ceramic

 **RoHS compliant.**



# Inside TRACK

with  
**Aaron Partridge,**

*Founder and Chief Scientist, SiTime*

Interview by JEAN-JACQUES DELISLE

**JJD: How have silicon microelectromechanical-systems (MEMS) timing solutions advanced in recent years?**

AP: Timing is actually the first application of MEMS. The first devices that had all the components we now call MEMS were presented in 1967 by H.C. Nathanson, and they were resonators. But getting MEMS timing to production took a long time, dozens of Ph.D.s, and many generations of DARPA funding.

We released the first commercial MEMS timing devices in 2007. Since then, it has been a process of improving performance and developing parts for particular applications. For example, our recently released low-power, 32-kHz XOs (oscillators) and temperature-controlled crystal oscillators (TCXOs; precision oscillators) are designed for timekeeping in mobile devices. They took years to develop, but they are now in high-volume production.

Things are moving very quickly as we improve performance and develop new capabilities. I like to think of it as a case for Moore's Law. Because we are a semiconductor company, we need to act like one. That means that every technology generation brings a whole new level of capability.

**JJD: What benefits do silicon and MEMS technology bring to timing solutions?**

AP: The big picture is pretty simple: Anytime silicon can do a job, it replaces the incumbent technology. Take film, for example. We don't

photograph with film anymore. Or look at the simple floppy disk; memory sticks replaced those. Of course, the list goes on. The reasons behind each change are a bit different, but there is a common thread. Simply put, silicon does a better job with higher reliability and more versatility at a lower cost. It is the same in timing. Quartz crystals have been around since 1920. Within their limits, they have worked well. Now, quartz is getting siliconized.

Why is this? It is the leverage brought by silicon. We have invested trillions of dollars in silicon—understanding the material, developing design tools, building fabs, and educating generations of engineers in how to use it. That investment is leverage. Let's say I want to build something in silicon. I can design with highly optimized and tested tools. I can get ultra-pure material from a variety of suppliers. I also can go to billion-dollar fabs that I don't need to build. I can even contract with a solid infrastructure of packaging and testing suppliers. Basically, I can use silicon's





economics of scale. What could compete against that?

**JJD: How are silicon-MEMS timing devices able to achieve such a high level of programmability?**

AP: When an artist chooses a medium, he or she adopts the capabilities and limitations of that medium. A painter works in two dimensions, while a sculptor works in three. A filmmaker works with motion and sound. In quartz, one is generally limited to producing output frequencies at the physical resonances of the crystals. For example, 25-MHz mechanical crystals produce 25-MHz output signals. In silicon, we have circuits in our medium, so we use them. We can build phase-locked loops (PLLs) and digital-state machines. We also have nonvolatile memory to store configurations, so we can build in programmability.

PLLs are now capable of shifting reference frequencies with extreme accuracy (down to sub-parts-per-billion) with low phase noise and at low power. At the same time, we can measure temperature with amazing accuracy—better than a thousandth of a degree at a hundred-hertz update rate. Put the two of these together and one can temperature-compensate an oscillator with fantastic accuracy. Why not allow the output frequency to be anything from 1 Hz to 500 MHz? The PLLs are there, so let's use them.

**JJD: How does CMOS integration lead to higher-performing timing products, and what are the extents of that benefit?**

AP: I should start by defining what we mean by "integration." There are two types: homogeneous and heterogeneous. With homogeneous, the CMOS and MEMS components are built on one die. In contrast, heterogeneous means that they are built on separate die and packaged together. We can do either, but heterogeneous integration gives the best performance. We can optimize the MEMS and circuit processes individually. So we build the resonators

on MEMS die and mount them directly onto CMOS die.

In oscillators, the first stages of the first amplifiers generally dominate the noise. When one analyzes this noise, one finds a term for the input capacitance. Increased capacitance results in more noise. In MEMS oscillators, the resonators are small and very close to the circuits, which decreases the capacitance to typically 1 pF for MEMS instead of 10 pF for quartz. One needs to be careful that the downstream circuit's noise contributions are small as well, but that 10× head start is a big advantage. So CMOS integration can lead to lower noise.

Next are the PLLs. It may be surprising to think this way, but well-designed PLLs can reduce signal noise. At frequency offsets outside the PLL bandwidth, they can supply tremendously low phase noise that is limited only by their output dividers and driver stages. So I often say, "PLLs are our friends!" Our low-jitter oscillators provide sub-picosecond integrated jitter, thanks to the PLLs. This is part of leveraging the silicon and an example of the performance benefits we get from CMOS.

**JJD: How have the Internet of Things (IoT) and wearables markets embraced MEMS timing?**

AP: I expect IoT to grow the semiconductor market dramatically. It will complete our third technology wave (agriculture, industrialization, communications). And MEMS timing will be at the heart of it. First, of course, every IoT device will need a clock. Most will communicate by radio. As a result, most will need precision for RF and low power for timekeeping, so that means multiple clocks. Next, many will be small and powered by batteries or energy harvesting. Small size and low power are core capabilities of MEMS. We are at the front edge of IoT and already we are seeing the pull—especially in wearables.

**JJD: How well are silicon-MEMS timing solutions suited for the military/defense or aerospace markets?**

AP: We are seeing interest from the military for our low-vibration sensitivity and high-shock survivability. The phase noise of quartz oscillators degrades under vibration to as much as 20 to 40 dB near carrier. In addition, quartz tends to break in shock. One can work around some of these problems in quartz, but it's not easy. On the other hand, MEMS naturally has lower vibration sensitivity and higher shock survival because it is small.

Here is a thought experiment: Drop a small animal out of a tree, like a squirrel. What happens? It hits the ground, runs back to the tree, and climbs up again. Now think about dropping a cow. What happens? Not a good outcome for the cow. This comparison may be a bit silly, but similar scaling laws apply in both our resonators and this example. The equations for mass to surface areas, resonant frequencies, and material strength are similar. Simply put, smaller things are not affected by acceleration and shock as much as larger things.

**JJD: What inspired MegaChips to acquire SiTime? How does MegaChips see SiTime aiding its business?**

AP: MegaChips' vision is to be a top-10 fabless semiconductor company. The company recognized SiTime's growth potential and technology and market leadership. According to Yole Développement, a market research firm, MEMS timing is projected to grow 60% to 70% per year. From SiTime's perspective, the adoption of MEMS timing could accelerate if SiTime were part of a larger company with more sales, reach, and relationships. The two companies were very complementary and we both saw that right away.

Our products work perfectly together. Where you have a chip, you need a timing device to drive it. And the other way, as well—when you have a timing device, it is driving somebody's chip. We already have important customers in common and we expect this to strengthen the adoption of our MEMS timing devices. **mw**

## PRINTING WIRELESS IOT SENSORS

**GIVEN THE INTERNET** of Things' (IoT) need for low power and wide environmental functionality in its technology, it may require design techniques like ambient power harvesting, ruggedness, and flexibility via conformal substrates. To gain greater understanding of battery-less IoT applications, A. Traille, A. Georgiadis, A. Collado, Y. Kawahara, H. Aubert, and M.M. Tentzeris have designed a scalable, low-cost, and ink-jet-printed wireless sensor platform.

To realize the microwave operation of inkjet-printed circuits on substrates, some commercial-off-the-shelf (COTS) components were used instead of organic thin-film transistors (OTFTs). Using a paper base, the researchers went about investigating dual-battery/energy-harvesting techniques with the goal of increasing lifespan and wireless range. With a transmission frequency of 904.4 MHz, the paper-based circuit houses a microcontroller unit (MCU) that encodes analog sensor data into an amplitude-shift-keying (ASK) modulated signal.

To impedance-match the RFID circuitry with the antenna, an impedance of  $60-j74 \Omega$  is the conjugate matched to the half-wave dipole antenna. The antenna structure is printed using silver nanoparticles. Wireless-link measurements are performed using a Tektronix real-time spectrum analyzer, the 30408A, and a UHF RFID reader antenna. Extrapolating the reading of  $-48.1$  dBm at 4.26 m, the researchers estimated that the link's effective range would be between 142 to 175 m. See "Inkjet-printed 'Zero-Power' wireless sensor and power management nodes for IoT and 'Smart Skin' applications," *2014 XXXIth URSI General Assembly and Scientific Symposium (URSI GASS)*, Aug. 2014, pp. 1-4.

## AMBIENT RF ENERGY SUPPORTS WIRELESS SENSORS

**F**OR A PLETHORA of intelligent wireless sensors to function throughout our environment, new ways of powering these devices must be explored. The viability of several energy-harvesting techniques—ranging from solar, thermal, and piezoelectric to wireless—have been investigated by Sangkil Kim, Rushi Vyas, Jo Bito, Kyriaki Niotaki, Ana Collado, Apostolos Georgiadis, and Manos M. Tentzeris from the Georgia Institute of Technology, the University of Calgary, and the Centre Tecnologic Telecomunicacions, Spain. The group focused on the wireless energy harvesting of low-power, far-field, ambient ultra-high-frequency and cellular-band radiation.

Ambient RF energy may have the lowest power density of available energies. Yet it is a very cost-effective option for powering a wireless sensor. To explore this option, the research team used a broadband (512 to 566 MHz) log-periodic antenna with a realized gain of

7 dBi on average for capturing power in the ultra-high-frequency (UHF) digital TV bands in Tokyo. CST Microwave Studio was used to design and optimize the antenna. This log-periodic structure was fabricated on 1.6-mm FR4. Slots were cut into the antenna's dipole elements to miniaturize the structure.

Utilizing inkjet-printed antenna structures on paper, the team made a quasi-omnidirectional antenna out of low-cost and lightweight material. The folder dual-band antenna is optimized at 915 MHz and 2.45 GHz, as the power density is much greater at these frequencies than it is in the spectrum dedicated to TV White Space. A single-stage rectifying circuit was used with this harvester to maximize RF-DC conversion efficiency.

See "Ambient RF Energy-Harvesting Technologies for Self-Sustainable Standalone Wireless Sensor Platforms," *Proceedings of the IEEE*, Nov. 2014, p. 1649-1666.

## ORGANIC SUBSTRATES AID ULTRA-MINIATURIZATION OF WLAN RECEIVER

**F**OR WIRELESS-LOCAL-AREA-NETWORK (WLAN) devices, system-on-package (SoP) technology using organic substrates has the potential to shrink footprints while increasing yields. To exceed system-on-a-chip (SoC)-only WLAN designs, the use of organic substrates and chip-last packaging techniques for WLAN SoPs has been investigated by a team of researchers from Georgia State University, including Srikrishna Sitaraman, Yuya Suzuki, Fuhuan Liu, Nitesh Kumbhat, Sung Jin Kim, Venky Sundaram, and Rao Tummala.

Integrated SoC WLAN receivers may suffer from very-low quality factors (Qs). As a result, using separate components for low-noise amplifiers (LNAs) and

bandpass filters (BPFs) could increase the performance of a receiver while decreasing its size. The team used a low-loss organic substrate, ZEONIF XL (X-L). Two designs were run with 3D EM simulation software—a package with an LNA and integrated BPF and one without a BPF.

With a low pass-band insertion loss of 2.3 dB, the BPF operates well with 15 dB of return loss. Considering a comparable wire-bonded, LNA-equipped WLAN receiver, the researchers claim their design is less than 1.5 times smaller. See "Ultra-miniaturized WLAN RF Receiver Module in Thin Organic Substrate," *IEEE Transactions on Components, Packaging and Manufacturing Technology*, Aug. 2014, p. 1276-1283.





# **HAND FLEX™ CABLES**

Hand Flex Cables conform to  
any shape required.

**\$9<sup>49</sup>** **IN STOCK**  
from ea. (qty. 1-9) **DC to 18 GHz**


**Get the performance of semi-rigid cable, and the versatility of a flexible assembly.** Mini-Circuits Hand Flex cables offer the mechanical and electrical stability of semi-rigid cables, but they're easily shaped by hand to quickly form any configuration needed for your assembly, system, or test rack. Wherever they're used, the savings in time and materials really add up!

**Excellent return loss, low insertion loss, DC-18 GHz.** Across their entire bandwidth, Hand Flex cables deliver excellent return loss (>26 dB typ for up to 50" runs) and low insertion loss (0.2 dB typ at 9 GHz for a 3-inch cable). So why waste time measuring and bending semi-rigid cables, when you can easily install a Hand Flex interconnect?

#### **Two popular diameters to fit your needs.**

Hand Flex cables are available in 0.086" or 0.141" diameters, with a turn radius of 6 or 8 mm, respectively. Straight SMA connectors are standard, and now we've added right-angle connectors to our Hand Flex lineup, for applications with tightly-packed components.

#### **Standard lengths in stock, custom models available.**

Standard lengths from 3 to 50" are in stock for same-day shipping. You can even get a Designer's Kit, so you always have a few on hand. Custom lengths, or two-right-angle models, are also available by preorder. Check out our website for details, and simplify your high-frequency connections with Hand Flex!  RoHS compliant





PAUL WHYTOK

## Universal Radio Platform Handles Digital and Legacy Analog

**A** PRIVATE MOBILE radio (PMR) common platform processor to support digital/analog Frequency Division Multiple Access (FDMA) PMR/LMR and 2-slot time division multiple access (TDMA) digital systems has been developed by UK-based low-power wireless semiconductor specialists CML Microcircuits ([www.cmlmicro.com](http://www.cmlmicro.com)).

With each system potentially having different requirements and specifications that affected the actual radio architecture design, the radio manufacturers' holy grail of a single universal cost-effective radio platform became a complex design challenge.

The rationale behind the CMX7241/7341 PMR Common Platform Processor sets out to address this. The CMX7241/7341 provides a common platform that can deliver FDMA digital PMR/LMR, TDMA digital PMR/LMR, and legacy analog. Based on CML's proprietary FirmASIC component technology, a Function Image (FI) can be uploaded into the device to determine the CMX7241/7341 overall functions and operating characteristics.

The first FI focuses on digital and analog FDMA PMR/LMR. It provides a complete feature set including auxiliary functions to support the whole radio. The company says that when combined with its CMX994 Direct Conversion Receiver IC, it presents a flexible, highly integrated radio platform solution.

### OPERATING FEATURES

Main operating features of the processor include automatic analog/digital

detection; digital PMR/LMR; ETSI TS 102 658, TS 102 490, and EN 301 166 compliance; embedded air interface physical and data link layers; and mode 1, 2, and 3 operation.

From an analog PMR/LMR perspective, the operational characteristics include: EN 300 086, EN 300 296, and TIA-603-D compliance; complete audio processing; sub-audio signaling; audio-band signaling; and an MPT 1327 modem.

The figure below shows a typical digital/analog PMR/LMR radio application. The CMX994 Direct Conversion Receiver provides maximum on-chip integration that allows a small RF receiver to be realized with minimal external components.

Improvements in semiconductor technologies have seen DCRx increasingly displace superhet as the technol-

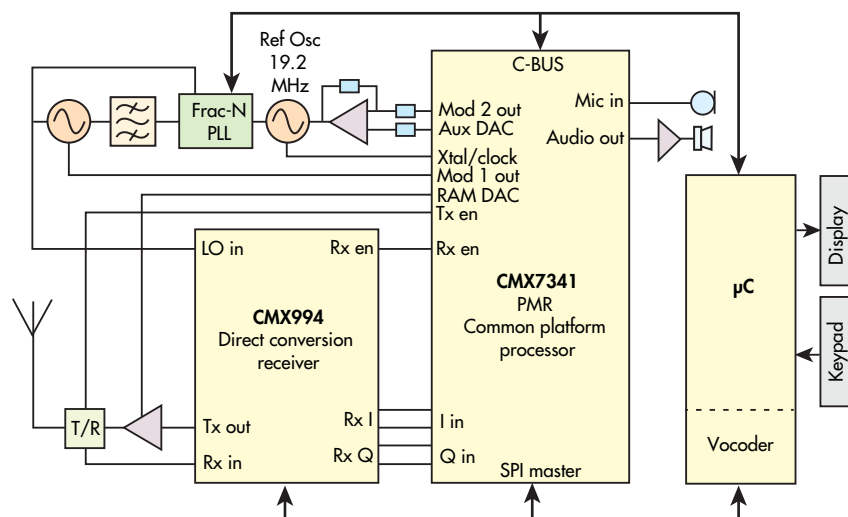
ogy choice for radio receivers across many different applications.

### DESIGN FLEXIBILITY

Earlier this year CML Microcircuits added the 16-FSK modulation to the CMX7164 Multi-mode Wireless Data Modem portfolio. Addition of the 16-FSK constant envelope modulation is expected to enhance the design flexibility of this modem IC, enabling telemetry systems to evolve into higher data throughput without the need to move to a linear modulation scenario.

The CMX7164 covers both constant envelope and linear modulation schemes, and also provides a good platform to support customer-specific modulation schemes.

The CMX7164 is available now, offering low-power 3.3V operation in small VQFN/LQFP packaging. [www.cmlmicro.com](http://www.cmlmicro.com)



Here is a block diagram illustrating the common-platform multi-mode analog/digital PMR/LMR radio.



### Keysight U2040 X-Series Wide Dynamic Range Power Sensors

The world's widest dynamic range: -70 to +26 dBm (96 dB)

Fast measurement speed: 10,000 readings-per-second

Choice of form factors: USB and LAN

Accuracy and repeatability across all common wireless signals

Internal zero and automatic calibration



Super fast.  
Super accurate.  
Super wide  
dynamic range.

Introducing a variety of power sensors that offer extremely high measurement speed and the world's widest dynamic range. Using Keysight BenchVue software for data capture/analysis, the sensors will allow you to obtain fast, accurate and repeatable measurements over a wide range of power levels. Choose from four USB models to test chipsets, radio systems, radar, mobile and handsets. Or choose the industry's first LAN and thermal vacuum-compliant power sensor for satellite testing.

**HARDWARE + SOFTWARE + PEOPLE = INSIGHTS**



USB

LAN

Download an app note on fast, accurate  
power measurements for wireless test.  
[www.keysight.com/find/rfpowertips](http://www.keysight.com/find/rfpowertips)



USA: 800 829 4444  
CAN: 877 894 4414

Scan to view video demo.

**KEYSIGHT**  
TECHNOLOGIES

Unlocking Measurement Insights

© Keysight Technologies, Inc. 2014

Agilent's Electronic Measurement Group has become **Keysight Technologies**.



# MAN AND MACHINE:



## Bonded Together with RF Glue

By embracing cost-sensitive and integrated approaches, unmanned systems, COTS, DASs/small cells, and test are opening doors to technology previously only seen in science fiction.

**T**his next year will see the advancement of a revolution in connectivity between man and data. The depth and design of this connectivity will bring us closer to technology and our bodies while enhancing our ability to compete electronically on the battlefield. The development of RF technologies, which are of course key to connected systems, is making possible technologies that were once relegated to pure fantasy (*Fig. 1*).

Among the highlights of upcoming technological developments are machines with greater mobility and intelligence; low-cost, military-grade multi-function devices; wireless data access virtually everywhere; and the ability to rapidly and accurately test the latest technologies.

From intelligent flying drones that mimic insects or birds of prey to pack mules for land-based troops, the U.S. Department

of Defense (DoD) is heavily invested in developing incredibly capable unmanned systems for land, air, and sea (*Fig. 2*). In doing so, it is partnering with other agencies, such as the Defense Advanced Research Projects Agency (DARPA) and the U.S. Office of Naval Research (ONR).

The resulting systems rely on RF technologies for communications, control, and the ability to “see” the world around them. Such heightened intelligence, in turn, leads to a demand for greater sensing and communications capabilities for reporting, threat identification, and coordination.

Looking at the current state-of-the-art in drones, last year saw the testing of pack-mule drones, the legged squad support system (LS3) by DARPA, and the development of add-on autonomy kits. Those autonomy kits, which hail from ONR and Lockheed Martin, can turn a variety of military vehicles (like a ground



support vehicle or V-22 Osprey) into semi-autonomous robots.

Much of the investment in drone technology has focused on devices that eliminate the need for human soldiers to participate in support roles, such as ferrying supplies and cargo across the battlespace. In addition to fatiguing and stressing soldiers, such tasks often result in casualties. Thus, the use of autonomy

**1. Projects like DARPA's Fast Lightweight Autonomy (FLA) program (left) seek to incorporate solutions found in nature to enable the latest tactical technology.**

kits and drones can help militaries save lives. At the same time, they can reduce spending and focus on force-multiplying and performance-enhancing technologies.

In a similar vein, much of the U.S. military's drone system development seeks to enable troops to

virtually extend their reach into a battlefield using remotely controlled robots. Such robots can operate semi-autonomously or via direct human control. Here, much also is saved in terms of training costs.

For example, a sergeant who is already familiar with video-game controls can learn to remotely pilot the latest combat equipment with much less time and effort—especially when compared to the level of education and training needed to ready a physicist/engineer/pilot to operate the latest combat craft. Recognizing this trend, the Navy has funded the development of an autonomous and controllable fighter aircraft. Also being considered is the use of machine swarms, which are undergoing testing, to combat high-number and enemy swarm threats.

Of course, the communications links and coordination electronics for these systems rely completely on wireless technologies. These wireless developments require more intelligent and integrated RF/microwave/millimeter-wave technologies, which can be rapidly reconfigured and reprogrammed. Over time, technologies that integrate high-performing computation hardware, RF hardware, and a sophisticated, flexible software plane will increasingly be employed. Those integrated technologies also will advance over time, thus better enabling these autonomous and remotely controlled machines to function on a battlefield that is brewing with complexity and threats.

Among the technologies that will be enhanced to provide the adaptability and control needed by these systems are software-defined radios, field-programmable gate arrays (FPGAs), gallium-nitride (GaN) on silicon, and reconfigurable RF devices. Due to the high numbers of these systems, modular and mass-manufacturing techniques also will be critical in enabling the next generation of defense robots.

### COMMERCIAL-OFF-THE-SHELF COMPONENTS

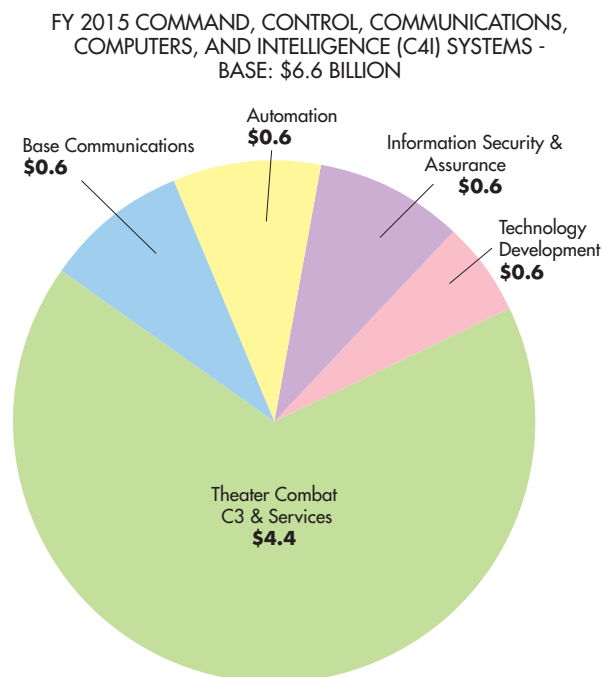
To cope with the need for cost-effective military systems that can still compete with the latest threats, both the military-technology supply chain and design approach must be reinvented (Fig. 3). Part of this trend revolves around using high-performing and rugged commercial-off-the-shelf (COTS) com-



**2. Using semi-autonomous robots as a force-multiplier could reduce the costs of fielding troops while increasing their effectiveness.**

ponents in modern military equipment and modular design. The old method of low-volume, highly custom components is now largely outdated, thanks to modern DoD requirements. Today's defense contractors/sub-contractors are designing and using components and subsystems that can meet the needs of both high-volume commercial/industrial applications and the stringent demands of the modern battlefield.

Specifically, size, weight, power, and cost (SWAP-C) is driving the use and development of COTS devices and modular-open-systems-architecture (MOSA) approaches. These design criteria



**3. DoD spending on command, control, communications, and computers (C4) is focused on technologies that rely on COTS components.**

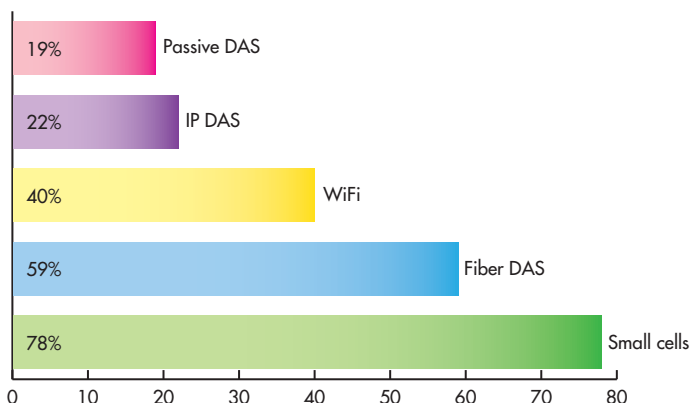
are hypercritical for electronic-warfare (EW) and radar systems, as they will be employed with unmanned vehicles in the land, air, and sea. These intelligence, surveillance, and reconnaissance (ISR); EW; and radar systems are also supposed to undergo more technical blending, as the hardware and software controlling them increasingly adopts the same technologies.

At the core of all of these devices, for example, are a software-defined radio (SDR), FPGAs, digital-signal-processing (DSP) units, general-purpose processors (GPPs), and very-high-speed domain-conversion technologies. As GaN is incorporated onto substrates like silicon, digital systems will integrate further.

In the near future, these devices will occupy the same module, if not the same integrated circuit (IC). Such high levels of integration are already being seen in next-generation EW technologies, such as Raytheon's next-generation jammer (NGJ). This active electronically steered array (AESA) jammer is both an extremely powerful radar and a remotely networked SDR.

GaN will continue to provide greater power density while solving thermal-control challenges. In the more distant future, carbon-based electronics will take GaN's place to provide even higher density. As a result of these advances, RF devices will merge closer to the analog and digital devices in the modular card or box-based systems built on open architectures. Examples include PXI/PCI, AXI, and VME card-slot-based

PREDICTED GROWTH IN THE NEXT THREE YEARS  
2013 survey of attendees, IBWAVE user group



4. As the demand for mobile data escalates, especially in urban environments, so too does the need for cell miniaturization and increased in-building wireless services.

modular hardware with an abstracted software layer.

By taking a proprietary approach—as Mercury Systems is doing with its OpenRFM architecture—or leveraging the Advanced Telecom Computing Architecture (ATCA), companies are working to modularize RF systems in combat aircraft. Their goal is to create an open standard based on easily replace-

# RF Solutions from JFW Industries



**Test Systems**  
**Terminations**  
**Variable Attenuators**  
**Power Dividers**

**Programmable Attenuators**  
**Fixed Attenuators**  
**RF Switches**  
**RF Test Accessories**



## JFW Industries

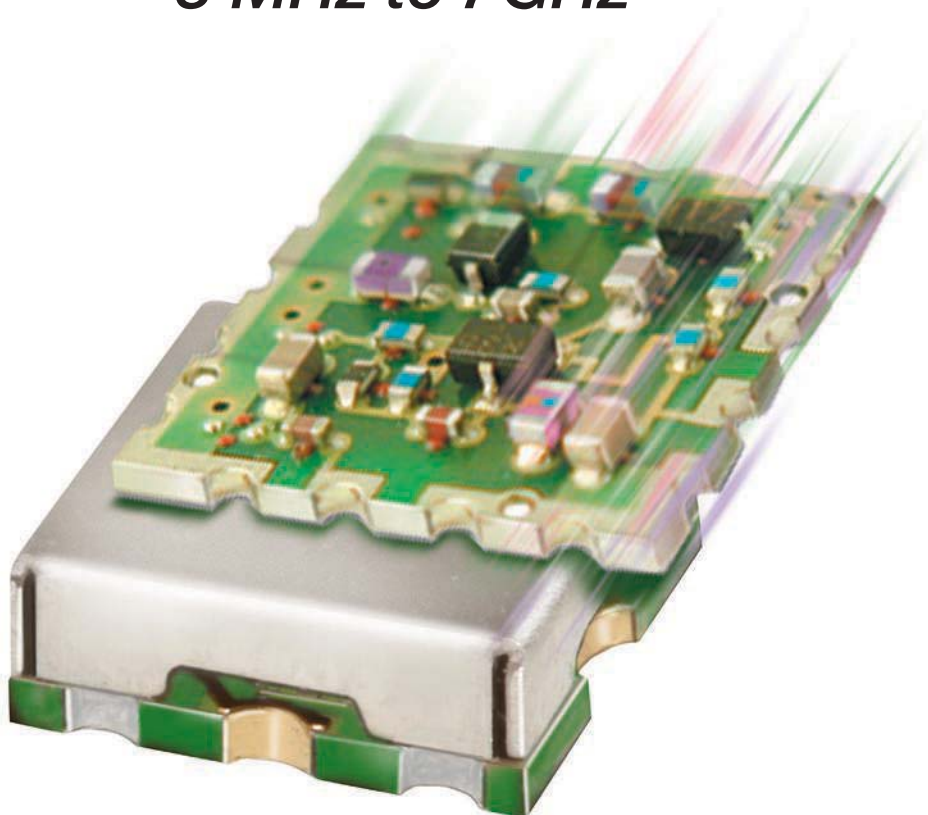
Call 317-887-1340 Toll Free 877-887-4JFW (4539)  
E-mail [sales@jfwindustries.com](mailto:sales@jfwindustries.com) Visit [www.jfwindustries.com](http://www.jfwindustries.com)



# ***CUSTOM VCOs***

*You Define It. We'll Design It.*

**3 MHz to 7GHz**



*Starting at*  
**\$49<sup>95</sup>\***  
*ea. (min. Qty. 10)*

***Send us your requirements using our online spec checklist for a response within 4 days!***

Need a VCO custom designed for your project? Mini-Circuits just made it easy. Go to [minicircuits.com](http://minicircuits.com) and enter your requirements into our online VCO spec checklist. Our engineers will review your application, run simulations and respond to discuss your request within four days or less. We can optimize models for wideband, linear tuning, dual output, low phase noise and more for costs as little as \$49.95\* ea. (minimum qty.10). Whether you need a rugged coaxial housing or surface mount packages as small as 0.25 x

0.25 x 0.1", we can probably create a solution for your needs. You can also use our unique Yoni2™ search engine on our website to search actual test data from our full engineering database. Just enter your desired performance parameters and click "search" for a complete list of models that will be close to your requirements. We're always here to support you, so send your request today, and our engineers will work with you to find the right VCO for your application!

***Go to*** [www.minicircuits.com/specCheckList/vco.html](http://www.minicircuits.com/specCheckList/vco.html)

***Enter your requirements, and click SUBMIT!***

***We promise you a fast response!***

\*Price for most designs. Up to \$99.95 for more complex designs.





able modules, which can support a variety of different configurations and functions. Such systems are built on a common hardware interface. Software abstractions dictate whether device behavior will be modified via a rapid module swap in the field or simple reprogramming.

This type of design approach offers great benefits for the defense industry, as it lowers the time spent on design, deploy-

ment, modernization, and maintenance. It also cuts the cost factors associated with future-proofing and upkeep. In the commercial and industrial computer-electronics industry, COTS and MOSA-focused designs comprising common hardware with software abstraction have already been embraced. They have proven to be a cost-effective and rapid method of fielding high-performance products.

### SMALL CELLS AND DASs

Outside of the military arena, the most significant worldwide trend is the rapid growth of mobile data traffic. Cisco predicts monthly mobile data traffic of greater than 15 exabytes by 2018. Combine that with urbanization, which leads to more tightly packed in-building and urban environments, and miniaturization of the cellular structure and high-speed mobile data connections in every nook and cranny becomes essential (Fig. 4). Video streaming and personal data services are big drivers in this regard.

In addition, public-safety demands for location and security information is requiring greater connectivity throughout urban environments. Substantial cellular offloading onto Wi-Fi networks also is occurring. Meanwhile, the demand for seamless high-speed mobile data encourages solutions that are cost effective to install and maintain.

This burden will ultimately fall on small cells and DASs that are built into (or onto) buildings and urban centers, such as stadiums (Fig. 5). Traditionally, small cells have operated as miniaturized macrocells, with higher capacity, lower cost per area, and operational expenditure (OPEX) benefits over DAS. DAS traditionally benefits from neutral host and macrocell parity.

Recently, DASs have also begun to integrate typical small-cell features, such as traffic steering and accessibility to a wide range of wireless networks and backhaul. As the winning features of DASs and small cells begin to blend, their benefits are likely to converge using the same highly integrated and flexible hardware.

These hybrid networks or distributed radio systems (DRSs) will likely employ



# KRYTAR®

**Microwave Components & Instruments**  
DC to 67 GHz



**Directional Couplers**  
to 67 GHz



**3 dB 90° Hybrid Couplers**  
to 40 GHz



**Directional Detectors**  
to 50 GHz



**Double Arrow 3 dB 180° Hybrid Couplers**  
to 26.5 GHz



**Detectors**  
Zero Bias  
Schottky  
Planar Doped  
Barrier Planar  
Tunnel Diode  
Threshold Detectors  
to 40 GHz



**MLDD Power Divider/  
Combiner** to 45 GHz



**RF & Microwave Power Meter**  
100 KHz to 40 GHz



**Adapters: DC to 50 GHz**  
In Series: SMA, 2.92 mm, 2.4 mm  
Between Series: 2.29 mm to 2.4 mm



**Coaxial Terminations**  
to 50 GHz



**Broadband Limiters**  
Pin-Pin Diode  
Pin-Schottky Diode to 18 GHz

**MIL Qualified Components Available**

 **KRYTAR®** 1288 Anvilwood Ave. Sunnyvale, CA 94089

Toll Free: (877) 734-5999 • Fax: (408) 734-3017 • [sales@krytar.com](mailto:sales@krytar.com)

[www.krytar.com](http://www.krytar.com) lists complete specifications and application ideas for all products



**40 Years of Excellence**  
KRYTAR  
Since 1975

Now  
available with  
**LabVIEW!**



# Micro Lambda's Bench Test Boxes... Simple and Easy to Use!

## MLBS-Synthesizer Test Box – 600 MHz to 20 GHz

Standard models cover the 0.6 to 2.5 GHz, 2 to 8 GHz, 8 to 20 GHz and 2 to 20 GHz frequency bands. All versions of the MLSP synthesizer product family can be easily inserted into the test box. Tuning consists of a control knob, key pad, USB and Ethernet connections. Units provide +10 dBm to +13 dBm output power levels and are specified over the lab environment of +15°C to +55°C and are CE certified.

Units are provided with a power cord, USB cable, Ethernet cable, CD incorporating a users manual, quick start guide and PC interface software.

## MLBF-Filter Test Box – 500 MHz to 50 GHz

Standard models utilize any Bandpass or Bandreject filter manufactured by Micro Lambda today. Bandpass filter models cover 500 MHz to 50 GHz and are available in 4, 6 and 7 stage configurations. Bandreject (notch) filter models cover 500 MHz to 20 GHz and are available in 10, 12, 14 and 16 stage configurations. Units are specified to operate over the lab environment of +15°C to +55°C and are CE certified.

Units are provided with a power cord, USB cable, Ethernet cable, CD incorporating a users manual, quick start guide and PC interface software.

See our complete line of wideband, low noise components



**MLSP-series  
Synthesizers**  
600 MHz to 20 GHz



**MLSW-series  
Synthesizers**  
600 MHz to 16 GHz



**MLTO-series  
TO-8  
Oscillators**  
2 to 16 GHz



**MLSMO-series  
Surface Mount  
Oscillators**  
2 to 16 GHz

[www.microlambdawireless.com](http://www.microlambdawireless.com)



**MICRO LAMBDA  
WIRELESS, INC.**

*"Look to the leader in YIG-Technology"*



centralized baseband functionality in combination with a cloud radio access network (CRAN) for the distribution of a common public radio interface (CPRI). Fiber networks will most likely carry the radio functions to remote radio heads (RRHs) throughout a building.

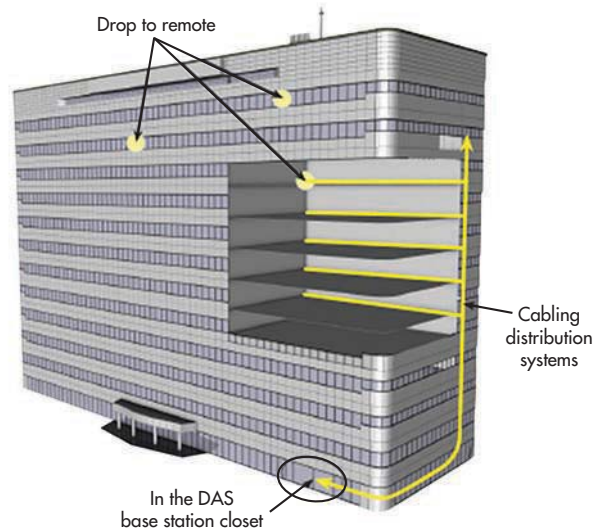
In addition, lower-cost common cabling, such as catV or other Ethernet lines with built-in power distribution, will be used to lower costs and complexity. Ericsson, SpiderCloud Wireless, and other companies are already building highly integrated and potentially cost-effective DAS units that use some of these concepts. It is likely that such features will continue to advance.

### THE NEXT WAVE IN SOFTWARE AND T&M

To keep up with the complexity and speed of the modern test environment, there has been significant movement away from large rack-mount and benchtop test and measurement instrumentation. This trend is not solely cost-driven, as fewer experienced engineers will be available to oversee and perform complex testing of the latest devices. As a result, there is a need for more automation, diversity of features, and ease of use.

At the same time, moving the computer out of a test and measurement instrument and onto a centralized device has helped shrink the cost and size of common instruments, such as spectrum analyzers, network analyzers, and oscilloscopes. PXI- and AXI-based test systems continue to improve as application-specific-integrated-circuit (ASIC) techniques advance the performance of instrumentation in the footprint of ICs.

Additionally, the software abstraction and common hardware environments are extending the features of traditional instruments to include many multifunctional instruments. Currently, these compound instruments are relegated to low-end performance. As the adoption and demand rise for this approach, however, more features will be integrated into these modular



**5. Often, traditional building materials are heavy attenuators of wireless signals. As a result, new building materials and design strategies are beginning to take into account the need for wireless connectivity throughout a structure.**

instruments. Eventually, this level of integration will be so high that software and branding will become the differentiating factor of an instrument (Fig. 6).

These trends could lead to different instrumentation manufacturers outsourcing to common hardware vendors. They will simply use operating-system platforms to compete in the development of apps and techniques. With PC-driven test instruments offering much lower prices for performance, cost competitiveness will also drive this development. This trend stems from smaller military budgets and the cost-centric purchasing of telecommunications companies.

Such cost-driven planning is feeding the development of automated testing and more sophisticated software control and analysis. The automation of instrumentation is necessary to efficiently test the enormous numbers of mobile devices, such as smartphones, tablets, and Internet of Things (IoT) devices with complex modulation schemes.

Looking into the future, another approach to handling hardware complexity and the merging of digital, analog, and RF domains is to build automated testing into the devices themselves. An automated self-test approach could—and inevitably will—remove the need for many of repetitive, simple tests on higher-cost devices. Yet external, higher-performing test equipment will still be needed to measure very-low-cost devices and for characterization/validation/compliance. **mtw**



**6. With the software interfacing of complex test environments, integrated software environments could soon enable remote operation and monitoring by experienced engineers off site. Technicians could then perform less complex local operations.**

# NEXT GENERATION POWER AMPLIFIERS



Significant size reduction  
Sizes reduced by 40-70%

Remote Monitoring & Control  
via embedded WEB server

## Next Generation Power Amplifier Systems

SKU 2126  
SKU 2066  
SKU 2162  
SKU 2170  
SKU 2175  
SKU 2179

**1  
kw**

**500 W  
250W**

20 - 500 MHz  
500 - 1000 MHz  
20 - 1000 MHz  
1000 - 3000 MHz  
80 - 1000 MHz  
2000-6000 MHz

**5U  
chassis**

**3U chassis  
4U chassis**

## Next Generation Building Block Modules

SKU 1163  
SKU 1193  
SKU 1199  
SKU 1191

125 W  
100 W  
100 W  
100 W

20 - 520 MHz  
20 - 1000 MHz  
1000 - 3000 MHz  
2500 - 6000 MHz

7 x 4 x 1.2"  
7 x 4 x 1.2"  
7 x 4 x 1.2"  
8 x 6.5 x 1"



[www.EmpowerRF.com](http://www.EmpowerRF.com)



**EMPOWER  
RF SYSTEMS, INC.**



# How to EM Simulate Large and Complex Objects

To reduce costly trial and error troubleshooting and speed design cycles, EM simulators are using specialized methods, software, and hardware techniques.

**WHAT APPROACHES WOULD** you take to electromagnetically (EM) simulate a large and/or complex structure or system? This question commonly faces engineers working on radar, macro-antenna placement, aircraft, or satellites. The dilemma also arises in scenarios where design geometries are complex or tens to hundreds of times the wavelength of the frequencies of interest (*Fig. 1*).

Until recent advances in computational methods, hardware, and intelligent computing, the answer was to simplify the problem until it could be managed with available technologies. But this approach is often inadequate for predicting even minor coupling or edge effects. For high-frequency or broadband simulations, the computation time could be enormous, too.

“As the electrical size (as measured in wavelengths) of an object increases, memory requirements and run time for

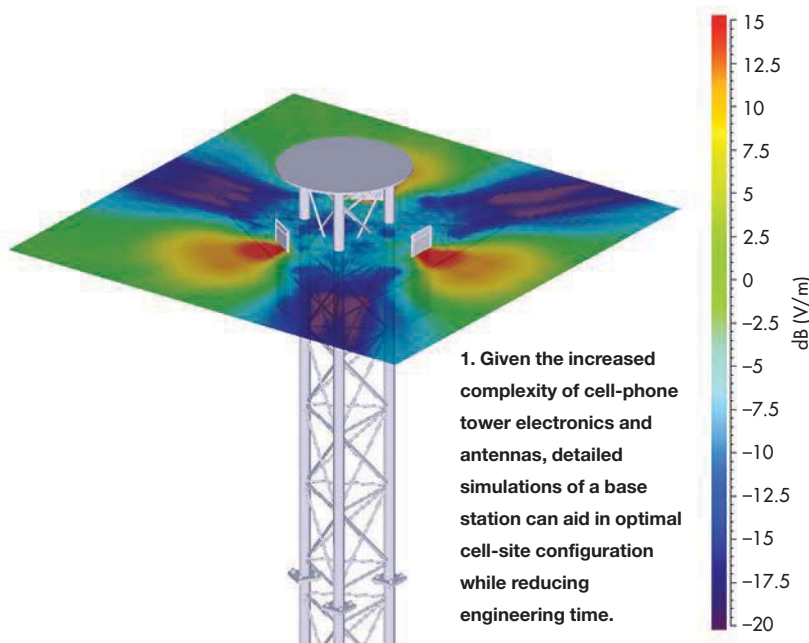
full-wave techniques—such as method of moments (MoM), finite-difference time domain (FDTD), finite element method (FEM), finite integral technique (FIT), etc.—increase rapidly,” says Matthew Miller, president of Delcross Technologies. “At some point, it is no longer practical to use a full-wave solver. It is at this point that users typically switch to an asymptotic, ray-based solution, such as geometric theory of diffraction (GTD) or physical theory of diffraction (PTD; *Fig. 2*).”

These techniques combine the physical mechanics of high-frequency or photonic ray/current properties with physics-based descriptions of interaction with conductors and induced currents. PTD (also known as the Physical-Optics solver method) relies on estimating the electric field on a conductor’s surface using ray optics. The approximated field results are then integrated over the surface to derive the resultant scattered field. The areas that are not illuminated by the EM rays are considered to have zero current and effect.

Such PTD methods are effective for large structures that have arbitrary or complex surfaces or structures with poorly reflective surfaces.

For example, PTD can be used to analyze large-reflector antenna radiation patterns and radar cross sections of large aerospace or naval structures based upon their scattering performance. Many modern EM-simulation software suites include corrections to the PTD method to account for creeping waves in shadowed regions, current corrections on edges and corners, and plane-wave basis functions. By compensating in this manner, the software suites increase computational efficiency.

One drawback of the PTD method is the exponential growth of computational requirements due the multiplying num-



ber of reflections. This factor necessitates the use of less physically accurate methods in those scenarios.

Because PTD relies on induced currents, it acts as a bridge between a full-wave solver (such as FEM or MOM) and a non-wave solver (like GTD). GTD, also known as Geometric Optics/Shooting and Bouncing Rays (SBR), employs both the ray-based optical propagation theory and the theory of reflection and refraction. The latter is used to model metallic and dielectric structures that are 10 times larger than the wavelength of interest (*Fig. 3*).

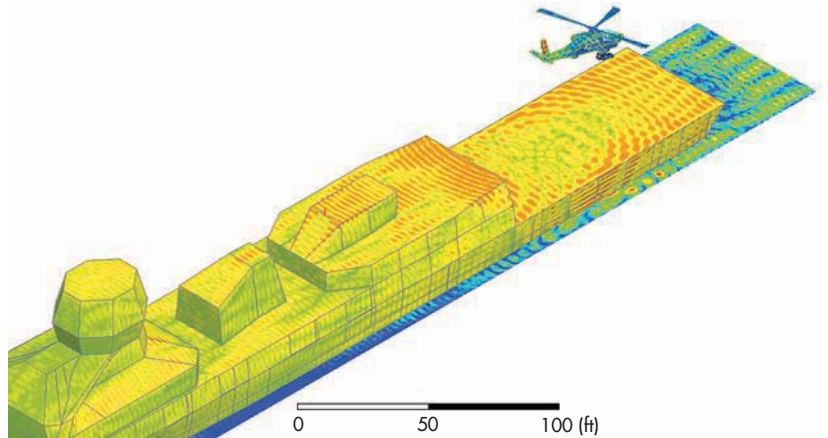
With GTD, the contact point for an object's bouncing ray is calculated for reflection, refraction, and transmission on the material boundaries. This behavior enables the GTD method to respond accurately to multiple layered objects, such as a dielectric-coated metallic surface.

The GTD approach also scales efficiently in response to the resource requirements of complex scattering problems and multiple reflections. Both path and geometric complexity ultimately increase the computational resources needed by the GTD method. To reduce the resource demand, simple primitive shapes will often be used to replace more complex surfaces, such as a rounded cone for the front of an aircraft. When size is the limiting factor computationally, methods like the Uniform Theory of Diffraction (UTD) can be used on simple structures more efficiently than PTD and GTD.

The UTD method uses quasi-optical approximation of near-field EM fields to take advantage of ray diffraction techniques. In doing so, it can estimate the diffraction coefficients of a combination of structure sources. The fields calculated from the phasors, which are generated from the diffraction coefficients, are then combined with incident and reflected fields for a complete field solution. Generally, the UTD method only operates well with structures composed of flat polygons or simple cylinders, where the geometry's edge dimensions are as long or longer than a wavelength.

A lot of the asymptotic methods fail at smaller and more complex structures. Yet many modern EM-simulation software offerings do feature dual simulation, which allows different components of a structure to be simulated with a combination of full-wave and asymptotic methods.

"One strategy is to link between full-wave methods, like FEM or MoM, and asymptotic methods, like PO," notes Matt Commens, lead product manager for HFSS ANSYS, Inc. "This approach can provide the balance between accuracy and rigor with detailed components in terms of size and scalability for platform analysis."

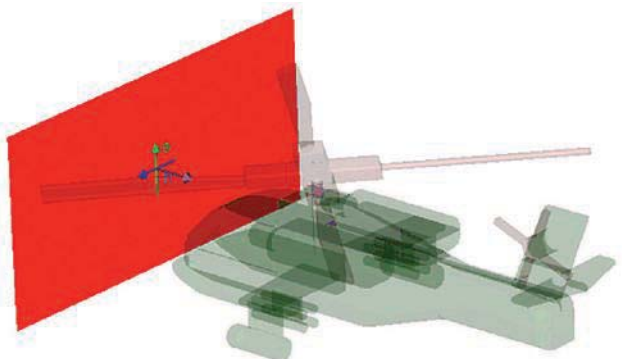


**2. For hard-to-test scenarios, such as a helicopter landing on a floating platform, EM simulation of a large environment can ensure proper operation of the electronic equipment needed for safe landing and vehicle control.**

As long as it has a solving pattern that is similar to the one used by the solutions, this approach allows fields or currents at the boundaries to transfer continuously from one domain to another. An example of a hybrid approach is simulating a complex antenna structure, such as a 3D feed horn, in close proximity to a large metallic object, such as a reflector dish or fuselage.

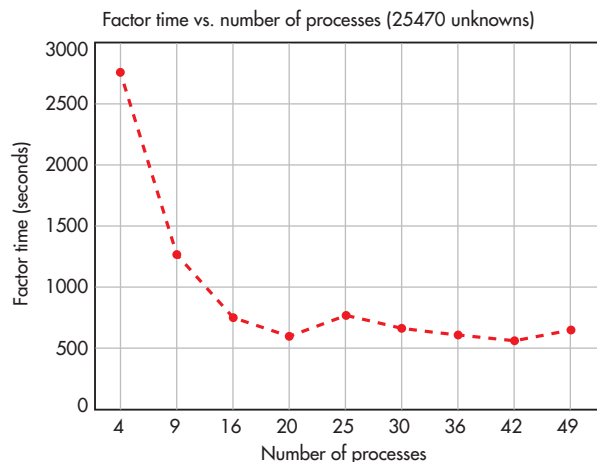
The full-wave solver would operate in the region around the complex structure. In contrast, the asymptotic method would account for the area in between the structures and across the surface of the larger structure.

Hybrid methods are capable of reducing simulation time and resources. Yet the complexity and sheer size of the structures in a simulation are often beyond common computational resources. Here, clever computation and hardware techniques can be used to increase computational capacity. One of these techniques, known as parallel processing, divides the computational effort of a simulation onto multiple cores. This



**3. Structures that are tens to hundreds of times larger than the wavelength can benefit from physical optics and ray-tracing techniques. In less simulation time, these approaches give engineers an idea of the potential radar signatures of various craft.**





**4. Using a bank of paralleled computer processors can reduce simulation times to a fraction of the time needed with a single processor.**

can be done as a division of frequency steps or as a subdivided segment of meshes, known as the Domain Decomposition Method (DDM).

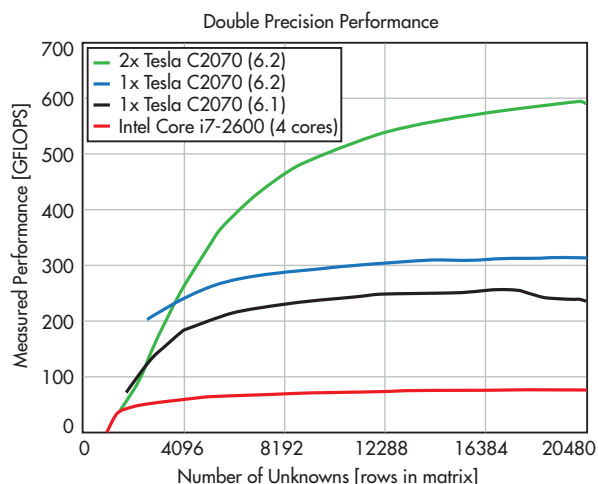
“With modern techniques and hardware, it is not out of the question to solve for the antenna with the platform and even solve for interactions between platforms,” says Comens. “An example of this is a helicopter in close proximity to a ship, where the interaction between antennas is modeled with the finite-element method and the Domain Decomposition Method. A visualization of the surface currents on the helicopter and ship platforms is established by a VHF antenna, which is located on the tail boom of the helicopter.”

These methods require that the EM simulator be specifically designed for parallel processing to have significant efficiency. Inevitably, parallel processing is less than 100% efficient when it comes to dividing computational resources (Fig. 4).

### BEEFING UP PROCESSING

A constant challenge for EM simulations is that the simple computer can only house a finite amount of random-access memory (RAM), storage space, and processing power. Leveraging the power of multiple computers can thus reduce computation time to a small fraction of what would traditionally be needed. Keep in mind that many solver methods require that RAM be scaled as the problem size scales. Given the minimum wavelength of the problem, distributed/shared memory methods also exist.

This approach divides the memory blocks of a simulation into various nodes within a cluster computing system. For many of these multi-node computing systems, a limiting factor of the simulation is the intercommunication capability between the nodes. Some EM-simulation software suites use techniques that enable a node to run relatively autonomously until a solution is produced and the results are aggregated.



**5. Many of the calculations performed with EM simulators involve large-matrix arithmetic and large series of simple arithmetic. As a result, GPUs can be used to substantially increase the processing capability of a machine.**

More recently, the highly specialized and core-abundant processing capability of a graphics-processing unit (GPU) also has been used to provide more processing units for an EM simulation. GPUs are traditionally used to compute massive amounts of parallel data in terms of vectors or matrices for the rendering of graphics and video. Compared to CPUs, they contain less control hardware. In fact, the standard GPU contains anywhere from hundreds to thousands of core processors.

The bulk of computations needed for EM simulations are large numbers of simple arithmetical computations to solve for differential, integral, and matrix systems of equations. As a result, GPUs are well suited to the task—so long as the necessary software exists to support the offloading of the simulation computations onto the GPU (Fig. 5). NVidia is piloting such a software infrastructure for its GPUs, called CUDA, which is being embraced by many simulation software companies.

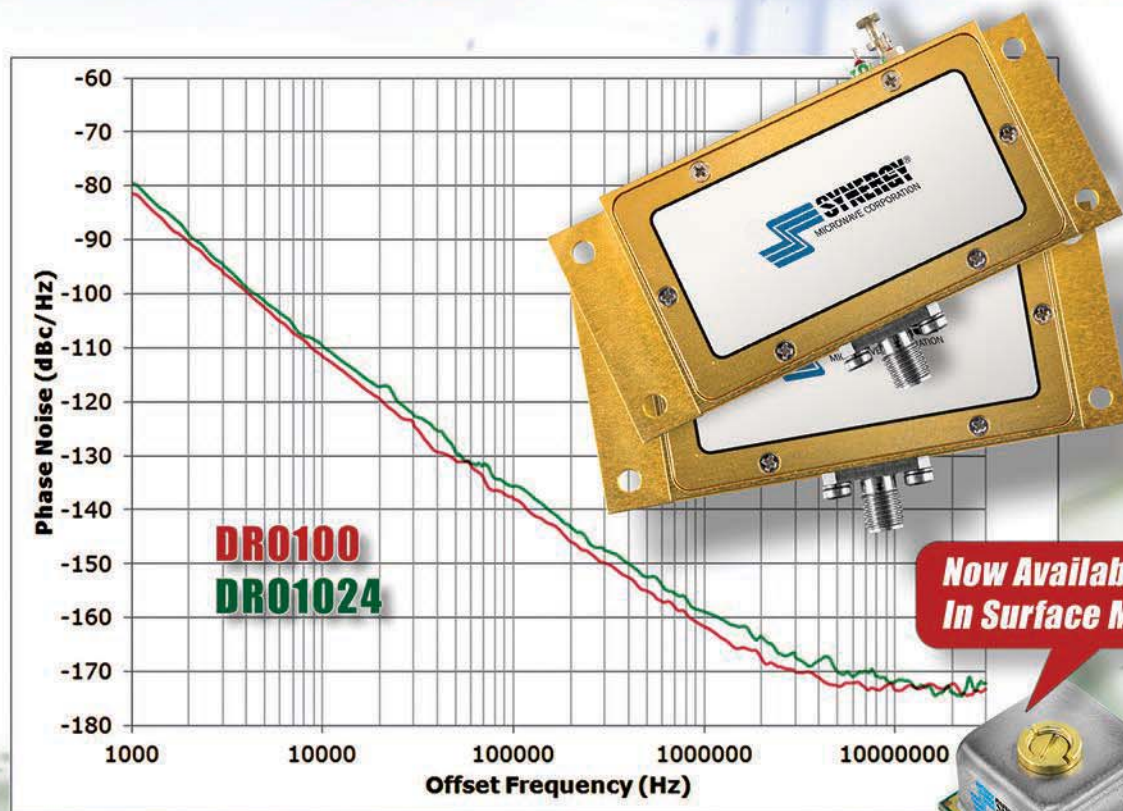
For all of the numerous solutions and offering now available, extremely massive or complex simulations still present a major challenge. The cost is unmanageable to house the necessary computational resources to simulate such structures with sufficient accuracy. The cloud at least offers an alternative to purchasing, setting up, and maintaining a private local computing station.

These services can allow for either the software and hardware or just hardware offloading of resources to distributed computing resources [often known as high-performance computing (HPC)]. Some of these services come equipped with the software pre-installed, which means that just servicing or licensing fees are needed to use the computational resources on a subscription or per-use basis. [ITW](#)

# Exceptional Phase Noise Performance Dielectric Resonator Oscillator

## DR0100 & DR01024

10 GHz 10.24 GHz



Patented Technology

**SDRO Series**

Package Dimensions:  
0.75" x 0.75 x 0.53"

**Now Available  
In Surface Mount!**

## Talk To Us About Your Custom Requirements.



Phone: (973) 881-8800 | Fax: (973) 881-8361  
E-mail: [sales@synergymw.com](mailto:sales@synergymw.com)  
Web: [WWW.SYNERGYMWAVE.COM](http://WWW.SYNERGYMWAVE.COM)  
Mail: 201 McLean Boulevard, Paterson, NJ 07504

# Plastic Packages Reduce Size And Cost For RFICs

Embracing IC plastic packaging for RF components, such as GaN power amplifiers, can cut cost and size while raising integration levels beyond the offerings of traditional packaging technologies.

**IN THE PAST FEW YEARS**, defense budgets have dropped, impacting military spending on RF/microwave technology. To satisfy the resulting performance and cost demands, new RF integrated-circuit (RFIC) technologies with superior performance and cost structures were developed. For example, transistor technology based on gallium nitride (GaN) has driven a rise in amplifier frequency, bandwidth, and efficiency.

As a result, industries outside of defense and aerospace, such as telecom and satcom, are beginning to hop on the GaN bandwagon. For these industries, though, cost remains a critical factor. By relying on plastic processes, GaN manufacturers hope to keep cost low while delivering all the benefits of GaN solutions.

For instance, in order to drop the price of GaN transistors for a wider market, developers of the technology have looked to replicate the success of silicon-based integrated-circuit (IC) technologies. Of course, some challenges must be overcome.

“The integration levels and coupling of digital functionality for calibration and digital signal processing will continue to be the major hurdles to overcome to realize future requirements,” explains Duncan Bosworth, director of marketing and applications for Analog Devices’ Aerospace and Defense Business. “Ever-more digital functionality will rely on ever-finer device geometries. But probably the biggest challenge is in determining the correct specifications for commercial-off-the-shelf (COTS) devices targeting multiple markets and applications.”

To tackle these diverse issues, a high-volume, low-cost, highly integrated, and common-material approach is needed. GaN-in-plastic processes use the already developed infrastructure and technology of plastic packaging over ceramic packaging. This approach has already been embraced to lower costs for the telecom industry

and budget-strapped military by some of the leading RF/microwave device manufacturers. Examples include Cree, Freescale, Hittite, MACOM, NXP, and Qorvo.

A concern remains as to whether the switch to plastic packaging compromises a device’s performance compared to traditional packaging methods. Based on the number of new power amplifiers (PAs) being released in plastic packages, the advantage might be on plastic’s side (*Fig. 1*). “There is no discernible performance degradation with plastic packaging up to about 4 GHz,” says Chris Hermanson, packaging engineer for Cree. “Several industries are adopting plastic packaging for RFICs—namely telecommunications, radar, and ISM.”

With some devices, the switch to plastic could mean a price drop of almost 50% versus ceramic packages with no loss to performance. The plastics used in these packages are generally thermoset polymers. When employed in mold compounds, they contain mostly glass/quartz filler and polymer resins. Under the heat and pressure of a mold, the material develops crosslinks during polymerization.

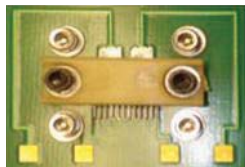
The resulting material is rather rugged and dimensionally stable over a wide operating-temperature range. Often, the material composition is designed to match the coefficient-of-thermal-expansion characteristics of printed-circuit-board (PCB) materials, with the goal of increasing long-term product reliability.

Packages made from this process are either overmolded or air-cavity plastic packages. They are a standard part of many of today’s mainstream IC manufacturing processes and testing.

Beyond cost, however, the thermal density of GaN devices raises significant concerns around heatsinking and temperature stability. Hermanson notes, “One of the main focus areas for developing plastic packages for RFICs is plastics with higher temperature capability.” As it turns out, plas-

**1. GaN PAs can be packaged in plastic in much the same way as they were packaged in previous ceramic technologies. Yet they benefit from more reduced sizes.**

(Courtesy of Freescale)





# Go wide.

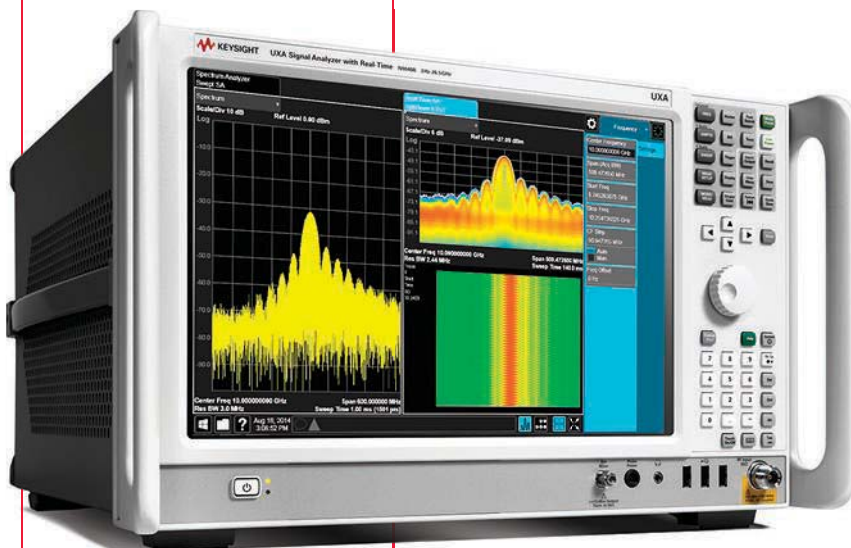
## Keysight UXA Signal Analyzer

510 MHz real-time analysis bandwidth

>75 dBc full-band spurious-free dynamic range

-136 dBc/Hz phase noise at 1 GHz, 10 kHz offset

14.1" capacitive touchscreen with streamlined UI



# Go deep.

The new UXA is the world's highest performing wideband signal analyzer. With real-time analysis bandwidth to 510 MHz and impressive phase noise, the UXA will give you the wide, deep views and performance headroom you need to troubleshoot hidden design problems. You can also simplify your measurement setup through an easy-to-use menu optimized for touch. Prove what your design can do. Get the UXA and see the real performance.

View our demo video and download an app note at [www.keysight.com/find/newUXA](http://www.keysight.com/find/newUXA)



USA: 800 829 4444  
CAN: 877 894 4414

Scan to view video demo.

 **KEYSIGHT**  
TECHNOLOGIES

Unlocking Measurement Insights

© Keysight Technologies, Inc. 2014

Agilent's Electronic Measurement Group has become **Keysight Technologies**.

tic packages can make use of copper-alloy lead frames, which actually offer heat-removal advantages over ceramic packages. Because the lead frames of ceramic packages must be matched to the relatively brittle ceramic material, the coefficients of thermal expansion (CTEs) of the materials are often not well matched to the PCB substrate. This aspect reduces long-term reliability and requires specialized alloys for ceramic packages.

As a product of these factors, GaN high-electron mobility transistors (HEMTs) in plastic packages have come to market offering power to 300 W to nearly 4 GHz. They commonly exhibit PA efficiency (PAE) as high as 70% across an instantaneous bandwidth into the gigahertz. Many of the transistors available today operate at 50-V drain bias conditions, which lower currents and shrinks the necessary size of the metallization through the signal path.

"In general, similar design techniques are employed with both ceramic and plastic package development," says Hermanson. "A lot of the complexity of the package parasitic design is in the wire-bonds, which require EM simulation no matter the medium...Plastic packages are much cheaper due to their fundamental construction."

Additionally, the higher voltage enables higher-impedance broadband-matching networks, which leads to smaller part sizes and lower device parasitics. For example, flanged ceramic packages typically require manual assembly. The larger leads tend to have lower impedances, which require larger passive components and are more difficult to match.

Given the small size of GaN-in-plastic transistors, they also can be designed for precision surface-mount assembly in fully matched integrated modules (Fig. 2). This capability further reduces size while increasing efficiency and lowering costs. Utilizing standard surface-mount-technology (SMT) packages and techniques enables commercial high-volume manufacturing and the resulting benefits of lower costs, component count, and ultimately higher yields.

Beyond these packaging gains, development has been ongoing to solve many of the manufacturing and reliability challenges of GaN-on-silicon (GaN-on-Si) transistors. An outcome of these efforts is the development of GaN on silicon carbide (SiC). However, because SiC is a rugged material, wafer-size limitations and the cost of SiC limit the economy-of-scale savings and automation of other IC technologies, such as silicon.

With the fabrication challenges of CTE mismatch and thermal management between GaN and Si solved, a GaN-on-Si

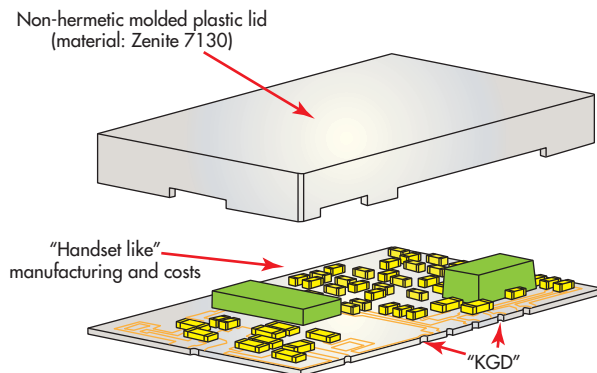
process could enable GaN transistors on wafer sizes to 8 in. This innovation would drastically reduce the cost of GaN devices while enhancing the integration of CMOS technology alongside the RF circuitry.

### MILITARY USES COMMERCIAL TACTICS

Commercial manufacturing methods specialize in providing increased reliability and reduced maintenance costs over time. Many new military initiatives may benefit from this modular device approach with the GaN developments currently being witnessed. The challenge would lie in developing GaN in plastic packages that could operate at higher frequencies with comparable performance to ceramic.

For example, modern radar is often based on antenna arrays, which require hundreds to thousands of transistors, switches, and phase-control components/modules. Using traditional methods, these radars are expensive and very difficult to upgrade. Modern SMT module approaches could render the production of array radars to an automated process with easily upgraded or repaired modular components.

The level of integration offered by GaN in plastic technologies also could reduce RF tactical module sizes and costs, allowing the military to produce smaller airborne systems with lower unit costs. This capability would aid the military's goal to field more capable drones and technologies that can reduce the effectiveness of an opponent's electronic assets. Such approaches also require



**2. Plastic packaging enables integration techniques that can transform multi-stage power modules into cost-effective, chip-sized components.** (Courtesy of MACOM)

more sophisticated tactical communications networks.

Here, for example, military LTE networks could use the same components as a commercial cell-based network with the added benefit of rapid network deployment enabled by airborne cellular sites. As budgets continue to tighten, there is a growing need to adopt lower-cost and more modular technology approaches for RF devices. This trend is putting pressure on RF power-device manufacturers to embrace commercial techniques without sacrificing performance.

For RFICs, GaN-in-plastic package technology is just the first step toward much higher integration and the utilization of proven commercial manufacturing processes. Innovations will overcome the material and fabrication challenges stemming from GaN-on-Si and high-power and high-frequency plastic packages. As those solutions evolve, more industries adopt these technologies to enable the next generation of telecommunications and tactical systems. **mw**

# Enhanced, Expanded, Perfected. Powerfilm™ attenuators go further.

The most important thing we build is trust

**COBHAM**

Inspired by original designs produced by Aeroflex / KDI decades ago, new Powerfilm surface-mount attenuators from Cobham Inmet are now produced in our new USA facility, and enhanced to include even more attenuation range and power than ever before. Employing a proprietary, highly reliable thick/thin film processing approach, these devices are optimized for your high-power signal conditioning, leveling, gain optimization and matching network challenges.

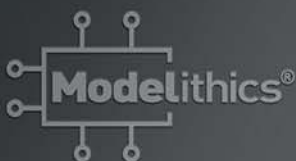
- Frequency Performance up to 18 GHz
- Attenuation Ranges up to 20 dB
- Power Ranges up to 100 Watts

They're easily designed-in, are readily available, and are priced competitively. Visit our website for detailed specifications.

## Cobham Inmet

888-244-6638

[www.cobham.com/Inmet](http://www.cobham.com/Inmet)



Start designing today with Modelithics Global Models™

Scalable equivalent circuit models and S-parameter data are available at **Modelithics.com**, in the simulator libraries of Agilent's ADS and Genesys software, and in AWR's Microwave Office suite.



*Cobham Inmet formerly Aeroflex / Inmet*



# Limiters Protect ADCs without Adding Harmonics

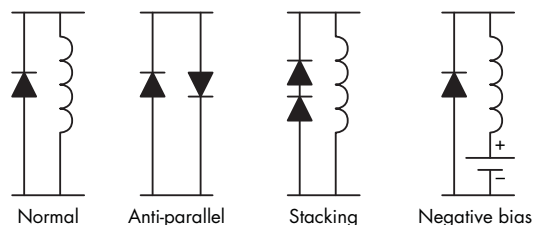
This experiment seeks to find a diode limiter that can protect high-speed ADCs from high-level overload signals while at the same minimize the amount of second-harmonic signals produced.

Modern receivers often use high-speed analog-to-digital converters (ADCs) to sample signals at intermediate frequencies (IFs) or even at radio frequencies (RFs), such as software-defined-radio (SDR) receivers.<sup>1</sup> However, the amplitude of an incoming signal may exceed an ADC's maximum permissible input level during large-signal conditions. To avoid damaging or degrading the ADC, amplitude limiting is necessary. While automatic-gain-control (AGC) circuitry can be effective for controlling IF amplitude excursion in traditional single-carrier systems, it is not desirable in modern multicarrier applications.<sup>2</sup>

One solution is to cap the IF amplitude excursion with a limiter. Unfortunately, it creates a new problem: The strong nonlinearity that is required of a good limiter also makes it an efficient generator of harmonics. The lower-order harmonics, especially second-harmonic signals, are particularly troublesome because they can fall inside the passband of a wideband ADC. ADC protection based on clamping with positive-negative (PN) or Schottky diodes are less linear than limiting with PIN diodes.

To minimize second-harmonic production in a PIN diode limiter, the authors investigated several circuit configurations and diode intrinsic-layer heights. The experimental results of those investigations, along with some proposed solutions and their tradeoffs, are presented here.

A number of different limiter circuit configurations are commonly used for protection purposes. The classic self-biased limiter configuration comprises a diode and a choke shunting a transmission line.<sup>3</sup> The choke serves as the



1. A number of different configurations were evaluated to find the most effective means of second-harmonic cancellation.

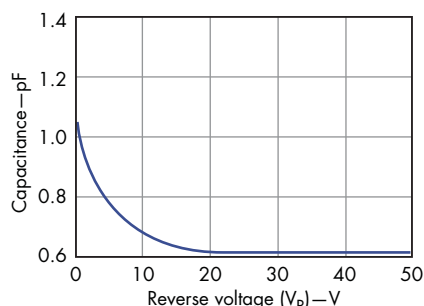
DC return in the diode's RF detector role. In the absence of a signal, the choke also discharges the charge stored in the diode and the DC blocking capacitors (Fig. 1).

Under small-signal conditions—i.e., below the limiting threshold—the rectified current is insufficient to lower the diode junction resistance. As a result, the diode appears as a capacitance shunted by a large resistance. The diode can be characterized by a dielectric relaxation frequency ( $f_{DR}$ ), which is given by:

$$f_{DR} = 0.5\pi\rho\epsilon$$

where:

$\rho$  = the intrinsic (I) layer bulk resistivity, and  
 $\epsilon = 1 \times 10^{-12}$  F/cm



2. The junction capacitance versus reverse voltage (C-V) of a 1.5- $\mu$ m PIN diode was measured at 1 MHz.

This capacitance varies inversely with the applied voltage (Fig. 2). An RF voltage can modulate this junction capacitance to produce distortion through the varactor effect. Since capacitive reactance decreases

with increasing frequency, the distortion becomes worse with increasing frequency—i.e., in the opposite direction to the forward-biased condition.<sup>4</sup>

Another diode limiter configuration, the anti-parallel configuration, is the basis of the bidirectional clamp<sup>5,6</sup> and the subharmonic mixer,<sup>7</sup> both of which use Schottky diodes. Since the even-order distortion generated by each diode will have opposite polarities, self-cancellation will occur to the extent that the diodes are matched. An anti-parallel configuration can be adapted with PIN diodes to reduce limiter distortion, with a bonus feature of the anti-parallel configuration being that it doesn't need a choke for the DC return.

A third diode limiter configuration—the stacked configuration—reduces the overall capacitance, because the two diodes are connected in series. An alternative explanation is that the voltage across each diode is halved compared to a single diode. Stacking has been successfully used to reduce distortion in field-effect-transistor (FET) attenuators.<sup>8,9</sup> Yet it remains to be seen if diode stacking can improve limiter linearity.

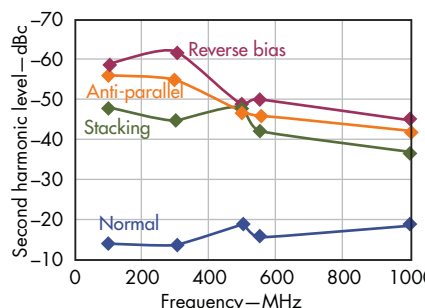
Reverse-bias ( $V_r$ ) techniques have been shown to reduce distortion in PIN diode switches,<sup>4</sup> and the mechanism is attributed to the negative bias preventing RF rectification.<sup>10</sup> Reverse-bias techniques also widen the diode's depletion zone. It is conceivable that the reduced junction capacitance is partly responsible for the improvement in linearity. Determining whether this method is the optimum means of reducing limiter distortion is a matter of sizing up the different diode limiter approaches.

Self-biased limiters typically use very thin PIN diodes in the 1- to 7- $\mu\text{m}$  range<sup>11</sup> because of their low turn-on thresholds. The 1.5- $\mu\text{m}$  PIN diode,<sup>12</sup> which forms the bulk of this work, has about a +10-dBm threshold.<sup>13</sup> But the thin diode's current-voltage (C-V) profile, which changes very abruptly around 0 VDC (Fig. 2), increases its susceptibility to varactor modulation.

On the other hand, thick diodes (e.g., 22.5  $\mu\text{m}$ ), have much flatter



**3. All the candidate solutions are evaluated using this common PCB test platform.**



**4. When fabricated using similar 1.5- $\mu\text{m}$  diodes, stacking, anti-parallel, and reverse biasing yield lower harmonic levels than the normal configuration.**

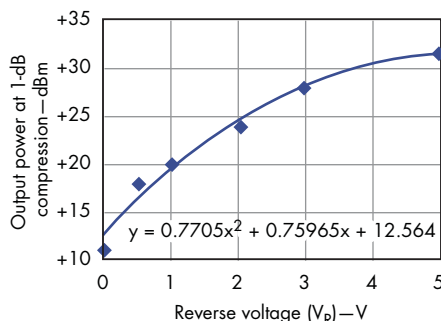
serves as the ground plane. The measurement reference planes were where the circuit board's SMA connectors interface with the coaxial cables that link the test board's signals to the test equipment.

Modification of a standard limiter circuit can reduce distortion by 18 to 30 dB. Below 500 MHz, more than 30-dB improvement can be achieved (Fig. 4). The greatest improvement was seen in the reverse-biased limiter (with  $V_r = 1$  V), followed by the anti-parallel configuration, and then the stacked configuration.

The harmonic distortion levels of these three candidate solutions become worse at higher frequencies in accordance with the theory of unbiased PIN diodes.

On the other hand, the distortion in the normal limiter diode configuration exhibits the opposite trend of improving with frequency—i.e., this configuration's turn-on threshold is equal to the test signal and therefore its diode is forward-biased.

Even though harmonic suppression increases with the reverse-voltage magnitude, values higher than 1 V are not viable because the threshold



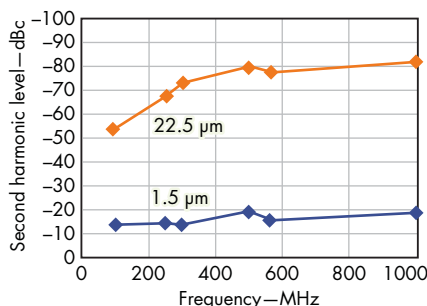
**5. Although harmonic suppression improves with the reverse voltage magnitude,  $V_r$ , a corresponding increase in the limiting threshold (the output power at 1-dB compression) caps the usable  $V_r$  value to  $\leq 1$  V.**

### COMPARING TURN-ON THRESHOLDS (POWER AT 1 dB) AT 900 MHz FOR DIFFERENT DIODE HEIGHTS AND CONFIGURATIONS

Diode height ( $\mu\text{m}$ )	Limiter configuration	Output power at 1-dB compression (dBm)
1.5	Normal	+10
1.5	Anti-parallel	+10
1.5	Stacked	+20
1.5	Reverse biased (1 V)	+20
22.5	Normal	>+30

is increased exponentially (Fig. 5). Since the diode capacitance changes very little between 0 and 1 V (Fig. 2), the distortion improvement is more likely due to the reverse bias preventing RF rectification. Stacking also raises the original +10 dBm threshold to about +20 dBm. Of all the evaluated solutions, only the anti-parallel arrangement does not increase the limiting threshold.

A thicker PIN diode can also reduce limiter distortion. Replacing the original 1.5- $\mu\text{m}$ -thick diode with a 22.5  $\mu\text{m}$  diode<sup>14</sup> lowers the second harmonic distortion by 40 to 60 dB in the evaluated frequency range (Fig. 6). The thick diode's distortion reduces with frequency before leveling off above about 500 MHz; this inflection point coincides with the dielectric relaxation frequency ( $f_{\text{DR}}$ ).



6. A 22.5- $\mu\text{m}$  diode reduces second-harmonic distortion by more than 40 dB versus over a conventional 1.5- $\mu\text{m}$  diode.

“A thicker PIN diode can also reduce limiter distortion. Replacing the original 1.5- $\mu\text{m}$ -thick diode with a 22.5- $\mu\text{m}$  diode lowers the second harmonic distortion by 40 to 60 dB in the evaluated frequency range.”

As predicted earlier, the 22.5- $\mu\text{m}$  diode limiter has an unusually high limiting threshold of >+30 dBm (see table). One possible way to achieve a more reasonable threshold with the 22.5- $\mu\text{m}$  diode is to utilize it in a quasi-active DC-driven limiter.<sup>15</sup> Instead of depending on RF rectification for the bias

current, the quasi-active DC-driven limiter sources the current through a DC amplifier (Fig. 7). Thereafter, the limiting threshold can be varied by changing the DC amplifier's gain.

On the downside, this configuration incurs much more space and cost than the self-biased limiter. Alternatively, if the ADC has an overflow indicator output, it can be used to drive the DC amplifier directly, thus saving on a detector and a coupler.

To evaluate the harmonic levels of these different diode limiter candi-

## Waveguide Components

OFF-THE-SHELF OR CUSTOM DESIGNS

• Attenuators • Couplers • Switches • Loads • Terminations • Adapters • Assemblies • Horns • Ferrite Components



# We're Ready When You Are... Next Day Delivery Of Catalog Components

From The Largest Inventory Of Waveguide Components In The Industry  
**RECTANGULAR, MM-WAVE, & DOUBLE-RIDGED COMPONENTS**

### CUSTOM DESIGNS

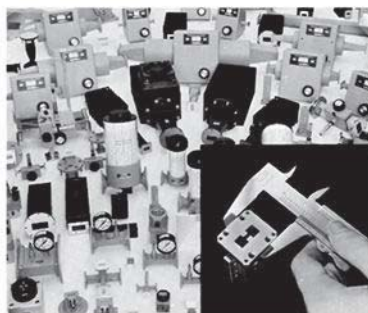
Custom designs are a Waveline specialty. If you don't see the product or design in our catalog, we probably have your "special" in our design files. Waveline now offers a complete line of Pin Diode Switches, Attenuators & Phase Shifters. Waveline has the expertise and capabilities to integrate waveguide and solid-state designs for subassemblies.

CALL OR WRITE

**waveline**

P.O. Box 718, West Caldwell, NJ 07006  
(973) 226-9100 Fax: 973-226-1565

E-mail: [wavelineinc.com](mailto:wavelineinc.com)





# USB & ETHERNET RF SWITCH MATRIX



DC to 18 GHz from **\$385** ea.

We're adding more models and more functionality to our line of RF switch matrices. All models now feature switch cycle counting with automatic calibration interval alerts based on actual usage, an industry first! This function improves test reliability and saves you money. Our new RC-series models feature both USB and Ethernet control, so you can run your test setup from anywhere in the world! Rugged aluminum cases on all models house our patented mechanical switches with extra-long life of 10 years/100 million cycles of guaranteed performance!\*

Our easy-to-install, easy-to-use GUI will have you up and running in minutes for step-by-step control, full automation, or remote operation. They're fully compatible with most third-party lab software,† adding capabilities and efficiency to existing setups with ease! Visit [minicircuits.com](http://minicircuits.com) today for technical specifications, performance data, quantity pricing, and real time availability – or call us to discuss your custom programming needs – and think how much time and money you can save!

## USB Control Switch Matrices

Model	# Switches (SPDT)	IL (dB)	VSWR (:1)	Isolation (dB)	RF P <sub>MAX</sub> (W)	Price \$ (Qty. 1-9)
<b>NEW</b> USB-1SP4T-A18	1 (SP4T)	0.25	1.2	85	2	795.00
USB-1SPDT-A18	1	0.25	1.2	85	10	385.00
USB-2SPDT-A18	2	0.25	1.2	85	10	685.00
USB-3SPDT-A18	3	0.25	1.2	85	10	980.00
USB-4SPDT-A18	4	0.25	1.2	85	10	1180.00
USB-8SPDT-A18	8	0.25	1.2	85	10	2495.00

## **NEW** USB and Ethernet Control Switch Matrices

Model	# Switches (SPDT)	IL (dB)	VSWR (:1)	Isolation (dB)	RF P <sub>MAX</sub> (W)	Price \$ (Qty. 1-9)
RC-1SP4T-A18	1 (SP4T)	0.25	1.2	85	2	895.00
RC-2SP4T-A18	2 (SP4T)	0.25	1.2	85	2	2195.00
RC-1SPDT-A18	1	0.25	1.2	85	10	485.00
RC-2SPDT-A18	2	0.25	1.2	85	10	785.00
RC-3SPDT-A18	3	0.25	1.2	85	10	1080.00
RC-4SPDT-A18	4	0.25	1.2	85	10	1280.00
RC-8SPDT-A18	8	0.25	1.2	85	10	2595.00

\*The mechanical switches within each model are offered with an optional 10 year extended warranty. Agreement required. See data sheets on our website for terms and conditions. Switches protected by US patents 5,272,458; 6,650,210; 6,414,577; 7,633,361; 7,843,289; and additional patents pending.

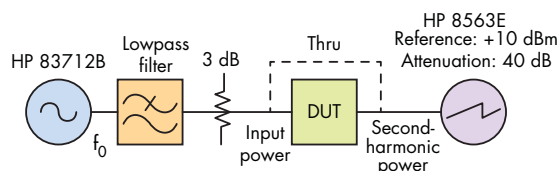
†See data sheet for a full list of compatible software.

**NEW  
FEATURE  
SWITCH  
CYCLE  
COUNTING**

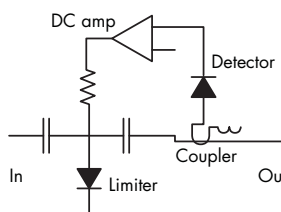


dates, a special test setup was assembled with the capability of measuring low-level signals (Fig. 8). Most commercial signal generators offer second-harmonic levels of around  $-30$  dBc. Since almost all of the limiters being evaluated would produce harmonic signal levels of less than the test signal generator being used in the experiments (a model 83712B from Hewlett-Packard Co.), low-pass filters were required to clean up the test signals.

Different low-pass filters were needed for each test frequency. An attenuator pad at the input of the device under test



8. This test setup was used for measurement of weak ( $-30$  dBc) second-harmonic levels.



7. A quasi-active DC-driven limiter can enable a usable limiting threshold with a  $22.5\text{-}\mu\text{m}$  PIN diode.

(DUT) buffers against mismatches when a limiter is turned on (ideally, an isolator could be used if available for each test frequency). To present the spectrum analyzer in the test setup from being overdriven, its attenuator is set to a relatively large value (30 to 40 dB). In order to verify that the test setup's residual harmonic level is lower than that of a DUT, the DUT is initially replaced by the "THRU" connection when making measurements.

The low-distortion limiter required by wideband ADCs can be realized by modifying the circuit configuration or the diodes' physical attribute. Stacking, anti-parallel, and reverse-biasing of limiter circuits can reduce the second-harmonic amplitude by tens of decibels over conventional limiter configurations. Selecting a thicker diode can also significantly reduce distortion, but this requires additional circuits to enable limiting at reasonable input-power levels.

With the exception of the anti-parallel configuration, all the other solutions suffer from higher turn-on threshold voltages. Hence, the latter approach is the most cost-effective solution. **mtw**

## ACKNOWLEDGMENT

The author wishes to thank Raymond W. Waugh for designing the test PCB.

## REFERENCES

1. P. Cruz, N.B. Carvalho, and K.A. Remley, "Designing and testing software-defined radios," IEEE Microwave Magazine, June 2010, pp. 83-94.
2. B. Brannon and B. Schofield, "Multicarrier WCDMA Feasibility," Analog Devices, Application Note AN-807, 2006, www.analog.com.
3. K.C. Gupta, "Microwave Control Circuits," in Microwave Solid-State Circuit Design, 2nd ed., I. Bahl and P. Bhartia, Eds., Wiley, Hoboken, NJ, 2003, pp. 682-683.
4. R.H. Caverly and G. Hiller, "Distortion in Microwave and RF Switches by Reverse Biased PIN Diodes," 1989 MTT-S International Microwave Symposium Digest, pp. 1073-1076.
5. R.W. Waugh, "Schottky diodes solve digital circuit problems," Hewlett-Packard Co., design tip, January 1999, www.hp.woodshot.com.
6. Avago Technologies, application note, "Non-RF applications for the surface mount Schottky diode pairs HSMS-2802 and HSMS-2822," www.avagotech.com.
7. M.V. Schneider Jr. and W.W. Snell, "Harmonically Pumped Stripline Down-Converter," MTT-S Transactions of Theory & Techniques, Vol. MTT-23, No. 3, March 1975, pp. 271-275.
8. D.R. Webster, M.T. Hutabarat, D.G. Haigh, and A.E. Parker, "Designing Low Distortion Continuously Variable Attenuators for Microwave Frequencies," IEEE Colloquium on Low Power IC Design, January 2001.
9. M. Granger-Jones, B. Nelson, and E. Franzwa, "A broadband high dynamic range voltage controlled attenuator MMIC with IIP3 > +47dBm over entire 30-dB analog control range," Proceedings of the 2011 IEEE Microwave Symposium, 2011.
10. L. Drozdovskaia, "Frequency properties of a reverse biased thick switching PIN diode," Applied Microwave & Wireless, February 2002, pp. 106-114.
11. Skyworks Solutions, datasheet, "Limiter diodes," www.skyworksin.com.
12. Avago Technologies, product specification, "HSMP-382x series and HSMP-482x series," www.avagotech.com.
13. Avago Technologies, application note 1050, "Low cost surface mount power limiters," 1999, www.avagotech.com.
14. Avago Technologies, product specification, "HSMP-386x series," www.avagotech.com.
15. Alpha Industries, application note 80300, "Characteristics of semiconductor limiter diodes."

## PMR Common Platform Processor

Delivering digital FDMA/TDMA PMR/LMR and legacy analogue

**Function Image™ 7241/7341FI-1.x - Available Now**  
Automatic Digital/Analogue Detection

- dPMR™ Mode 1/2/3
  - AI Physical Layer 1
  - AI Data Link Layer 2
  - Packet data
  - Vocoder support
- Analogue PMR/LMR
  - Complete Voice Processing
  - Sub-audio Signalling
  - Audio-band Signalling
  - FFSK/MSK MPT1327 Support

**Function Image™ Roadmap - DMR, NXDN™, PDT**

**CML Microcircuits**  
COMMUNICATIONS SEMICONDUCTORS

Search Online 'CMX7241 or CMX7341'  
Visit [www.cmlmicro.com](http://www.cmlmicro.com) for further information

A CML Microsystems Plc Company



# Routing. Conditioning. Streamlined.

The most important thing we build is trust

# COBHAM

One perfectly integrated, dependable signal routing and conditioning box. That's your goal. That's Cobham Weinschel's promise. And that's why defense programs such as JSF, SSEE, JTRS, GMR, and EPLARS have put their faith in us. Our subsystems are easy to control and configure and perform various duties as:

- Antenna Interface and Control Units
- RF Distribution and Interface Units
- Fading Simulators
- Attenuators and Switch Matrices

Features include high port-to-port isolation, low phase noise, dynamic ranges up to 95 dB, and high power capability through 40 GHz.

From ATE to EW, we have the answers. Call us.

**Cobham Weinschel**

888-244-6638

[www.cobham.com/Weinschel](http://www.cobham.com/Weinschel)



*Cobham Weinschel formerly Aeroflex / Weinschel*





## Design Feature

CHANG-ZE LI | Doctor  
School of Air and Missile Defense, Air Force Engineering University,  
Xi'an, Shanxi, 710051, People's Republic of China; e-mail:  
babelun\_2003@163.com

CHUANG-MING TONG | Professor  
School of Air and Missile Defense, Air Force Engineering University, Xi'an,  
Shanxi, 710051, People's Republic of China  
State Key Laboratory of Millimeter Waves, Nanjing 210096, People's  
Republic of China; e-mail: chmtong@126.com

LI-HUI QI | Doctor  
Office of PLA in 786 Factory, Xi'an, Shanxi, 710051, People's Republic of  
China; e-mail: qh101@126.com

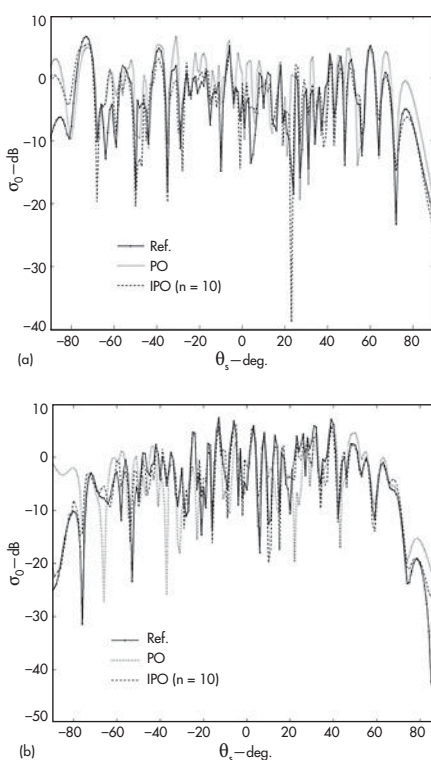
MINGYANG JI | Master  
School of Air and Missile Defense, Air Force Engineering University,  
Xi'an, Shanxi, 710051, People's Republic of China; e-mail: jiming-  
yang602@163.com

# Model Depicts EM from Rough Surfaces

Predicting the scattering of electromagnetic radiation from rough surfaces can provide invaluable data for radar and other systems that must process such target information.

Gauging electromagnetic (EM) scattering from rough surfaces is of great interest for a number of fields, including for remote sensing and interpreting remote radar signals. EM wave scattering has been studied for some time, especially with the development of radar and sonar systems.<sup>1-3</sup> Generally, there are two means of obtaining radar data from rough surfaces: by experimental engineering and through computer simulation. Engineering can be expensive, however, and depends mostly on the environment and the radar devices.

Computer simulation can provide radar echoes for cases where experimental studies are scarce and expensive. Rough surfaces can be extremely complex with their random geometries, even on a large scale, encouraging the use of cost-effective computer simulations for a better understanding of the EM scattering effects. EM multipath effects at low grazing angles (LGAs) can make even numerical simulation difficult. This, in turn, poses a challenge in terms of effectively simulating radar echoes from rough surfaces for acceptable costs.



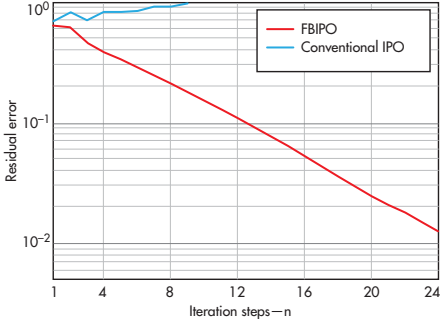
**1. The curves show the validity of the IPO approach for studying Gaussian rough surfaces, both for (a) HH polarization and (b) VV polarization.**

For the case where  $\lambda$  represents EM wavelength, a large-scale rough surface may be on a scale of  $10,000\lambda^2$  or more,<sup>4</sup> a considerable computational challenge for a simulation. Generally, such problems entail two kinds of computational methods: analytical and numerical. For numerical methods, such as the method of moments (MoM)<sup>5</sup> and the multilevel fast multipole algorithm (MLFMA),<sup>6</sup> rigorous results can be obtained under certain computational costs. However, such methods are limited to solving large-scale scattering problems.

Conventional analytical methods, like Kirchhoff's approximation (KA)<sup>7</sup> and the small perturbation method (SPM),<sup>8</sup> can provide reasonable results with low computational costs, albeit with some conditions. For example, these methods work best for moderate incident angles of an EM wave or a small amount of roughness for the rough surface. For composite scattering problems from rough surfaces, analytical methods are often used for solutions. Computational

precision is more important than cost in many cases.

The use of iterative physical optics (IPO)<sup>9</sup> is one means of extending the validity of Kirchhoff's approximation; this



**2. This depicts a convergence comparison for the two iteration methods.**

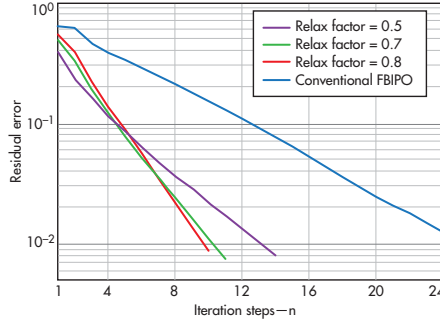
approach can deal with the rougher surface, such as the wind-driven Pierson-Moskowitz (P-M) variety,<sup>10</sup> rather than one that is unrealistic or simplified. Also, a forward-backward methodology (FB)<sup>11</sup> and its modification with an under-relaxation iteration method will be employed to improve the convergence and robustness of this analysis.

Thirdly, based on the scattering characteristics of a rough surface, the far-field approximation (FaFFA)<sup>12</sup> and local iteration methodology<sup>13</sup> are proposed to reduce the computational complexity and further improve the efficiency of the whole iteration process. Hence, this model for analyzing EM scattering from rough surfaces can greatly reduce the computational costs, including both the amount of computer random-access memory (RAM) and central-processing-unit (CPU) time required.

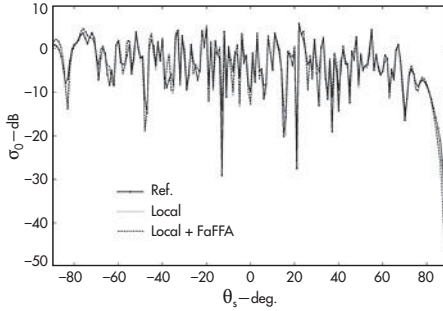
Analyzing the scattering problems of rough surfaces is usually considered as a large-scale scattering problem, such as related to  $10,000\lambda^2$ .<sup>4</sup> It is usually more feasible to solve such problems by means of analytical methods than numerical methods. Many researchers are focused on the use of Kirchoff approximation (KA) in such cases, also known as the use of physical optics.

The surface of the sea is considered a good typical rough surface for the current study, with seawater a finite conductivity media in a realistic engineering application. According to Huygens' principle, the volume-induced current can be changed to the equivalent surface current. The electric surface current,  $J_s$ , and the equivalent magnetic surface current,  $M_s$ , must both be considered. When the curvature radius,  $\rho$ , of the rough surface satisfies  $\rho \gg \lambda$ , the tangent plane approximation is valid so that the diffraction and multipath scattering of the rough surface can be ignored. The induced currents ( $J_s$ ,  $M_s$ ) can be solved by Fresnel's equations<sup>14</sup> under the computational costs of order  $O(N)$ , where  $N$  is an unknown number.

A trapezoidal integration rule is used with a sampling density of  $16 \text{ points}/\lambda^2$  (in contrast to 100 points or patches/ $\lambda^2$  for



**3. This is a convergence comparison for the under-relaxation iteration.**



**4. Shown is a comparison of the different acceleration techniques.**

the sea water while  $\mathbf{n}'$  denotes the outer normal vector of the scattering surface. For a frequency of 1.25 GHz, temperature of  $+20^\circ\text{C}$ , and salinity of 32.54%, the relative permittivity,  $\epsilon_r$ , is  $72.64 + j69.36$  with  $Z_s$  of  $34.92 - j13.99$  [with  $j = -(-1)^{0.5}$ ].

The magnetic-field integral equation (MFIE) is used as the basis for computing the IPO. Considering the iteration process in the  $n$ th iteration step, the MFIE with  $J_s$  and  $M_s$  can be written as:

$$J_s^{(n+1)} = 2\hat{\mathbf{n}} \times \mathbf{H}^i + 2\hat{\mathbf{n}} \times \int_{S_s} \left\{ -\frac{jk}{\eta_0} [M_s^{(n)} + \frac{1}{k^2} \nabla' \cdot M_s^{(n)} \nabla] G - J_s^{(n)} \times \nabla G \right\} ds' \quad (1)$$

where  $\mathbf{H}_i$  represents the incident magnetic field. For the induced electric current, the initial value can be obtained by the physical optical current on the surface excited by the incident fields. Defining the interaction error,  $\xi_s$ , in the  $n$ th iteration step, is as shown in Eq. 2:

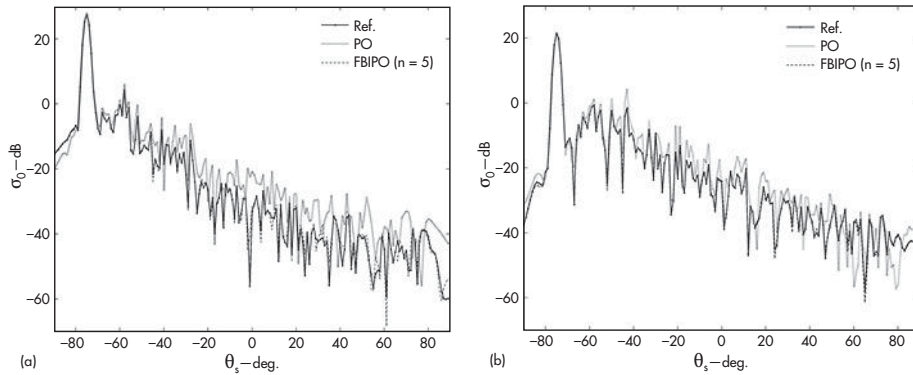
$$\xi_s^{(n)} = \frac{|J_s^{(n+1)} - J_s^{(n)}|}{|J_s^{(n)}|} \quad (2)$$

Once  $\xi_s$  is less than a target residual error (such as 0.01),

the MoM and MLFMA), which is much less than the computational cost of the numerical method. Besides, the above condition limits the KA application region. It doesn't satisfy the conditions for a realistic wind-driven PM rough surface and a motivation to improve the calculation accuracy.

Borrowing the impedance boundary condition (IBC)<sup>15</sup> to solve the dielectric rough surface scattering problem in the high-frequency band, the relationship between the induced electric current,  $J_s$ , and the equivalent magnetic current,  $D_s$ , can be written as  $M_s = -Z_s \mathbf{n}' \times J_s$ . Hence, the total number of unknowns can be cut in half.

Parameter  $Z_s$  is the surface impedance of the sea scatterer, determined by the permittivity ( $\epsilon$ ) and permeability ( $\mu$ ) of



5. These traces show the validity of FBPO for the P-M rough surface, both for (a) HH polarization and (b) VV polarization.

the interaction process is assumed to have converged and reached a stable state. Accordingly, the iteration process will be stopped at that point.

Since the IPO process is derived from the MFIE, the interaction effects from among all the patches of rough surface are taken into account, helping to improve the computational accuracy and extend the validity region of KA compared with a conventional PO. As an experiment, an isotropic Gaussian rough surface was used for analysis. The basic parameters were as follows: for one Monte Carlo (MC) realization, its size was  $60\lambda \times 60\lambda$ ; the correlation length,  $l_c$ , was  $2\lambda$ ; the root-mean-square height of the rough surface,  $h_{rms}$ , was  $1\lambda$ ; and the curvature radius,  $\rho$ , was  $1.73\lambda$ . For this experiment, the incident angle,  $\theta_i$ , was set to 60 deg., with  $\epsilon_r = 72.64 + j69.36$ .

Obviously, these parameters do not satisfy the full KA conditions. The copolarization, including the horizontal-horizontal (HH) polarization and the vertical-vertical (VV) polariza-

tion comparisons of the radar scattering coefficient ( $\sigma_0$ ), are given out using the PO, IPO, and rigorous MLFMA yardsticks (with the MLFMA considered as the reference in the current work, and identified as Ref. in the figures). It should be noted that a two-dimensional (2D) tapered illumination window<sup>16</sup> was employed to suppress the edge effects in the applied numerical method.

Figure 1 shows the validity of the IPO approach compared with the MLFMA method. The IPO method shows good agreement with the rigorous method after 10 iterations, even though the surface is very rough (see above sea states) at a large incident angle. The general Kirchhoff approximation is valid, but only for the small incident angle ( $\theta_i < 30$  deg.).<sup>14</sup>

Even though the proposed method can offer improvements when running on PCs with limited RAM, it can be time consuming in performing the IPO. The time required is obvious when performing a Monte Carlo simulation of a large-scale rough surface. There must be some ways to improve the computational efficiency of the IPO approach while also reducing the CPU time.

After desecrating and testing the integral form of Eq. 1 using the basis function and IBC approximation, the original IPO method of Eq. 1 can be rewritten according to classical Jacobi iteration. This yields the updated form of current  $J^{(n+1)}$



MMICs

DETECTORS

LIMITERS

Sometimes, the best way to envision the future, is to invent it.

High performance broadband. It's what we're about.

From ultra low noise MMIC amplifiers, driver and power amplifiers, network matched and high sensitivity detectors and limiters with operation to 40 GHz, Eclipse MDI has you covered.

Eclipsing your expectations. We're about that too.



www.eclipsemdi.com  
408.526.1100



GaAs PHEMT MMIC Low Noise Amplifiers  
GaAs PHEMT MMIC Driver Amplifiers  
GaAs PHEMT MMIC Power Amplifiers  
Broadband Schottky Detectors  
Pin-Schottky Diode Limiters





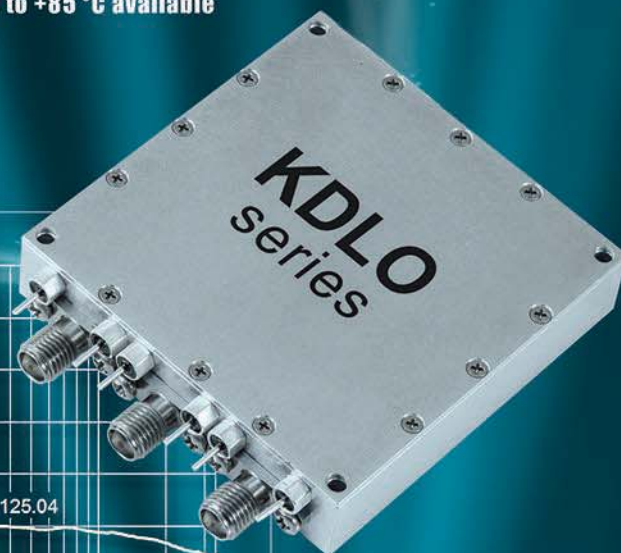
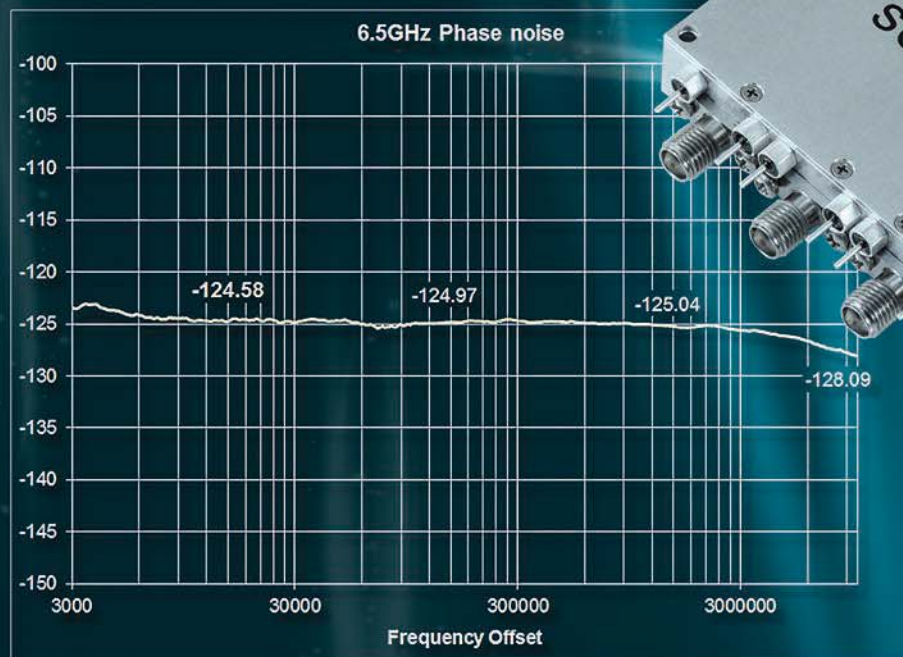
# DUAL or SINGLE LOOP SYNTHESIZER & PLO MODULES

## Features:

- Proprietary digital Integer and Fractional PLL technology
- Lowest digital noise floor available -237 dBc/Hz figure of merit
- Output frequencies from 100 MHz locked crystal to 15 GHz
- Available with reference clean up dual loop, or single loop for very low noise reference
- Parallel fixed band stepping or SPI interface synthesized up to octave bandwidths
- Reference input range 1 MHz to 1.5 GHz
- Dual RF output or reference sample output available
- +12 dBm standard output power +16 dBm available
- Standard module size 2.25 X 2.25 X 0.5 Inches (LxWxH)
- Standard operating temperature -10 to 60 °C, -40 to +85 °C available

## Applications:

- SATCOM, RADAR, MICROWAVE RADIO,
- LOW NOISE CLOCK STANDARDS



**Talk To Us About Your Custom Requirements.**



Phone: (973) 881-8800 | Fax: (973) 881-8361  
E-mail: [sales@synergymw.com](mailto:sales@synergymw.com)  
Web: [WWW.SYNERGYMWAVE.COM](http://WWW.SYNERGYMWAVE.COM)  
Mail: 201 McLean Boulevard, Paterson, NJ 07504

COMPARING DIFFERENT CALCULATION METHODS FOR THEIR TIME CONSUMPTION			
Method	FBIPO	Local FBIPO	Local FBIPO + FaFFA
Time (s)	7116	4608	1913

for the rough surface in terms of the current of the previous iteration. For the  $i$ th surface patch,  $i = 1, 2, \dots, N$ :

$$J_i^{(n+1)} = \frac{\left( J_i^i - \sum_{j=1}^{i-1} Z_{ij} J_j^{(n)} - \sum_{j=i+1}^N Z_{ij} J_j^{(n)} \right)}{Z_{ii}} \quad (3)$$

where  $Z_{ij}$  = the coupling effects from the  $j$ th surface patch to the  $i$ th surface patch, and  $J_i^i$  = the excited element associated with the incident magnetic field.

Equation 3 can be rewritten in matrix notation as Eq. 4:

$$\bar{\bar{D}} J^{(n+1)} = J^i + (\bar{\bar{U}} + \bar{\bar{L}}) J^{(n)} \quad (4)$$

where:

$\bar{\bar{D}}$  = the diagonal matrix;

$\bar{\bar{L}}$  = the lower triangular matrix; and

$\bar{\bar{U}}$  = the upper triangular matrix.

It is often difficult to achieve convergence of the IPO process for very rough surfaces. Therefore, it is necessary to apply some modifications or techniques to improve the convergence. The iteration currents are updated in the forward and backward passes. The most recently updated currents in forward-backward iterative physical optics (FBIPO)<sup>11</sup> are used in the two passes by means of an intermediate solution.

The forward pass for  $i = 1, 2, \dots, N$  can be computed as:

$$J_i^{(n+1/2)} = \frac{\left( J_i^i - \sum_{j=1}^{i-1} Z_{ij} J_j^{(n+1/2)} - \sum_{j=i+1}^N Z_{ij} J_j^{(n)} \right)}{Z_{ii}} \quad (5)$$

The backward pass for  $i = N, N-1, \dots, 1$  can be computed as:

$$J_i^{(n+1)} = \frac{\left( J_i^i - \sum_{j=1}^{i-1} Z_{ij} J_j^{(n+1/2)} - \sum_{j=i+1}^N Z_{ij} J_j^{(n+1)} \right)}{Z_{ii}} \quad (6)$$

The matrix form of these iterative equations can be rewritten in the following manners. For the forward iteration, the

equation can be rewritten as Eq. 7:

$$(\bar{\bar{D}} - \bar{\bar{L}}) J^{(n+1/2)} = J^i + \bar{\bar{U}} J^{(n)} \quad (7)$$

For the backward iteration, it can be rewritten as Eq. 8:

$$(\bar{\bar{D}} - \bar{\bar{U}}) J^{(n+1)} = J^i + \bar{\bar{L}} J^{(n+1/2)} \quad (8)$$

To improve convergence and reduce the chance for divergence of the iterative solution for a very rough surface, a relaxation parameter  $\bar{\omega}$  will be introduced into the iterative solution. With this new parameter, the updated currents can be renewed as  $J^{(n+1)} = \bar{\omega} J^{(n+1/2)} + (1 - \bar{\omega}) J^{(n)}$ . Therefore, the under-relaxation FBIPO algorithm can also be rewritten. The forward iteration is rewritten as Eq. 9:

$$(\bar{\bar{D}} - \bar{\omega} \bar{\bar{L}}) J^{(n+1/2)} = \bar{\omega} J^i + \left[ (1 - \bar{\omega}) \bar{\bar{D}} + \bar{\omega} \bar{\bar{U}} \right] J^{(n)} \quad (9)$$

while the backward iteration is rewritten as Eq. 10:

$$(\bar{\bar{D}} - \bar{\omega} \bar{\bar{U}}) J^{(n+1)} = \bar{\omega} J^i + \left[ (1 - \bar{\omega}) \bar{\bar{D}} + \bar{\omega} \bar{\bar{L}} \right] J^{(n+1/2)} \quad (10)$$

As can be seen, the matrix-vector product  $\bar{\bar{L}} J^{(n+1/2)}$  is used in both Eqs. 9 and 10, so this product need only be computed once. Similarly, the product

$\bar{\bar{U}} J^{(n)}$  in Eq. 9 can be obtained from Eq. 10 in the previous iteration. Only one complete matrix-vector product need be computed for a single forward-backward iteration.

Essentially, the Jacobi iteration is replaced by the Gauss-Seidel iteration. The same rough surface in Fig. 2 is then used to state the effectiveness of under-relaxation FBIPO. Instead of the tapered EM wave, here the plane wave is illuminating the rough surface. It leads to stronger EM scattering interaction among the surface patches.

In Fig. 2, the conventional IPO cannot converge for this surface; by contrast, the FBIPO is able to converge. Meanwhile, as shown in Fig. 3, the under-relaxation iterations are also being tested under different parameters:  $\bar{\omega} = 0.5, 0.7, 0.8$ , and 1.0, respectively. When  $\bar{\omega} = 1$ , the conventional FBIPO is represented.

As can be seen from Fig. 2, 24 iteration steps are required to reach convergence for a residual error of  $\xi = 0.01$  in the conventional FBIPO, but only 10 iteration steps are needed to reach a convergence for a residual error of  $\xi = 0.008$  in the under-relaxation FBIPO of  $\bar{\omega} = 0.8$ . This parameter is used in the current report.

Because impedance element storage is avoided, CPU time is conserved. This becomes a big drawback for any Monte Carlo realization in terms of random surface analysis. For both outer and inner iterations, a FaFFA<sup>12</sup> is subsequently employed to speed the electromagnetic coupling interaction between observation point and source point, both of which originate

from the speed-up technique in the MLFMA.

Assuming that  $r_t$  is an observation point in an observation group  $m$  and  $r_s$  is a source point in a source group  $n$ ,  $r_m$  and  $r_n$  represent the centers of the observation and source groups, respectively. Under far-field conditions—i.e.,  $|r_{tm} + r_{ns} \approx r_{mn}|$ —the scale Green's function can be approximated by Eq. 11:

$$\frac{e^{-jk|r_t - r_s|}}{4\pi|r_t - r_s|} = \frac{e^{-jk|r_{tm} + r_{mn} + r_{ns}|}}{4\pi|r_{tm} + r_{mn} + r_{ns}|} \approx \frac{e^{-jk|r_{mn}|} e^{-jk\hat{r}_{mn} \cdot (r_{tm} + r_{ns})}}{4\pi|r_{mn}|} \quad (11)$$

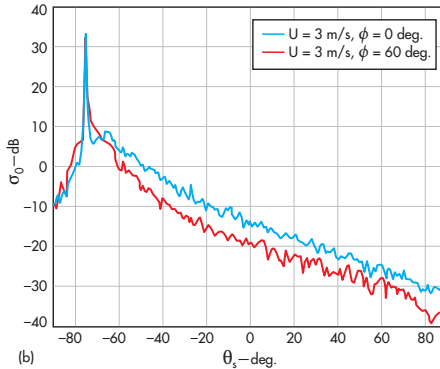
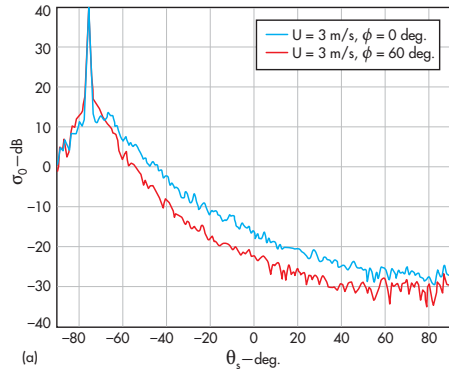
where:

$$\hat{r}_{mn} = (r_m - r_n) / |r_m - r_n|.$$

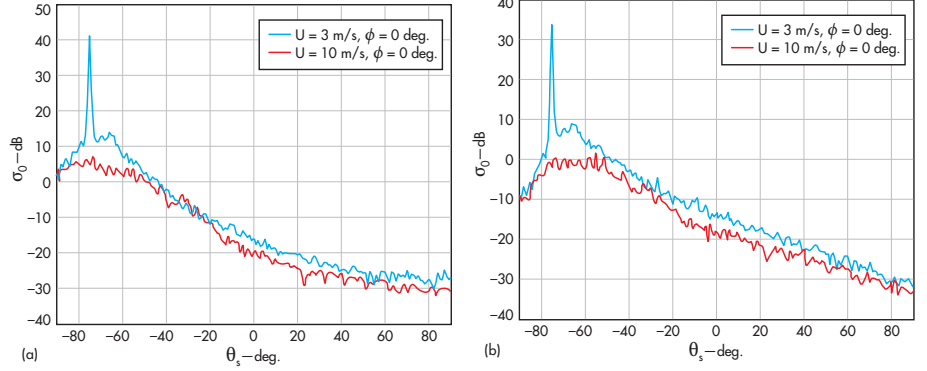
In terms of the FaFFA model, the interaction separates three sets of aggregation, translation, and disaggregation in far regions. The matrix-vector multiplication can be accelerated by means of the fast multipole method (FMM).<sup>6</sup> Also, the complexities of the multiplication process can be greatly reduced from  $o(N^2)$  to  $o(N \log N)$ .

Generally, all interactions between near-field regions and far-field regions are considered in the iteration process. But, in fact, only the interactions between local regions are dominant, especially for a nearly planar rough surface. In the current experiment, the local interaction threshold was set to  $20\lambda$ .

If  $r_t$  and  $r_s$  are the observation point and source point on a rough surface,  $S_s$ , iterations for patches where  $|r_t - r_s| > 20\lambda$  are omitted, as a result of something called the local iteration.<sup>13</sup> The complexities of the multiplication for the FaFFA model were found to be much less than the conventional iteration model, reducing even to  $o(N)$  for an extra large-scale rough surface rather than  $o(N^2)$ .



7. This is a comparison of the different wind direction cases.



6. This is a comparison of different wind speed cases, both for (a) HH polarization and for (b) VV polarization.

The same surface as in the last section was used to test the effectiveness of the FaFFA model and, as can be seen in Fig. 4, good agreement was obtained in comparisons of the FaFFA and local iteration. The table shows the time consumptions when using different methods.

In actual engineering, a wind-driven P-M rough surface<sup>10</sup> is widely used for the rough surface instead of a Gaussian surface. The 2D P-M spectrum can be computed by Eq. 12;

$$W(K, \varphi) = \frac{\alpha}{2K^4} \exp \left\{ -\frac{\beta g^2}{K^2 U^4} \right\} \frac{\cos^2 \varphi}{\pi} \quad (12)$$

where:

$K$  = the spatial wave number in the horizontal x-y plane;  
 $U$  (m/s) = the wind speed at a height of 19.5 m above the mean surface,  $\bar{z} = 0$ ;

$\varphi$  = the wind direction;

$g = 9.81$  m/s;  $\alpha = 8.1 \times 10^{-3}$ ; and  $\beta = 0.74$ .

The EM frequency used in Eq. 12 is 1.25 GHz with a rough surface of  $160\lambda \times 12\lambda$ ,  $U = 3$  m/s, the wind direction  $\varphi = 90$  deg., and the EM incident angle  $\theta_i = 75$  deg.

Good agreement was obtained in the comparisons in Fig. 5. Also, different scattering cases were examined corresponding

to different wind speeds:  $U = 3$  and 10 m/s and wind directions of  $\varphi$  of 0 and 60 deg. as simulated by the proposed model. Some conclusions can be drawn from the results in Figs. 6 and 7, concerning a wind-driven sea surface.

When the wind speed increases, the sea surface becomes rougher and the distribution of scattered EM energy is more dispersive and

(continued on p. 78)



# Analyze Quasi-TEM Rectangular Coax Couplers

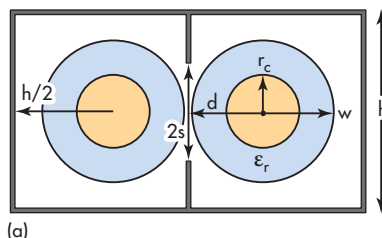
By digging into the even- and odd-mode electromagnetic parameters of quasi-TEM rectangular coax couplers, some simple modifications can be implemented for improved performance.

**D**irectional couplers are versatile performers in test setups and other RF/microwave systems in which signal power must be channeled and measured. In general, the choice of a directional coupler has involved a tradeoff between cost and performance. Hopefully, the use of modeling and simulation software can make the choice of directional coupler a bit less of a tradeoff.

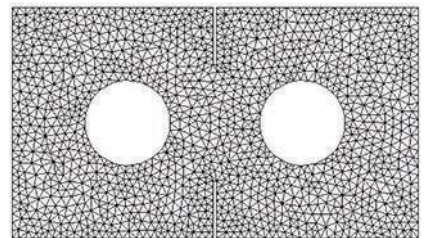
Traditional broadband couplers suffer from either high cost or low performance. For example, broadband waveguide couplers are bulky and costly. Stripline and microstrip directional couplers have attractive broadband characteristics, but they are affected by significant losses and low power-handling capabilities.

In contrast, coaxial structures would be ideal for their circuit losses and their high power-handling capabilities.

1. These two views of a quasi-TEM rectangular coaxial coupler with metal diaphragm show (a) the cross-sectional view and (b) the 3D view.

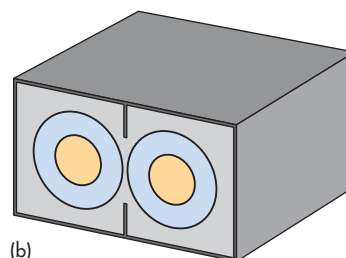


2. This illustrates the FEM meshes of the EM simulator performed on the quasi-TEM rectangular coaxial coupler with metallic diaphragm.



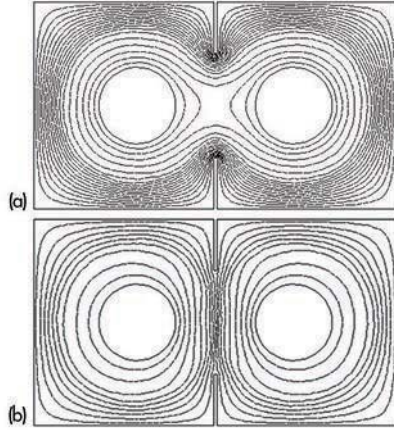
ities.<sup>1</sup> Coupled coaxial lines have long histories of use in microwave filters, couplers, and other high-frequency components. The current project is focused on developing a new type of extremely low-cost, low-loss, broadband, high-performance coupler.

The practical solution adopted for these couplers is to partially fill rectangular coaxial cables and insert thin metal diaphragms with a properly shaped aperture between the two inner conductors. The resulting air gap between the dielectric substrate and the ground plane will exhibit less circuit losses than the convention-



ally shaped aperture between the two inner conductors. The resulting air gap between the dielectric substrate and the ground plane will exhibit less circuit losses than the convention-

3. These diagrams show potential distributions of the quasi-TEM rectangular coaxial coupler with metal diaphragm for (a) the even mode and (b) the odd mode (for  $w/r_c = 1.94$  and  $s/h = 0.25$ ).



al coaxial cables<sup>2,3</sup>. Metallic diaphragms partially separate the inner conductors and easily control the coupling factor by means of adjusting the aperture half-width value ( $s/h$  ratio). This new structure can be realized without major difficulties and with simple, low-cost mechanical construction.

Figure 1 provides a graphical depiction of a rectangular coaxial coupler with metallic diaphragm, both in a cross-sectional view (a) and in a three-dimensional (3D) view (b) of the quasi-transverse-electromagnetic (TEM) rectangular coaxial coupler. Each coaxial line of this quasi-TEM coupler is assumed to be lossless, with an inner conductor radius of  $r_c$  and an outer conductor of height  $h$  and width  $(h/2 + d)$ .

The coaxial lines are partially filled with dielectric material of radius,  $w$ , and relative dielectric constant,  $\epsilon_r = 2.03$ . A portion of each cable is cut out and coupled through thin metal diaphragms with negligible thickness to form the quasi-TEM coupled line. The cut depth is shown as  $d$  on the cross section, and the coupling level is adjusted by changing the aperture half-width ( $s/h$  ratio).

Various numerical techniques can be used to determine the accurate electromagnetic (EM) parameters of the quasi-

TEM coupled lines. For example, analysis of high-frequency structures by means of the finite-element method (FEM) may reveal a great deal about the expected EM behavior of those structures.<sup>4,5</sup> The FEM is especially convenient for the computation of electric and magnetic fields in homogeneous media. Also, it has high computation accuracy and fast computation speed.

This numerical method was essentially applied for the characterization of the electromagnetic parameters: the even- and odd- mode characteristic impedances ( $Z_{0e}$ ,  $Z_{0o}$ ); the even- and odd-mode effective dielectric constants ( $\epsilon_{\text{effe}}$ ,  $\epsilon_{\text{effo}}$ ); the coupling coefficient,  $k$ ; and the inductance and capacitance matrices ( $[L]$  and  $[C]$ , respectively) of the quasi-TEM rectangular coaxial coupler with metallic diaphragms, where:<sup>4,5</sup>

$$[L] = \begin{bmatrix} L_0 & M \\ M & L_0 \end{bmatrix} [C] = \begin{bmatrix} C_0 & -\gamma \\ -\gamma & C_0 \end{bmatrix} \quad (1)$$

In Equation 1:

$L_0$  = the proper inductance of the isolated lines;

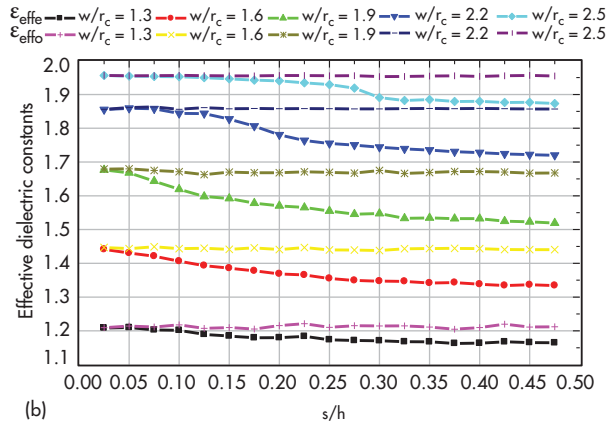
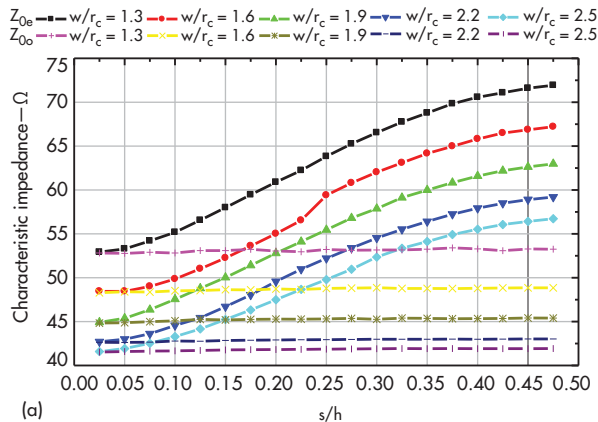
$C_0$  = the proper capacitance of the isolated lines;

$M$  = the mutual inductance of the quasi-TEM coupled lines; and

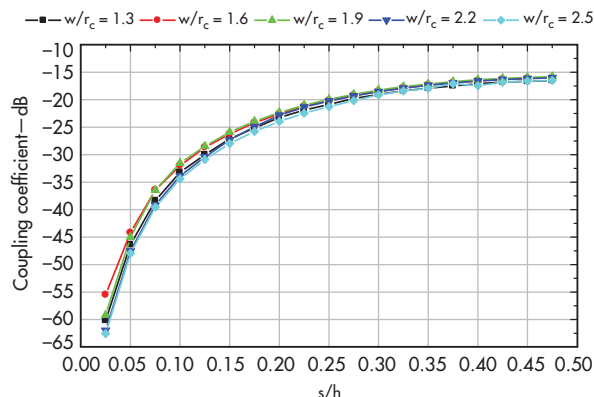
$\gamma$  = the coupling capacitance of the quasi-TEM coupled lines.

To find the EM parameters of a quasi-TEM rectangular coaxial coupler with metallic diaphragms, analysis was performed on a structure portrayed in Fig. 1 with  $d/r_c = 2.04$ . An FEM-based numerical tool was applied to show the effects of the metallic diaphragms ( $s/h$  ratio) and the dielectric radius ( $w/r_c$  ratio) on the quasi-TEM coupler's EM parameters.

Figure 2 shows the FEM meshes of the partially filled, rectangular coaxial coupler with metallic diaphragms using triangular elements. The potential distributions are pre-



4. These plots show even- and odd-mode (a) characteristic impedances and (b) effective dielectric constant values as functions of the  $s/h$  ratio for different values of  $w/r_c$ .



5. This plot shows the influence of the  $s/h$  ratio on the coupling coefficient for various values of  $w/r_c$ .

sented in Fig. 3 for the even and odd modes with  $s/h$  of 0.25 and  $w/r_c$  of 1.94. For different  $s/h$  and  $w/r_c$  ratios, varying respectively between 0.025 and 0.475 and 1.3 and 2.5, the results obtained by FEM analysis can be seen in Figs. 4 through 7.

The EM parameters obtained through the FEM analysis were used to design and build a 20-dB directional quasi-TEM rectangular coaxial coupler with metallic diaphragms. All four ports of the coupler were matched to  $50\ \Omega$ , as shown in

Fig. 8. The fixed parameters of the 20-dB directional coupler include a characteristic impedance of  $(Z_{0e} Z_{0o})^{0.5} = 49.62\ \Omega$  and an operating frequency of 7 GHz.

The features of the coupler obtained from the analytical results include an inner conductor radius of 1 mm; a coupler height of 5.4 mm; a  $d/r_c$  ratio of 2.04; a  $w/r_c$  ratio of 1.94 and an  $s/h$  ratio of 0.25; a coupler length ( $l$ ) of 8.4 mm, even-mode characteristic impedance ( $Z_{0e}$ ) of  $54.8\ \Omega$ ; odd-mode characteristic impedance ( $Z_{0o}$ ) of  $44.93\ \Omega$ ; even-mode effective dielectric constant ( $\epsilon_{\text{effe}}$ ) of 1.577; odd-mode effective dielectric constant ( $\epsilon_{\text{effo}}$ ) of 1.7; and  $[L]$  and  $[C]$  found as follows:

$$[L] = \begin{bmatrix} 195.87 & 19.95 \\ 19.95 & 195.87 \end{bmatrix} \left( \frac{nH}{m} \right) [C] =$$

$$\begin{bmatrix} 106.263 & -9.672 \\ -9.672 & 106.263 \end{bmatrix} \left( \frac{pF}{m} \right)$$

(2)

Using MATPAR software, the S-parameters of the designed quasi-TEM rectangular coaxial coupler with metallic diaphragms (with respect to  $50\ \Omega$ ) were plotted in Fig. 9.<sup>6</sup> MATPAR is a software package that makes it possible for users of MATLAB software, developed by MathWorks ([www.mathworks.com](http://www.mathworks.com)) to take advantage of parallel computers for



## Test Solutions

... from SRS!

**2 GHz Signal Generator**  
SG382 ... \$3900

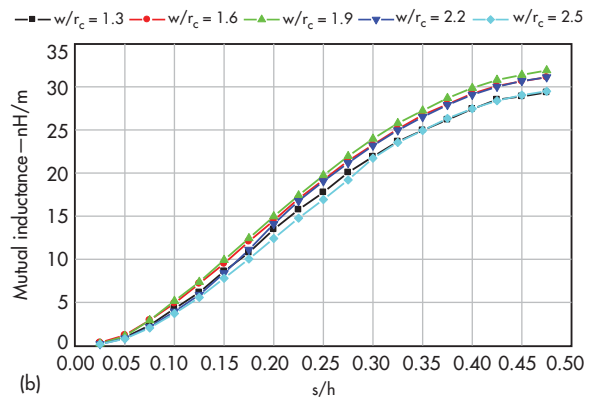
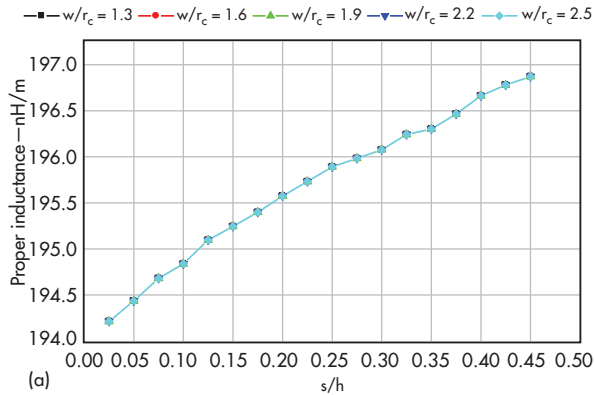
**10 MHz Rubidium Std.**  
FS725 ... \$2695

**Distribution Amplifiers**  
FS735 ... from \$950

**2 GHz Clock Generator**  
CG635 ... \$2995







6. The impact of the  $s/h$  ratio can be seen here on (a) the proper inductance and (b) the mutual inductance for various values of  $w/r_c$ .

large problems, helping to accelerate the processing of complex problems.

For this type of quasi-TEM rectangular coaxial coupler with metallic diaphragms, there are no numerical or experimental results readily available in the scientific literature. To check the numerical FEM calculations, some parallel processing was required on another solver, using the same geometrical and physical parameters for the quasi-TEM directional coupler in both simulation methods.

For a “reinforcement” to the FEM calculations, simulations in 3D were performed using CST MICROWAVE STUDIO software (Fig. 1) developed by Computer Simulation Technology ([www.cst.com](http://www.cst.com)).<sup>7</sup> By employing the CST MICROWAVE STUDIO’s Transient Solver, the resulting scattering parameters (with respect to  $50\ \Omega$ ) for a quasi-TEM rectangular coaxial coupler measuring  $9.48 \times 5.40 \times 8.40\ \text{mm}^3$  were plotted, as shown in Fig. 10, for frequencies ranging from 0.25 to 14.00 GHz.

*Building on our rich 30 year history of designing high performance scientific and engineering test equipment, SRS now offers a broad line of RF instrumentation.*

*SRS products are not only affordable, but they offer incredible performance — like the new SG386 DC to 6 GHz Signal Generator which has outstanding*

*specifications and sells for about 1/3 the price of competing instruments.*

*Please visit us at [www.thinkSRS.com](http://www.thinkSRS.com), or call us at 408-744-9040 for details on these products as well as our full line of instrumentation.*

**Frequency Counter**  
SR620 ... \$4950

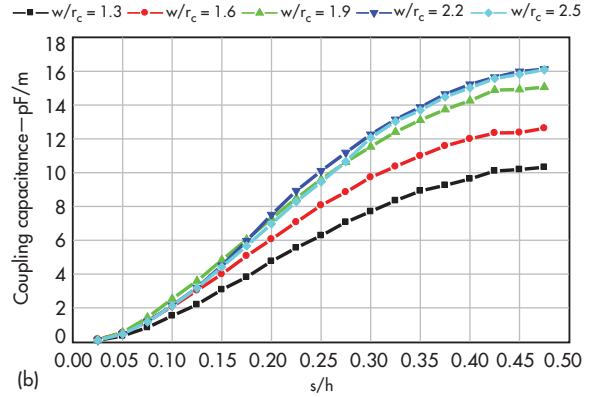
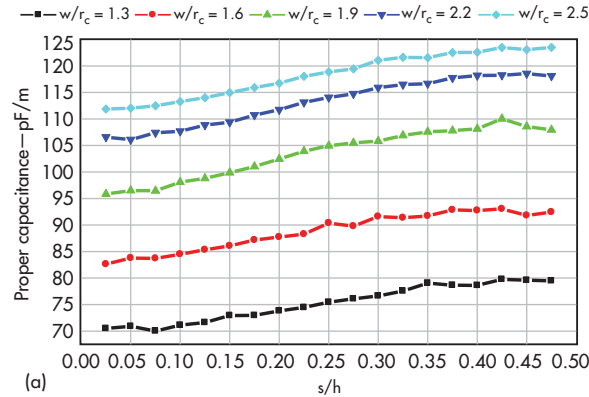
**30 MHz Function/Arb Generator**  
DS345 ... \$1595

**4 GHz Signal Generator**  
SG384 ... \$4600

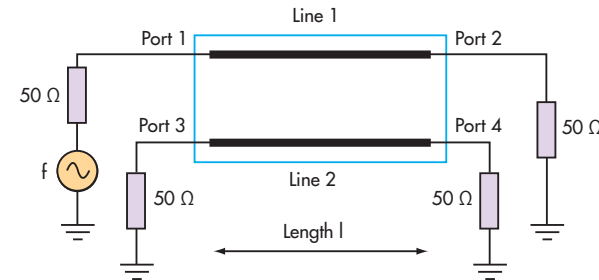
**10 MHz Rb Oscillator**  
PR510 ... \$1495

**6 GHz Signal Generator**  
SG386 ... \$5900





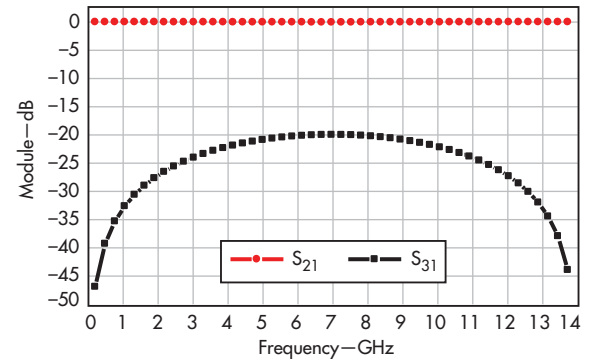
7. These plots illustrate (a) proper capacitance and (b) coupling capacitance as functions of  $s/h$  ratio for various values of  $w/r_c$ .



8. This diagram provides some additional details on the quasi-TEM directional coupler.

The results of Figs. 9 and 10 obtained respectively under MATPAR and CST environments show a good agreement of the frequency responses of S-parameters. They indicate the desired 20-dB coupling occurring from 5 to 9 GHz, which permit the designed quasi-TEM rectangular coaxial coupler with metallic diaphragms to have good coupling over a large frequency range.

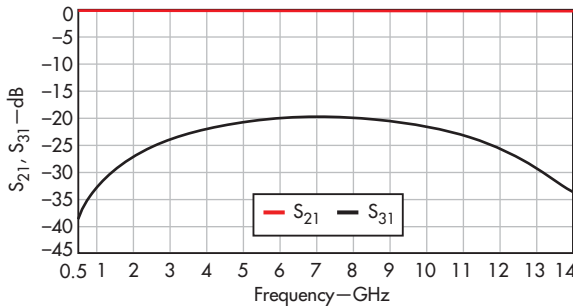
In summary, this article has highlighted a new type of low-cost, low-loss, high-performance broadband quasi-TEM rectangular coaxial coupler with metallic diaphragms. Its EM parameters were evaluated and design curves were developed. The curves were used as the basis for designing a 50- $\Omega$ , 20-dB, quasi-TEM rectangular coaxial coupler



9. This plot shows scattering parameters  $S_{21}$  and  $S_{31}$  for the quasi-TEM rectangular coaxial coupler as a function of frequency through 14 GHz as obtained in the MATPAR simulation environment.

with metal diaphragms measuring just  $9.48 \times 5.40 \times 8.40$  mm<sup>3</sup> and operating at 7 GHz.

Computer simulations performed under MATPAR and CST design environments were reinforced by results obtained from measurements with commercial test equipment. The close agreement of the simulated and measured results represent progress in the design and modeling of quasi-TEM rectangular coaxial couplers with metallic diaphragms. **MMW**

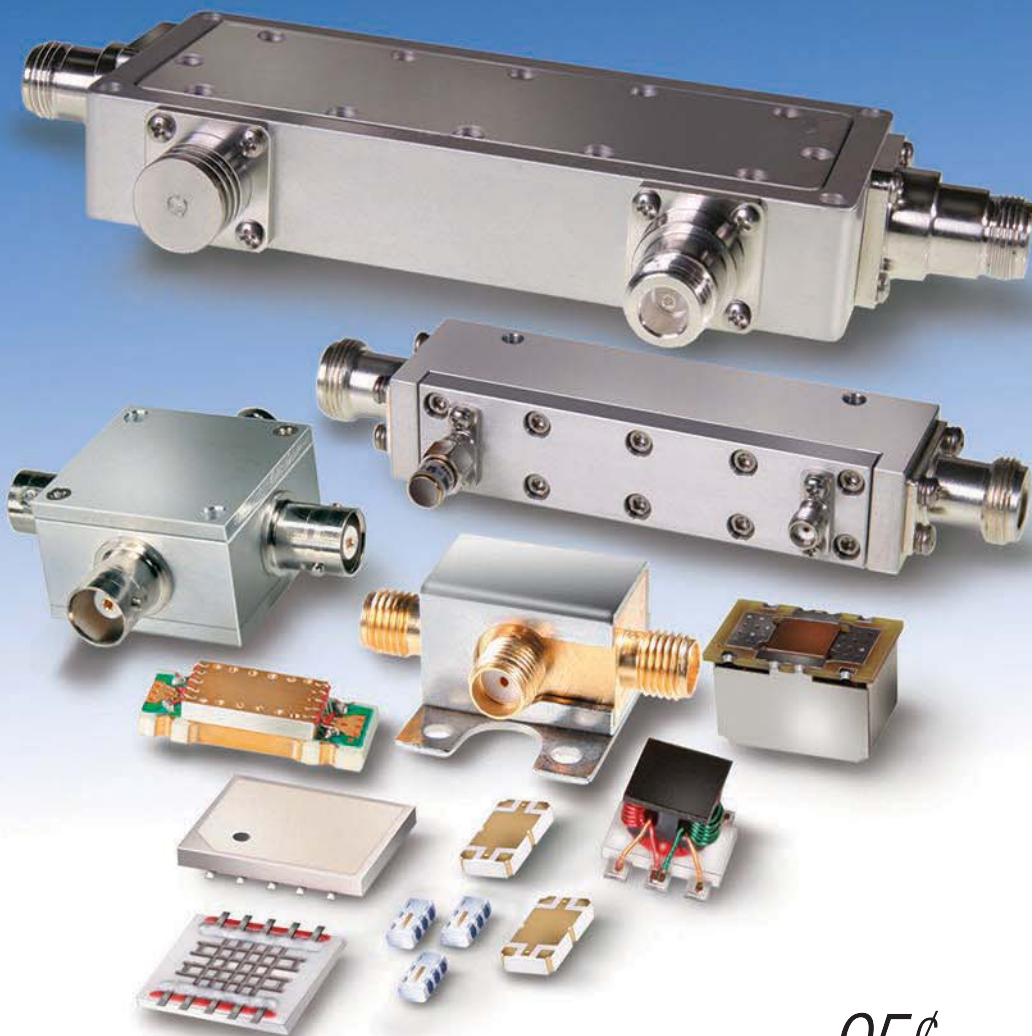


10. This plot shows the scattering parameters for the quasi-TEM coupler as a function of frequency through 14 GHz as obtained under the CST simulation environment.

# REFERENCES

1. H. An, R.G. Bosisio, and K. Wu, "Ultra-Wideband Directional Couplers with Coaxial Cable," Canadian Conference on Electrical and Computer Engineering, Vol. 2, 1995, pp. 1160-1163.
2. G.L. Ragan, "Microwave Transmission Circuits," MTT Radiation Laboratory Series, Vol. 9, McGraw-Hill, New York, 1948.
3. Hatsuda, Takeshi, "Computation of Impedance of Partially Filled and Slotted Coaxial Line," IEEE Transactions on Microwave Theory & Techniques, Vol. MTT-15, No. 11, November 1967, pp. 643-644.
4. N. Benahmed and M. Feham, "Finite Element Analysis of RF Couplers with Sliced Coaxial Cable," Microwave Journal, Vol. 43, No. 11, November 2000, pp. 106-120.
5. A. Lallam, N. Benabdallah, N. Benahmed, and Y. Bekri, "Analyze EM Parameters of Slotted Tube Couplers," Microwaves & RF, Vol. 47, No. 3, March 2008, pp. 76-86.
6. A.R. Djordjevic, M. Bazdar, G. Vitosevic, T. Sarkar, and R.F. Harrington, Scattering Parameters of Microwave Networks with Multiconductor Transmission Lines, Artech House, Norwood, MA, 1990.
7. CST-Computer Simulation Technology, 2010, www.cst.com.

# Directional / Bi-Directional COUPLERS



**5 kHz to 18 GHz up to 250W** from **95¢** ea. (qty. 1000)

**Now!** Looking for couplers or power taps? Mini-Circuits has ~~326~~ **279** models in stock, and we're adding even more! Our versatile, low-cost solutions include surface-mount models down to 1 MHz, and highly evolved LTCC designs as small as 0.12 x 0.06", with minimal insertion loss and high directivity. Other SMT models are designed for up to 100W RF power, and selected core-and-wire models feature our exclusive Top Hat™, for faster, more accurate pick-and-place.

At the other end of the scale, our new connectorized air-line couplers can handle up to 250W RF input power, with low insertion loss and exceptional coupling flatness! All of our couplers are RoHS compliant. So if you need a 50 or 75Ω, directional or bi-directional, DC pass or DC block coupler, for military, industrial, or commercial applications, you can probably find it at [minicircuits.com](http://minicircuits.com), and have it shipped today!



[www.minicircuits.com](http://www.minicircuits.com) P.O. Box 350166, Brooklyn, NY 11235-0003 (718) 934-4500 [sales@minicircuits.com](mailto:sales@minicircuits.com)



# Filters Build Upon MCSRRs

Several different types of bandpass filters are constructed using multi-split complementary split-ring resonators (MCSRRs), series capacitive gaps, and grounded stubs on low-cost circuit material.

Wireless communications systems and applications continue to expand, and many components have kept pace by shrinking in size to meet the needs of newer and smaller wireless electronic products. But some components, such as filters, still pose a challenge in terms of miniaturization, and the use of left-handed materials has presented great promise for their miniaturization.<sup>1</sup>

Some microwave components can be shrunk in size and improved in performance through the use of left-handed materials, including antennas, baluns, couplers, filters, and phase shifters. Microwave circuit designs typically employ some form of transmission line as the propagation medium, loaded by split-ring resonators (SRRs) or lumped series capacitances and shunt inductances.

By applying multi-split complementary split-ring resonators (MCSRRs), series capacitive gaps, and working in microstrip, the current researchers were able to develop multiple-pole, narrowband bandpass filters capable of providing reliable filtering functions in extremely small sizes.

Bandpass filters are essential to the operation of many wireless communications systems, and many different filter structures have been explored in recent years. Bandpass filter designs on printed-circuit-board (PCB) materials have included complementary split ring resonators,<sup>2</sup> multilayer-multichip-module (MCM-D) technology,<sup>3</sup> and composite right/left-

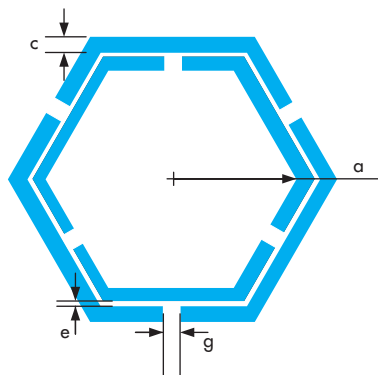
handed transmission (CRLH) technology.<sup>4</sup> But these bandpass filter structures have only had one passband with a relatively narrow bandwidth.

With the growing number of wireless activities and applications, a multiple-band filter is a key requirement that's been pursued by numerous engineering teams and researchers. As a possible solution, in the current report, a planar multiple-band microwave filter based on simplified CRLH (SCRLH) material has been proposed.<sup>5-7</sup>

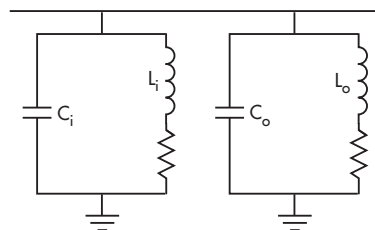
Microstrip filter structures can be quite complex, though. As part of this earlier filter solution proposal, a dual-mode resonant structure was designed and an ultrawideband (UWB) bandpass filter was detailed based on SCRLH material.<sup>8,9</sup> But the design approach was not useful for implementing double-band or multiple-band filters as in the current work.

By way of a potential solution, a novel structure based on MCSRRs is proposed for the design of multiple-narrowband bandpass filters (MNBPFs), as well as wideband bandpass filters. The proposed filter features multiple passbands and a relatively small size. By adjusting the size of the grounded stubs, the center frequencies of the multiple-band filter's passbands are able to be tuned. When these frequencies overlap, it forms a wideband filter.

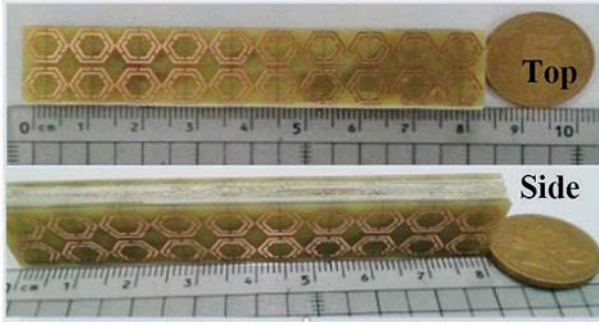
The proposed filter design offers four passbands, with center frequencies at 4.49, 4.97, 5.47, and 5.92 GHz and with



1. This is the topology of the MCSRRs, based on 0.8-mm-thick FR-4 substrate material.



2. This equivalent circuit represents the MCSRRs.



3. The photos present top and side views of the fabricated MCSRRs.

better than 20-dB return loss. The target 3-dB passband for the companion wideband filter that is part of this proposal is 5.89 to 7.06 GHz with less than 1.5-dB passband insertion loss.

The theory of metamaterials was introduced almost 50 years ago by Veselago.<sup>1</sup> The current researchers present a MCSRR structure based on magnetic resonance to achieve negative permeability. Figure 1 shows the topology of these MCSRRs. From the diagram, it can be seen that a structure with two multiple-split hexagons is established at the top of the substrate. A dielectric material of FR-4 substrate with 0.8-mm thickness was used as the filter circuit material. The geometric values for the MCSRRs (for the diagram in Fig. 1) are as follows:  $a = 3$  mm,  $c = 0.3$  mm,  $e = 0.1$  mm, and  $g = 0.2$  mm.

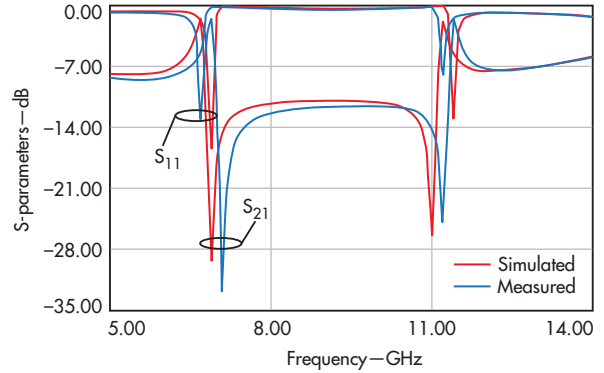
According to electromagnetic (EM) theory, an equivalent capacitance will be produced between two closed metal rings separated by a dielectric material. In the present report, an opening was etched in every opposite side of the circuit board, resulting in the equivalent capacitance disappearing. For the equivalent circuit shown in Fig. 2, the circuit elements  $C_i$ ,  $L_i$ ,  $C_o$ , and  $L_o$  were used to explain the magnetic resonances of the inside and outside rings, respectively. Using those same circuit elements, the two resonant frequencies,  $\omega_1$  and  $\omega_2$ , can be found from these simple equations:

$$\omega_1 = 1/(L_i C_i)^{0.5} \quad (1)$$

and

$$\omega_2 = 1/(L_o C_o)^{0.5} \quad (2)$$

THE FILTERS AT A GLANCE				
Type	Band	Center frequency (GHz)	3-dB passband	Filter BW
MNBPF	Band 1	4.49	4.44-4.55	2.5%
	Band 2	4.97	4.87-5.08	4.2%
	Band 3	5.45	5.36-5.56	3.4%
	Band 4	5.92	5.88-5.95	1.2%
Wideband		6.91/6.94	5.89-7.06	18.1%



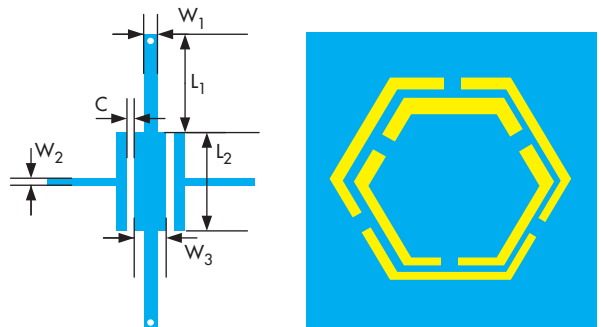
4. The curves compare simulated and measured results for the MCSRRs.

Figure 3 presents photographs of fabricated MCSRRs, with views of the top and side, while Figure 4 contains simulated and measured results of performance. From these results, it can be seen that a double-band magnetic resonator has been proposed.

It should also be apparent that the performance levels for insertion and return losses agree closely between measurements and simulations. At the resonator frequency, the insertion losses and return losses are less than 10 dB, which should only be possible by merit of a circuit material with negative permeability.

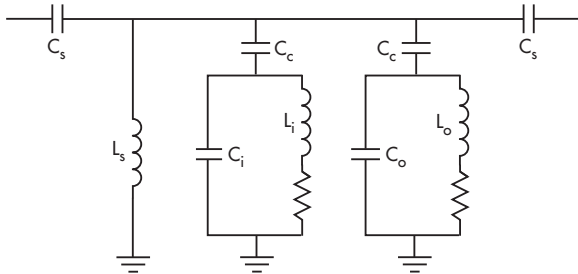
Figure 5 presents both the layout (right) and schematic diagram (left) for the proposed multi-narrowband filter. The filter layout was formed by etching an MCSRR unit onto the bottom of the circuit substrate, with series capacitive grounding stubs etched onto the top of the circuit substrate. The key to achieving the desired results with this proposed filter is the MCSRR unit. It can be used to improve the performance of the filter while also decreasing the filter's size.

At this point, it should be noted that the double-band magnetic-resonator unit can have two poles; the microstrip structure must feature two poles at the electronic resonance frequencies in order to yield a multi-narrowband filter (MNBPF) for each of the poles.



5. These are the schematic (left) and layout (right) views of the proposed multi-narrowband filter.

“According to EM theory, an equivalent capacitance will be produced between two closed metal rings separated by a dielectric material.”



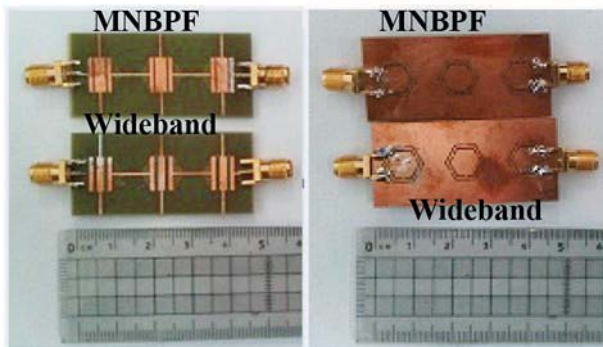
6. This represents the equivalent circuit of the proposed filter.

The equivalent circuit of the proposed filter (Fig. 6) should help to explain the theory behind the filter's operation. The coupling of the line is described by means of capacitance  $C_c$ . The grounded stubs are modeled by means of the shunt inductance,  $L_p$ . The series capacitances are accounted for by  $C_s$ .

From this equivalent circuit, it is possible to obtain several resonant frequencies for the filter. Series capacitance  $C_s$  and inductance  $L_s$  were used to explain resonant frequency  $f_0$ , while capacitance  $C_c$  and the MCSRRs were used to explain the present of frequencies  $f_1$  and  $f_2$ .

To fabricate the MNBPF, the following dimensions were selected and used:  $W_1 = 3$  mm;  $L_1 = 8.8$  mm;  $W_2 = 0.55$  mm;  $L_2 = 6.3$  mm;  $W_3 = 0.5$  mm; and  $C = 0.44$  mm. The geometric values of MCSRRs were  $a = 8.8$  mm and  $c = e = g = 0.5$  mm. The filters were fabricated on FR-4 circuit substrate material with 0.8-mm thickness and relative dielectric constant,  $\epsilon_r$ , of 4.4. The radius of the viahole is 0.1 mm.

Figure 7 offers photographs of the proposed filters, which were characterized by a commercial microwave vector network analyzer (VNA). Both the simulated and measured results of the MNBPF's performance is shown in Figure 8. As those results reveal, the filter has four discrete bands, with center frequencies at 4.49, 4.97, 5.47, and 5.92 GHz, and return losses of less than 20 dB for each band.



7. These photographs show prototypes of the proposed filters.

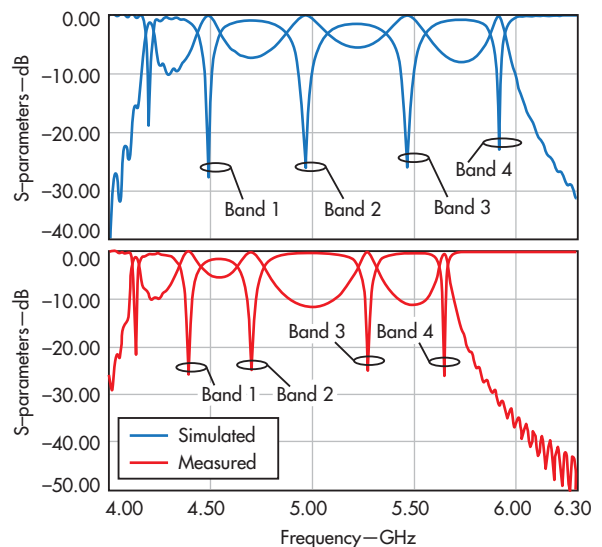
It was previously known that the poles (and frequencies) of a multipole narrowband filter could be designed and tuned by choosing the size/dimensions of the microstrip transmission lines. In theory, a wideband filter with continuous passband could also be obtained with the same approach and design structure. To design a wideband bandpass filter, the size would be etched with the dimensions of:

$W_1 = 0.8$  mm and  $W_3 = 0.3$  mm.

Figure 9 shows the simulated and measured filter responses for the resulting structure. Return losses are more than 10 dB, while insertion loss is less than 1.5 dB in the 3-dB passband from 5.89 to 7.06 GHz. This wideband filter has two zeros at 6.91 and 6.94 GHz in the passband. A short summary of the filter characteristics can be found in the table, "The Filters At A Glance."

It was known that the performance of the wideband filter could be enhanced through the application of cascade approaches. As a result, a third-order cascade technology was adapted for the wideband filter. At the same time, the size of the filter remained acceptable for many wireless systems and applications, even with the use of the cascade technology.

As was shown, an MNBPF and a wideband bandpass filter based on MCSRRs could be fabricated with essentially the same structure. The multiple-band filter offers great potential for meeting filtering requirements in wireless systems where space is tight, and the fact that the same basic structure can be reused to fabricate a wideband bandpass filter makes the design even more versatile. [mtw](#)



8. These plots show the measured and simulated responses for the MNBPF.





# CERAMIC FILTERS

**LOW PASS BANDPASS HIGH PASS**

**NOW!**

**Passbands Covering DC to 18 GHz**

from **99¢** ea. qty. 3000

**Over 200 models as small as 0.06 x 0.03"!** These tiny, hermetically sealed filters utilize our advanced Low Temperature Co-fired Ceramic (LTCC) technology to offer superior thermal stability, high reliability, and very low cost. Supporting a wide range of applications with high stop band rejection and low pass band insertion loss in tiny packages, they're a perfect fit for your system requirements. Visit [minicircuits.com](http://minicircuits.com) for comprehensive data sheets, PCB layouts, free high-accuracy simulation models, and everything you need to choose the model for your needs. Order direct from our web store, and have them in your hands as soon as tomorrow!

**Now available in small-quantity reels** at no extra charge:  
Standard counts of 20, 50, 100, 200, 500, 1000 or 3000.  
Save time, money, and inventory space!

**Wild Card Filter Kits, KWC-LHP, only \$98**



- Choose any 8 LFCN or HFCN models
- Receive 5 of each model
- A total of 40 filters for a great value
- Order your KWC-LHP Filter Kit TODAY!

**RoHS compliant** U.S. Patents 7,760,485 and 6,943,646

**Free, High-Accuracy Simulation Models for ADS**

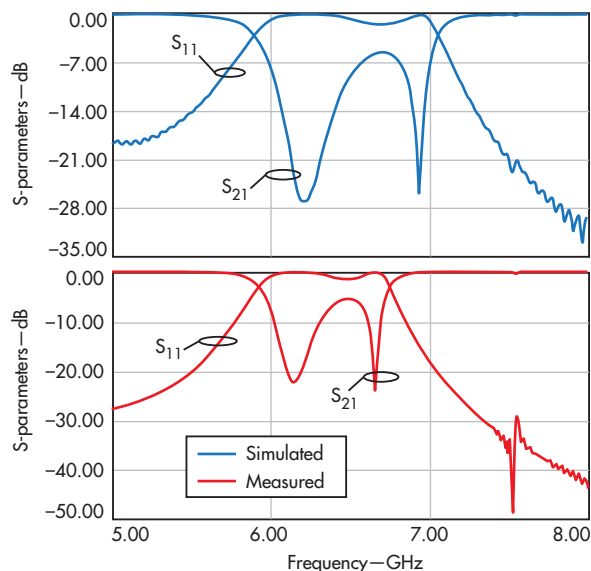


[www.modelithics.com/mvp/Mini-Circuits.asp](http://www.modelithics.com/mvp/Mini-Circuits.asp)



## ACKNOWLEDGMENT

The authors would like to thank the *National Nature Science Foundation of China* for financially supporting this research under Grant No. 61274020.



9. These plots show the measured and simulated responses for the wideband filter.

## EM Model

(continued from p. 67)

specular scattering becomes weaker. The scattering for a crosswind is more anisotropic in its spectral pattern, which is coherent for sea states. As currently reported, this analysis method provides the capability to simulate the radar echoes from rough sea surfaces for remote sensing applications.

In summary, the proposed IPO model helps solve the computational cost and time issues of solving for large-scale scattering of EM energy from rough 2D surfaces, such as the sea surface. The different methods reported help accelerate the convergence of the IPO and improve its robustness. **mw**

## ACKNOWLEDGEMENT

This work was supported by the National Natural Science Foundation of China (Grant No. 61372033).

## REFERENCES

1. G. Brown, "Backscattering from a Gaussian-distributed perfectly conducting rough surface," *IEEE Transactions on Antennas and Propagation*, Vol. 26, 1978, pp. 472-482.
2. W. Yang, Z.Q. Zhao, and Z.P. Nie, "Fast Fourier transform multilevel fast multipole algorithm in rough ocean surface scattering," *Electromagnetics*, Vol. 29, 2009, pp. 541-552.
3. C. Li, S.Y. He, J. Yang, Z. Zhang, B.X. Xiao, and G.Q. Zhu, "Monostatic scattering from two-dimensional two-layer rough surfaces using hybrid 3DMLUV-ACA method," *International Journal of Applied Electromagnetics and Mechanics*, Vol. 42, 2013, pp. 1-11.
4. H.X. Ye and Y.Q. Jin, "Parameterization of tapered incident wave for electromag-

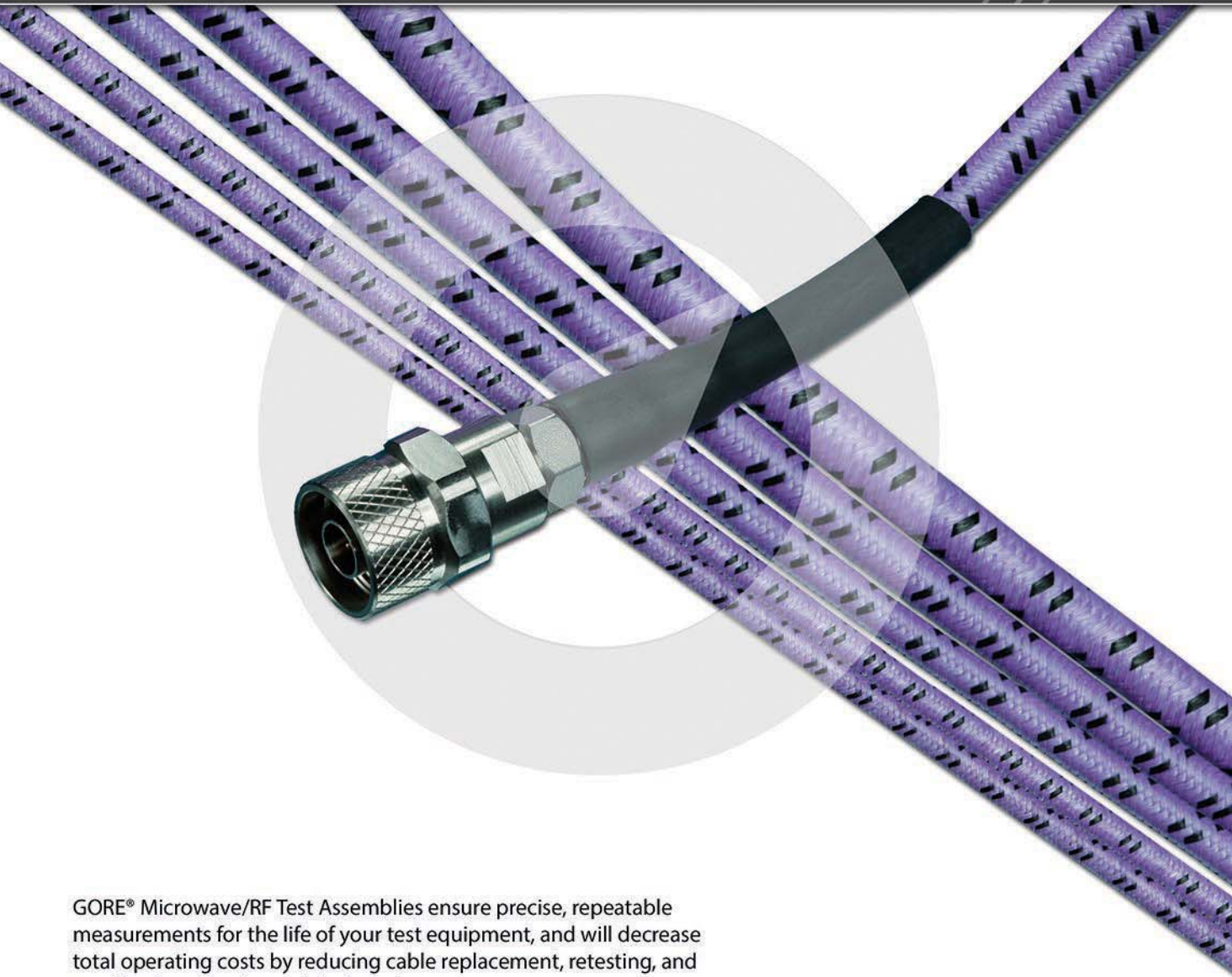
## REFERENCES

1. V.G. Veselago, "The electrodynamics of substances with simultaneously negative the values of  $\epsilon$  and  $\mu$ ," *Soviet Physics Uspekhi*, Vol. 10, February 1968, pp. 509-514.
2. Jordi Bonache, Ignacio Gil, Joan García-García, and Ferran Martín, "Novel Microstrip Bandpass Filters Based on Complementary Split-Ring Resonators," *IEEE Transactions on Microwave Theory & Techniques*, Vol. 54, 2006, pp. 265-271.
3. J. Bonache, G. Posada, G. Carchon, W. De Raedt, and F. Martín, "Compact (<0.5 mm<sup>2</sup>) K-band Metamaterial Bandpass Filter in MCM-D Technology," *Electron Letters*, Vol. 43, 2007, pp. 45-46.
4. Marta Gil, Jordi Bonache, Joan García-García, Jesús Martel, and Ferran Martín, "Composite Right/Left-Handed Metamaterial Transmission Lines Based on Complementary Split-Rings Resonators and Their Applications to Very Wideband and Compact Filter Design," *IEEE Transactions on Microwave Theory & Techniques*, Vol. 55, 2007, pp. 1296-1304.
5. Miguel Durán-Sindreu, Gerard Sisó, Jordi Bonache, and Ferran Martín, "Planar Multi-Band Microwave Components Based on the Generalized Composite Right/Left Handed Transmission Line Concept," *IEEE Transactions on Microwave Theory & Techniques*, Vol. 58, 2010, pp. 3882-3891.
6. George V. Eleftheriades, "A Generalized Negative-Refractive-Index Transmission-Line (NRI-TL) Metamaterial for Dual-Band and Quad-Band Applications," *IEEE Microwave Wireless Component Letters*, Vol. 17, No. 6, 2007, pp. 415-417.
7. Jin Xu and Wen Wu, "Miniaturised Dual-Wideband Bandpass Filter Using Novel Dual-Band Coupled-Line Sections," *Electron Letters*, Vol. 49, 2013, pp. 1162-1163.
8. F. Wei, C.-J. Gao, B. Liu, H.-W. Zhang, and X.-W. Shi, "UWB Bandpass Filter with Two Notch-Bands Based on SCRLH Resonator," *Electron Letters*, Vol. 46, 2010, pp. 1134-1135.
9. Hui Wang, Yu-Qian Yang, Wei Kang, Wen Wu, Kam-Weng Tam, and Sut-Kam Ho, "Compact Ultrawideband Differential Bandpass Filter Using Self-Coupled Ring Resonator" *Electron Letters*, Vol. 49, 2013, pp. 1156-1157.

- netic scattering simulation from randomly rough surface," *IEEE Transactions on Antennas and Propagation*, Vol. 53, 2004, pp. 1234-1237.
5. R.F. Harrington and J.L. Harrington, *Field Computation by Moment Methods*, Oxford University Press, London, England, 1996.
6. J.C. Song, C. Lu, and W.C. Chew, "Multilevel fast multipole algorithm for electromagnetic scattering by large complex objects," *IEEE Transactions on Antennas and Propagation*, Vol. 45, 1997, pp. 1488-1493.
7. E.I. Thorsos, "The validity of the Kirchhoff approximation for rough surface scattering using a Gaussian roughness spectrum," *The Journal of the Acoustical Society of America*, Vol. 83, 1988, pp. 78-92.
8. S.O. Rice, "Reflection of electromagnetic waves from slightly rough surfaces," *Communications on Pure and Applied Mathematics*, Vol. 4, 1951, pp. 351-378.
9. W. Yang, Z. Zhao, C. Qi, W. Liu, and Z.P. Nie, "Iterative hybrid method for electromagnetic scattering from a 3-D object above a 2-D random dielectric rough surface," *Progress In Electromagnetics Research*, Vol. 117, 2011, pp. 435-448.
10. E.I. Thorsos, "Acoustic scattering from a 'Pierson-Moskowitz' sea," *Journal of the Acoustical Society of America*, Vol. 88, 1990, pp. 335-349.
11. R.J. Burkholder and T. Lundin, "Forward-backward iterative physical optics algorithm for computing the RCS of open-ended cavities," *IEEE Transactions on Antennas and Propagation*, Vol. 53, 2005, pp. 793-799.
12. W.C. Chew, T.J. Cui, and J.M. Song, "A FAFFA-MLFMA algorithm for electromagnetic scattering," *IEEE Transactions on Antennas and Propagation*, Vol. 50, 2002, pp. 1641-1649.
13. J. Hu, Z.P. Nie, L. Lei, and Y.P. Chen, "Solving 3D electromagnetic scattering and radiation by local multilevel fast multipole algorithm," *IEEE International Symposium on Microwave, Antenna, Propagation and EMC Technologies for Wireless Communication Proceedings*, 2005, pp. 619-622.
14. L. Tsang and J.A. Kong, *Scattering of Electromagnetic Waves, Advanced Topics*, Wiley-Interscience, New York, 2001.
15. A.W. Glisson, "Electromagnetic scattering by arbitrarily shaped surfaces with impedance boundary conditions," *Radio Science*, Vol. 27, 1992, pp. 935-943.
16. E.I. Thorsos, "The validity of the Kirchhoff approximation for rough surface scattering using a Gaussian roughness spectrum," *Journal of the Acoustical Society of America*, Vol. 83, 1988, pp. 78-92.

# Performance Over Time

GORE® Microwave/RF Test Assemblies offer unmatched precision, repeatability and durability.



GORE® Microwave/RF Test Assemblies ensure precise, repeatable measurements for the life of your test equipment, and will decrease total operating costs by reducing cable replacement, retesting, and recalibration. Gore's portfolio includes:

- **GORE® PHASEFLEX® Microwave/RF Test Assemblies** – Provide excellent phase and amplitude stability with flexure.
- **110 GHz Test Assemblies** – Engineered to be flexed, formed and repositioned while maintaining excellent electrical performance.
- **VNA Microwave Test Assemblies** – Provide exceptional performance for precision test applications with frequencies through 67 GHz.
- **General Purpose Test Assemblies** – Excellent electrical performance for everyday test applications.



[gore.com/test](http://gore.com/test)

*Choose GORE® Microwave/RF Test Assemblies.  
For the life of your test equipment.*



GORE, PHASEFLEX, the purple cable and designs are trademarks of W. L. Gore & Associates.



## Design Feature

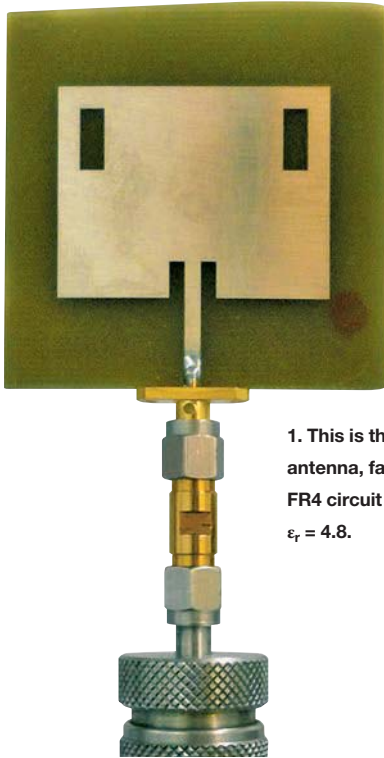
MOHAMMAD MAHDI SHAFIEI | Research Assistant  
Department of Electrical Engineering, Faculty of Engineering, University of Malaya, Malaysia

MAHMOUD MOGHAVVEMI | Professor  
Centre of Research in Applied Electronics (CRAE), Department of Electrical Engineering, Faculty of Engineering, University of Malaya, Malaysia

DR. WAN NOR LIZA MAHADI | Doctor  
ElectroMagnetic Radiation and Devices Research Group (EMRD), Department of Electrical Engineering, Faculty of Engineering, University of Malaya, Malaysia

# Antenna Tackles

**This slotted microstrip antenna handles both bands at 2.4 and 3.6 GHz with tight directional radiation patterns to provide efficient service for both Wi-Fi and WiMAX wireless communications applications.**



**1. This is the experimental antenna, fabricated on FR4 circuit material with  $\epsilon_r = 4.8$ .**

**A**s wireless applications continue to expand, antennas that can handle more than one frequency band are gaining in importance. For two of the more popular wireless frequency bands—those for Wi-Fi/WiMAX applications at 2.4 and 3.6 GHz—a compact microstrip patch antenna was developed with versatile frequency characteristics. The microstrip circuit is capable of multiple resonant frequencies.

When the antenna is designed for 2.4 GHz, its higher resonance frequency will be around 3.7 GHz or beyond the target 3.6-GHz frequency. By adding two rectangular slots on the patch area, the higher resonance frequency shifts down in frequency (from 3.7 to 3.6 GHz). Because the slots are cut inside the patch area, the radiation pattern of the antenna remains unaffected, and a dual-resonance antenna can be realized without an increase in size. The antenna achieves desirable directional radiation patterns at both 2.4 and 3.6 GHz.

Many dual-band antennas have been designed and fabricated for wireless applications in recent years.<sup>1-10</sup> Most have been designed for omnidirectional purposes, such as in cell phones and for wireless links in computers. But for indoor wireless access points (APs) or point-to-point (P2P) communications, more directivity is usually required.<sup>11-13</sup> As an example, Wi-

Fi/WiMAX antennas, operating at 2.4-/3.6-GHz frequency bands, are usually designed with directional patterns for the highest gain,<sup>14,15</sup> as well as for compact size and low profile. Although an assortment of dual-band antennas have been developed recently,<sup>16,17</sup> many are stacked<sup>18-21</sup> or suffer high-profile<sup>22-24</sup> configurations.

As a possible solution, a dual-band directional slotted microstrip antenna was developed for Wi-Fi/WiMAX applications. It consists of a rectangular patch acting as the radiator, plus two rectangular slots that are added to the structure symmetrically to modify the resonance frequency. This dual-band antenna achieves high directivity in both lower and upper bands. Computer simulations analyzed the return loss and radiation patterns of the antenna, with results validated by experimental measurements.

Figure 1 shows the dual-band rectangular microstrip antenna, realized by means of two symmetrical rectangular slots on the patch area; the slots are added symmetrically. The dimensions of the patch area are  $L = 29$  mm and  $W = 38$  mm. The inset microstrip feed dimensions are 2.2 mm in width and 17.3 mm in length.

The slot length is 8.5 mm, with a width of 3.5 mm. The antenna is fabricated on double-sided FR4 circuit-board material, 1.6 mm in height, with a relative dielectric constant,  $\epsilon_r$ , of 4.4. The back side of the antenna is the ground plane. A microstrip line feeds the antenna, and impedance matching is achieved by means of inset feed. The signal is connected to the microstrip line by an SMA connector soldered at the edge.

Having the relative permittivity ( $\epsilon_r$ ) and height of the substrate ( $h$ ), we want to design the antenna to correspond to the first resonance frequency of  $f_r = 2.4$  GHz. The width of the antenna can be achieved via Eq. 1. Practically speaking, fields will not be confined to  $L$  or  $W$ . Due to the fringing field effect, a fraction of the field lies outside the physical dimensions. Therefore, the effective antenna length is  $2\Delta L$  larger than its physical length, as demonstrated by Eqs. 1-4<sup>25,26</sup>:

# Wi-Fi and WiMAX

$$W = 1/2f_r(\mu_0\epsilon_0)^{0.5} \times [2/(\epsilon_r + 1)]^{0.5} \quad (1)$$

$$\epsilon_{\text{eff}} = (\epsilon_r + 1)/2 + (\epsilon_r - 1)/2[1 + (12h/W)]^{0.5} \quad (2)$$

$$\Delta L = (0.412/h)[(\epsilon_{\text{eff}} + 0.3)(W/h + 0.264)/(\epsilon_{\text{eff}} - 0.258)(W/h + 0.8)] \quad (3)$$

$$L = 1/[2f_r(\epsilon_{\text{eff}})^{0.5} \times (\mu_0\epsilon_0)^{0.5}] - 2\Delta L \quad (4)$$

For a matching procedure by inset feed line, the gap has the same width as the microstrip line, and the feed position from the center (x) is calculated by Eq. 5<sup>27</sup>:

$$R_{\text{in}} = R_{\text{edge}} \sin^4(\pi x/L) \quad 0 \leq x \leq L/2 \quad (5)$$

where:

$R_{\text{in}}$  = the input impedance to match with the antenna, and

$R_{\text{edge}}$  = the input impedance of the rectangular patch at its feeding edge.

The antenna's fundamental TM<sub>10</sub> mode supports the 2.4-GHz band. By adding slots with proper shapes and at appropriate positions inside the patch, a dual-band antenna can be realized without an increase in size—leaving its radiation patterns unperturbed, in turn.<sup>28</sup> Adding two slots reduces the higher-order TM<sub>02</sub> mode and realizes the desired higher frequency band for the antenna.

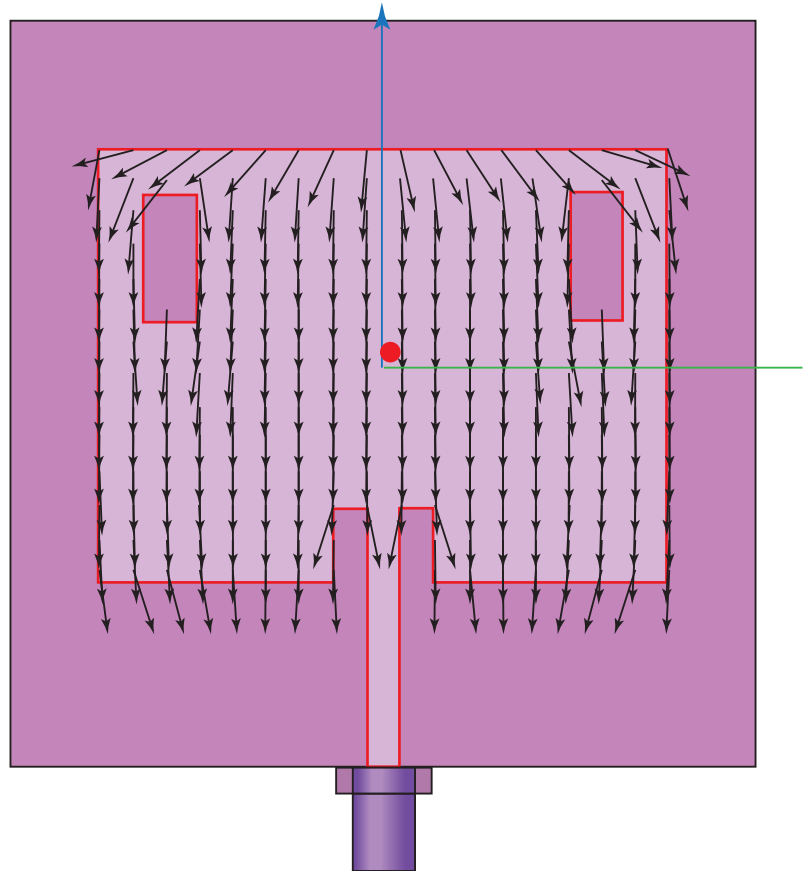
## MODELING AND MEASURING

To better understand the performance of the dual-band antenna, the surface-current distributions of the design were studied in Figure 2 for 2.4 GHz and in Figure 3 for 3.6 GHz. The TM<sub>10</sub> mode is dominant at 2.4 GHz, with surface currents showing a half-wavelength change along the patch's length. Adding slots had less effect on the surface current distribution at lower-frequency bands. Since the TM<sub>02</sub> mode is dominant at 3.6 GHz, when a pair of slots is cut from

places where the current for the TM<sub>02</sub> mode is maximum, a maximum reduction in the higher-frequency band will occur.

The slots modify the antenna's current distribution and increase the electrical length of the antenna. Although the changes in the position of the feed inset alter the input impedances at the dual frequencies, both frequencies will remain almost constant. The perturbation in surface current distributions increases with the length of the slots.<sup>28</sup>

The two rectangular slots reduced the higher-order orthogonal TM<sub>02</sub> mode resonance frequency from 3.7 GHz to 3.6 GHz, owing to the excitation of the higher-order TM<sub>02</sub> mode. Because both slots are parallel to the current for the TM<sub>10</sub> mode, and the slot length is larger than its width, the



2. This plot shows the surface current distribution on the microstrip antenna at 2.4 GHz.

lower-frequency performance remains almost constant when the slot length is increased. At higher frequencies, based on the positions of the slots, the slot can increase the length of the surface currents.

To evaluate the dual-band antenna design, it was fabricated on FR4 and measurements of return loss were performed (Fig. 4). The return loss was compared with and without slots, and test results were found to agree closely with computer simulations for the slotted antenna. The cut slots affect the higher resonance frequency band, but have little impact on the lower resonant frequency band.

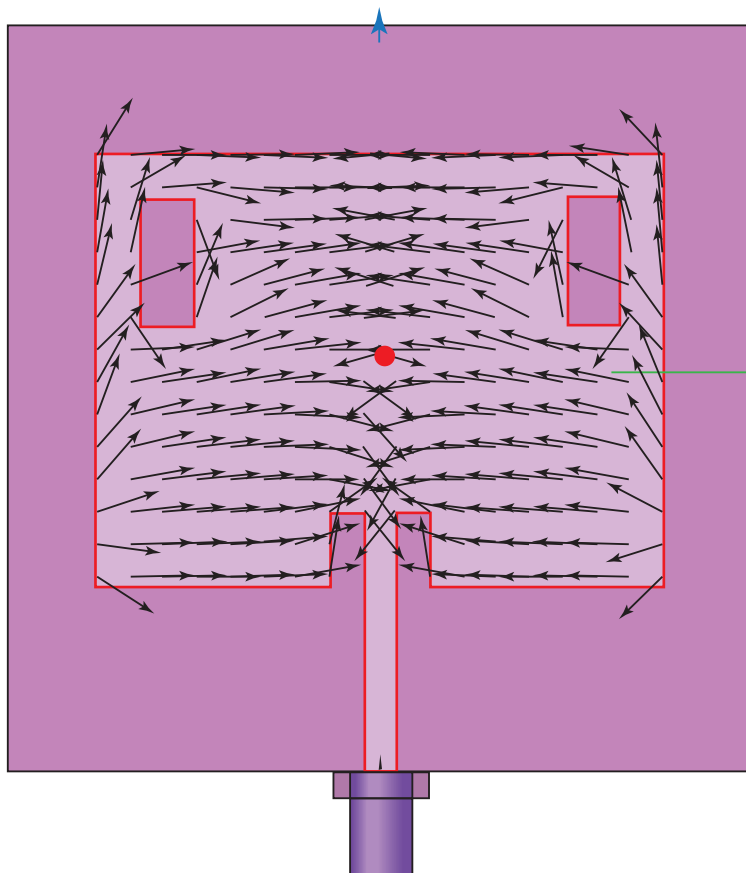
Measurements of  $S_{11}$  for the antenna's lower-frequency bandwidth were better than -10 dB from 2.412 to 2.478 GHz. This frequency band covers channels 1 to 13 for Wi-Fi applications and the antenna can be used for Wi-Fi applications for channels 1, 6, and 11 in the IEEE 802.11b protocol; for channels 1, 5, 9, and 13 in IEEE 802.11g/n; and for channels 3 and 11 in the IEEE 802.11n protocol. The return loss for the higher-frequency band was better than -10 dB from 3.58 to 3.65 GHz, suitable for WiMAX applications.

Free-space E- and H-plane pattern measurements were also made on the prototype antenna, with gain of  $\theta$  and gain of  $\phi$  presented in Figures 5 and 6, respectively. The radiation pattern gain ( $\theta$ ) is a maximum for 2.4 GHz at 0 deg. when  $\phi = 90$  deg. The gain  $\theta$  is leaning toward 0 deg. due to the ground plane. The pattern is almost symmetrical for  $\phi = 0$  deg., although it is particularly weak, with almost no current contributing to it. The added slots do not change the surface current distributions at lower-frequency bands, so the radiation patterns are almost similar at 2.4 GHz with or without slots.

The effects of the slots are more pronounced at higher frequencies. The radiation pattern for 3.6 GHz is a maximum at 90 and 270 deg., with two nulls at 0 and 180 deg. Although the gain  $\theta$  when  $\phi = 90$  deg. is lower than when  $\phi = 0$  deg., the difference is not as great as at the lower-frequency band. The radiation pattern is closer to being omnidirectional at the higher resonant frequency.

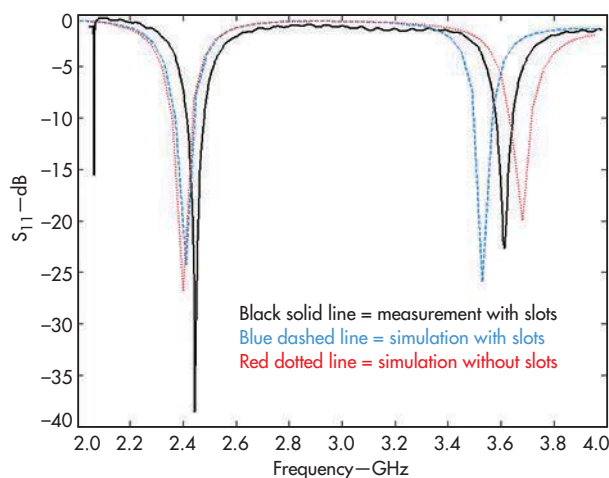
When the length of the slots increases, the surface currents are directed along the length of the slots. By increasing the lengths of the slots, the radiation pattern becomes more broadsided.

The gain  $\phi$  exhibits almost similar patterns for  $\theta = 0$  deg. and  $\theta = 90$  deg. at 2.4 GHz. The antenna patterns are omnidirectional, with two nulls at 90 and 270 deg. At 3.6 GHz, adding slots reduced the magnitude of the gain  $\phi$  compared to that



3. This plot shows the surface current distribution on the microstrip antenna at 3.6 GHz.

at 2.4 GHz. The pattern shape after adding slots for  $\theta = 0$  deg. remained similar, and only the magnitude level dropped. For  $\theta = 90$  deg., the magnitude level remained unchanged, but two dents were detected at  $\phi = 188$  deg. and  $\phi = 350$  deg.

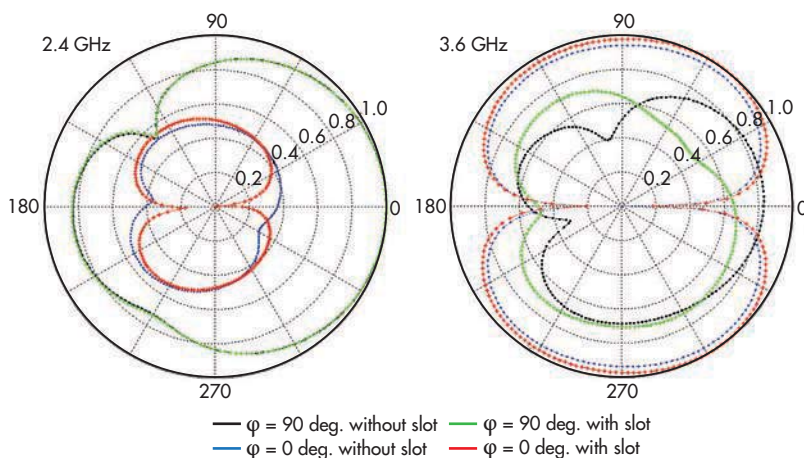


4. The plots show measured and simulated return loss for the dual-band antenna.



In short, it was possible to produce a dual-band antenna for Wi-Fi/WiMAX using a rectangular microstrip patch, with two rectangular slots on the patch area and inset feeding. The two frequency bands step from the TM<sub>10</sub> and TM<sub>02</sub> microstrip modes.

The antenna provides lower-frequency coverage of 2.412 to 2.478 GHz and higher-band coverage of 3.58 to 3.65 GHz, with proper radiation patterns in both of those bands. Overall, the antenna's simple planar structure helps facilitate the fabrication of Wi-Fi/WiMAX applications. **mw**



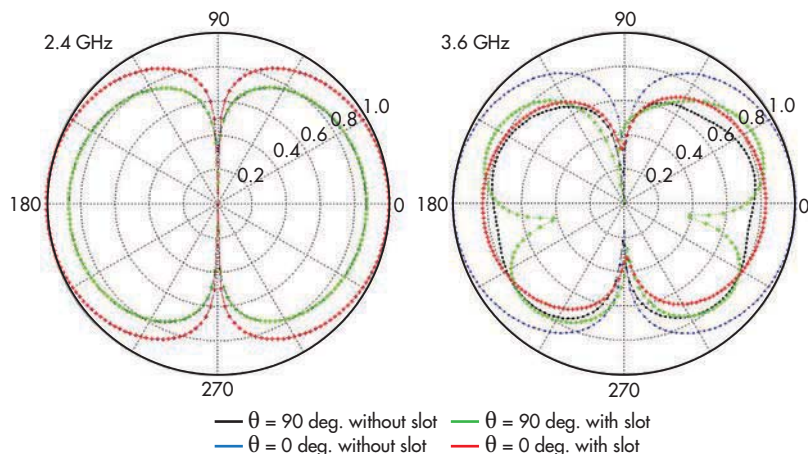
5. The curves show the gain  $\theta$  for the patch antenna with and without slots.

## REFERENCES

1. K. Ding, T. Yu, Q. Zhang, and K. Luo, "Dual-band Circularly Polarized Aperture Coupled Annular-ring Microstrip Antenna for GNSS Applications," in *Frequenz*, Vol. 68, 2014, p. 19.
2. V. Sharma and M.M. Sharma, "Wideband Gap Coupled Assembly of Rectangular Microstrip Patches for Wi-Max Applications," in *Frequenz*, Vol. 68, 2014, p. 25.
3. A. Narbudowicz, B. Xiu Long, and M.J. Ammann, "Dual-Band Omnidirectional Circularly Polarized Antenna," *IEEE Transactions on Antennas and Propagation*, Vol. 61, 2013, pp. 77-83.
4. C. Shih-Hsun and L. Wen-Jiao, "A Novel Dual Band Circularly Polarized GNSS Antenna for Handheld Devices," *IEEE Transactions on Antennas and Propagation*, Vol. 61, 2013, pp. 555-562.
5. X.L. Sun, S.W. Cheung, and T.I. Yuk, "Dual-Band Monopole Antenna With Frequency-Tunable Feature for WiMAX Applications," *IEEE Antennas and Wireless Propagation Letters*, Vol. 12, 2013, pp. 100-103.
6. P. Borah, A.K. Bordoloi, N.S. Bhattacharyya, and S. Bhattacharyya, "Bridged 'V'-shaped patch antenna for dual-band communication," *Electronics Letters*, Vol. 48, 2012, pp. 419-420.
7. F. Mirzamohammadi, J. Nourinia, and C. Ghobadi, "A Novel Dual-Wideband Monopole-Like Microstrip Antenna With Controllable Frequency Response," *IEEE Antennas and Wireless Propagation Letters*, Vol. 11, 2012, pp. 289-292.
8. M. Gaffar, M.A. Zaman, S.M. Choudhury, and M.A. Matin, "Design and optimisation of a novel dual-band circularly polarised microstrip antenna," *IET Microwaves, Antennas & Propagation*, Vol. 5, 2011, pp. 1670-1674.
9. O. Quevedo-Teruel, M.N.M. Kehn, and E. Rajo-Iglesias, "Dual-Band Patch Antennas Based on Short-Circuited Split Ring Resonators," *IEEE Transactions on Antennas and Propagation*, Vol. 59, 2011, pp. 2758-2765.
10. M.A. Al-Joumayli, S.M. Aguilar, N. Behdad, and S.C. Hagness, "Dual-Band Miniaturized Patch Antennas for Microwave Breast Imaging," *IEEE Antennas and Wireless Propagation Letters*, Vol. 9, 2010, pp. 268-271.
11. Q. XuLin, L. RongLin, C. YueHui, and M.M. Tentzeris, "Analysis and Design of a

- Compact Dual-Band Directional Antenna," *IEEE Antennas and Wireless Propagation Letters*, Vol. 11, 2012, pp. 547-550.
12. C.R. Medeiros, E.B. Lima, J.R. Costa, and C.A. Fernandes, "Wideband Slot Antenna for WLAN Access Points," *IEEE Antennas and Wireless Propagation Letters*, Vol. 9, 2010, pp. 79-82.
13. R. Gardelli, G. La Cono, and M. Albani, "A low-cost suspended patch antenna for WLAN access points and point-to-point links," *IEEE Antennas and Wireless Propagation Letters*, Vol. 3, 2004, pp. 90-93.
14. Z. Hongjiang, Y. Abdallah, R. Chantalat, M. Thevenot, T. Monediere, and B. Jecko, "Low-Profile and High-Gain Yagi Wire-Patch Antenna for WiMAX Applications," *IEEE Antennas and Wireless Propagation Letters*, Vol. 11, 2012, pp. 659-662.
15. T. Wu, L. Rong-Lin, E. Soon Young, M. Seong-Sik, L. Kyutae, J. Laskar, et al., "Switchable Quad-Band Antennas for Cognitive Radio Base Station Applications," *IEEE Transactions on Antennas and Propagation*, Vol. 58, 2010, pp. 1468-1476.
16. G. Ghobadi and M. Majdzadeh, "Compact Antenna Snares WiMAX/WLAN," *Microwaves & RF*, May 2014.
17. X.-D.Y. Yin-Song Li, Yu Bai, and Tao Jiang, "Dual-Band Antenna Handles WLAN/WiMAX," *Microwaves & RF*, June 2011.
18. K. Jain Satish and S. Jain, "Performance Analysis of Coaxial Fed Stacked Patch Antennas," in *Frequenz* Vol. 68, 2014, p. 7.
19. M. Chen and C.C. Chen, "A Compact Dual-Band GPS Antenna Design," *IEEE Antennas and Wireless Propagation Letters*, Vol. 12, 2013, pp. 245-248.
20. T. Fujimoto and S. Fukahori, "Broadband dual-band stacked square microstrip antenna with shoring plates and slits," *IET Microwaves, Antennas & Propagation*, Vol. 6, 2012, pp. 1443-1450.
21. M.I. Sabran, S.K.A. Rahim, A.Y.A. Rahman, T.A. Rahman, M.Z.M. Nor, and Evizal, "A Dual-Band Diamond-Shaped Antenna for RFID Application," *IEEE Antennas and Wireless Propagation Letters*, Vol. 10, 2011, pp. 979-982.

22. H.T. Hsu and T.J. Huang, "Generic dipole-based antenna-featuring dual-band and wideband modes of operation," *IET Microwaves, Antennas & Propagation*, Vol. 6, 2012, pp. 1623-1628.
23. H. Tiwari and V. Kartikeyan Machavazam, "A Stacked Microstrip Patch Antenna Loaded With U-Shaped Slots," in *Frequenz*, Vol. 65, 2011, p. 167.
24. P. Lindberg, E. Ojefors, Z. Barna, A. Thornell-Pers, and A. Rydberg, "Dual wideband printed dipole antenna with integrated balun," *IET Microwaves, Antennas & Propagation*, Vol. 1, 2007, pp. 707-711.
25. R. Garg, *Microstrip antennas design handbook*, Artech House, Boston, MA, 2001.
26. M.M. Shafiei and M. Roslee, "A Compact Slotted Bowtie Patch Antenna," in *The 2009 International Symposium on Antennas and Propagation (ISAP 2009)*, Bangkok, Thailand, 2009, pp. 349-352.
27. T.A. Milligan, *Modern Antenna Design*, 2nd ed., IEEE Press/Wiley Interscience, Hoboken, NJ, 2005.
28. A.A. Deshmukh and K.P. Ray, "Formulation of Resonance Frequencies for Dual-Band Slotted Rectangular Microstrip Antennas," *IEEE Antennas and Propagation Magazine*, Vol. 54, 2012, pp. 78-97.



6. The curves show the gain  $\phi$  for the patch antenna with and without slots.

# LTE DEVICE TESTING: FROM THEORY TO MEASUREMENT

**T**HE HIGH DATA rates, carrier aggregation, and multiple-input multiple-output (MIMO) operation of LTE devices creates a complex transmitter (Tx) and receiver (Rx) measurement environment. In an application note titled, "Introduction to LTE Device Testing: From Theory to Transmitter and Receiver Measurements," National Instruments helps to decipher LTE device testing from the signal structure to measuring spurious emissions. Three categories are covered in this document: LTE and LTE Advanced (LTE-A) structure/theory of operation, LTE Tx measurements, and LTE Rx measurements.

The note describes LTE and its use of the orthogonal frequency-division multiplexing (OFDM) scheme. For the uplink, LTE is modulated with OFDM-access (OFDMA). It uses multiple subcarriers grouped into resource blocks in order to accommodate multiple users. Using

single-carrier frequency division multiple access (SC-FDMA) and fast Fourier transform (FFT) techniques, that uplink approach can apply pre-coding before the symbols are modulated onto subcarriers. This method reduces the peak-to-average power ratio (PAPR) of the transmission. Up to eight input antenna and eight output antenna are possible in release 10 of the LTE-A standards. In addition, up to five carriers can be aggregated to create a higher data rate without using higher-order modulation schemes.

Going on to describe the Tx measurements, the note details power, signal-quality, and spectrum measurements for LTE transmitters. The bulk of LTE Tx testing is done according to the 3GPP TS 36.521 section of the LTE standard. It requires a combination of a vector signal generator (VSG) and vector signal ana-

lyzer (VSA). Both the lowest and highest bandwidth configurations are required for testing LTE devices under various modulation schemes for maximum output-power tolerance.

In the LTE standard, 3GPP TS 36.521 section 7 describes the necessary Rx measurements from a reference sensitivity level to adjacent-channel selectivity and spurious emissions. The note specifies that these measurements only apply to the handset receiver and not to typical receiver components, such as low-noise and power amplifiers. The primary figure of merit for an LTE Rx is receiver throughput, which is a measure of the data rate through the Rx hardware. This is exemplified with LTE sensitivity being defined as the lowest average power level required for the Rx to achieve 95% of the throughput maximum.

**National Instruments,  
11500 N Mopac Expwy,  
Austin, TX 78759-3504  
(877) 388-1952,  
www.ni.com**

## ENHANCE ACTIVE LOAD-PULL IN DOHERTY POWER AMP

**FOR TELECOMMUNICATIONS APPLICATIONS,** Doherty power-amplifier (PA) configurations can offer excellent power efficiency while accommodating the high peak-to-average-power ratios (PAPRs) of the latest modulation schemes. Load-pull techniques are highly valuable in optimizing and tuning these PA configurations to better performance. In an application note from Mesuro, "Application of the Mesuro Active Load-Pull System in Doherty Power Amplifier Design and Optimization," the authors disclose techniques for defining Doherty PA performance and enhancing PA designs.

The note describes how a Doherty amplifier acts like an active load-pull system between two amplifiers, connected to each other by the impedance transformer. The impedance at the output of each device varies as a function of the envelope magnitude. This factor requires certain output dynamics to be de-embedded to capture the internal behavior of a Doherty PA and optimize the bias voltages. To generate measurement data with a reference at the current generator plane, the resulting currents and voltages are combined with the synthesis of the input drive, output load impedance, and bias conditions.

For the bias conditions, each device needs to be estimated with direct-current (DC) measurements and steadily refined using the RF waveforms in isolation. Load-pull aids in deciding the optimum impedance. The main amplifier is initially tested and refined. The bias and load-pull waveforms from these earlier tests are used to aid in refining the auxiliary, or peaking, amplifier's behavior. It should be noted that reliability is an issue with the auxiliary amplifier. The note cautions engineers to keep the generated voltages below the breakdown threshold of the auxiliary amplifier while operating in the high-impedance state.

After effectively biasing the devices and analyzing their performance in isolation, a matching network between the devices can be designed. During this process, the note explains how tradeoffs must be made. Here, iterative testing will provide the best insight into the realistic performance of the manufactured design. This analysis process can be used with immature device processes to help gain in-depth understanding of process limitations, and even aid in illuminating possible redesign approaches for enhanced functionality.

**Mesuro Ltd.,  
Pencoed Technology Park,  
Pencoed, UK CF35 5HZ,  
www.mesuro.com**

# UP TO 100 Watt AMPLIFIERS

**NOW! 100 kHz to 18 GHz**



**\$995**  
from ea. qty. (1-9)

**High-powered performance across wide frequency ranges.** These class A/AB linear amplifiers have set a standard throughout the RF & microwave industry. Rugged and reliable, they feature over-voltage and over-temperature protection, including the ability to withstand opens and shorts! And they're all in stock, whether with a heat sink/fan (for design labs and test benches), or without (for quick integration into customer assemblies). Go to [minicircuits.com](http://minicircuits.com), where it's easy to select the models that meet your needs, including new features like TTL-controlled RF output. Place an order today, and you can have them in your hands as soon as tomorrow—or if you need a custom model, just give us a call for an engineer-to-engineer discussion of your requirements!

Model	Frequency (MHz)	Gain (dB)	Pout @ Comp.		\$ Price (Qty. 1-9)
			1 dB (W)	3 dB (W)	
ZVE-3W-83+	2000-8000	35	2	3	1295
ZVE-3W-183+	5900-18000	35	2	3	1295
ZHL-4W-422+	500-4200	25	3	4	1570
<b>NEW</b> ZHL-5W-422+	500-4200	25	3	5	1670
<b>NEW</b> ZHL-5W-2G+	800-2000	45	5	6	995
ZHL-10W-2G	800-2000	43	10	13	1295
• ZHL-16W-43+	1800-4000	45	13	16	1595
• ZHL-20W-13+	20-1000	50	13	20	1395
• ZHL-20W-13SW+	20-1000	50	13	20	1445
LZY-22+	0.1-200	43	16	32	1495
ZHL-30W-262+	2300-2550	50	20	32	1995
ZHL-30W-252+	700-2500	50	25	40	2995
LZY-2+	500-1000	47	32	38	2195
LZY-1+	20-512	42	40	50	1995
• ZHL-50W-52+	50-500	50	40	63	1395
• ZHL-100W-52+	50-500	50	63	79	1995
• ZHL-100W-GAN+	20-500	42	79	100	2395
ZHL-100W-13+	800-1000	50	79	100	2195
ZHL-100W-352+	3000-3500	50	100	100	3595
ZHL-100W-43+	3500-4000	50	100	100	3595
LZY-5+	0.4-5	52.5	100	100	1995

Listed performance data typical, see [minicircuits.com](http://minicircuits.com) for more details.

• Protected under U.S. Patent 7,348,854



[www.minicircuits.com](http://www.minicircuits.com) P.O. Box 350166, Brooklyn, NY 11235-0003 (718) 934-4500 [sales@minicircuits.com](mailto:sales@minicircuits.com)





The Original Electronics Parts Search & Procurement Tool



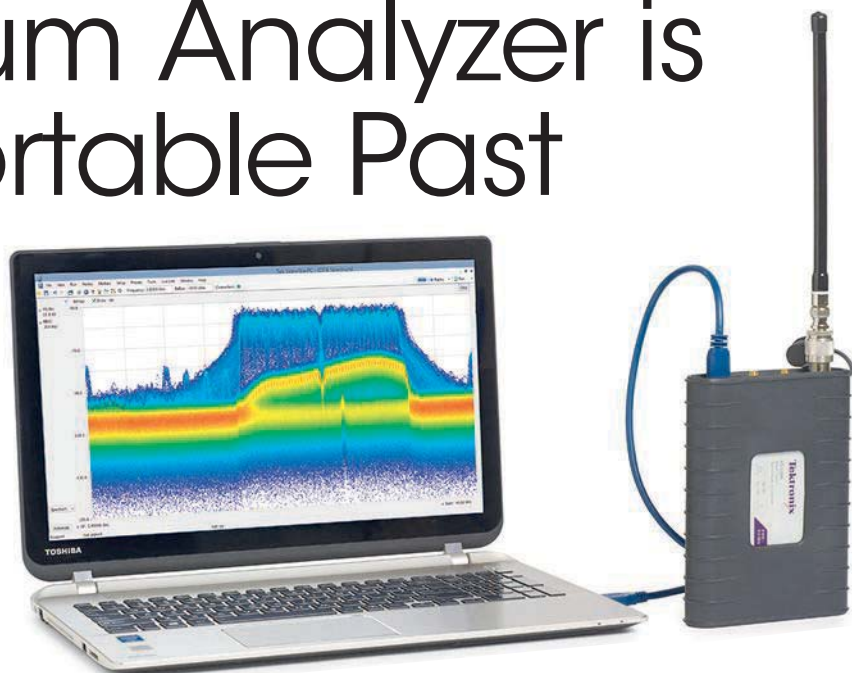
# SEARCH PARTS FAST

*Your Trusted Source*

**[www.SourceESB.com](http://www.SourceESB.com)**

# Spectrum Analyzer is Truly Portable Past 6 GHz

Fitting into a housing about the size of an old-fashioned transistor radio, this very modern spectrum analyzer teams with a computer to accurately scrutinize spectrum past 6 GHz.



1. The RSA306 spectrum analyzer works with measurement software running on a laptop or other PC to form a lightweight, portable measurement system ranging from 9 kHz to 6.2 GHz.

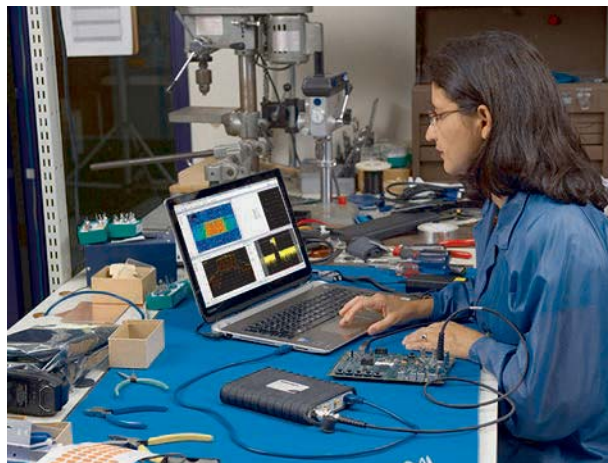
**SPECTRUM ANALYZERS** have long been among the most popular, invaluable RF/microwave test equipment. By offering as much measurement power in the RSA306 portable spectrum analyzer for such a low price, Tektronix ([www.tek.com](http://www.tek.com)) now makes this instrument more accessible to a greater number of users.

As an added bonus, this truly is a “green” measuring tool, requiring only 4 W of operating power for spectrum measurements from 9 kHz to 6.2 GHz. The compact instrument works with the processing functionality of a PC and Tektronix’s supplied SignalVu-PC software to provide all of the capabilities of a full-sized spectrum analyzer at a fraction of the size and price.

The compact RSA306 (*Fig. 1*) is not the spectrum analyzer of years past—which is to say, one of those hefty portable units with carrying handles (the 492 and 494 series) upon which Tektronix built its reputation. This new, portable instrument weighs a mere 1.2 lb and is the firm’s first spectrum analyzer with a Universal Serial Bus (USB) 3.0 connection, but it certainly won’t be Tektronix’s last. It is designed for use with a laptop or other PC running with the proper measurement software.

The essential spectrum-analyzer functionality is contained within the RSA306’s portable-radio-sized housing; it relies on the computer for control, processing, and screen display to show captured signals across an instantaneous real-time bandwidth of 40 MHz. The analyzer has a frequency range of 1 kHz to 40

MHz. The RSA 306 measures just  $5.0 \times 7.5 \times 1.2$  in. ( $127 \times 190.5 \times 30.5$  mm), making it a perfect fit for both field and laboratory. It uses a Type-N female RF/microwave input connector and SMA female connectors for the external frequency reference input and trigger/sync input signals.



2. The RSA306, PC, and software combine to provide a flexible benchtop measuring system that can perform an extensive amount of signal analysis.

The RSA306 (*Fig. 2*) achieves a frequency accuracy of 3 ppm across its full operating temperature range; amplitude measurement ranges from  $-160$  to  $+20$  dBm. Absolute amplitude measurement accuracy is  $\pm 1$  dB + the absolute amplitude accuracy for room-temperature measurements (from  $+18$  to  $+28^{\circ}\text{C}$ ). The spectrum analyzer can perform stepped measurements, with dwell times per step from 50 ms to 100 s.

Resolution-bandwidth (RBW) filter range spans from 10 Hz to 10 MHz and can achieve in-phase/quadrature (I/Q) measurement resolution of 17.9 ns for an acquisition bandwidth of 40 MHz. This rugged little analyzer minimizes noise: its second-harmonic distortion is typically less than  $-55$  dBc from 10 to 300 MHz at a reference level of 0 dBm, and typically less than  $-50$  dBc from 10 MHz to 3.1 GHz at a reference level of  $-40$  dBm.

The analyzer's displayed average noise level (DANL) is specified as  $-130$  dBm/Hz from 100 kHz to 42 MHz;  $-145$  dBm/Hz from 2 to 5 MHz;  $-160$  dBm/Hz from beyond 5 MHz to 1 GHz;  $-158$  dBm/Hz from beyond 1 GHz to 2 GHz;  $-155$  dBm/Hz from beyond 2 GHz to 4 GHz; and  $-150$  dBm/Hz from beyond 4 GHz to 6.2 GHz. The instrument's phase noise for a carrier of 10 MHz is  $-108$  dBc/Hz offset 1 kHz from the carrier;  $-118$  dBc/Hz offset 10 kHz from the carrier;  $-120$  dBc/Hz offset 100 kHz from the carrier; and  $-122$  dBc/Hz offset 1 MHz from the carrier.

At the other extreme, the RSA306's phase noise for a 6-GHz carrier is  $-70$  dBc/Hz offset 1 kHz from the carrier;  $-75$  dBc/Hz offset 10 kHz from the carrier;  $-85$  dBc/Hz offset 100 kHz from the carrier; and  $-105$  dBc/Hz offset 1 MHz from the carrier.

It is important to remember that the PC contributes to the performance of the RSA306 spectrum analyzer, not just to controlling the analyzer. The RSA306 requires a PC with Windows 7 or Windows 8 or 8.1 with a 64-bit operating system and a USB 3.0 connection to link the PC with the spectrum analyzer. To take full advantage of the RSA306's features and performance, an Intel Core i7 4th generation processor is required.

The portable analyzer ships with SignalVu-PC software, which will run on most laptop or desktop PCs and provides tremendous flexibility in the measurement and analysis of signals within the RSA306's range. In addition to using SignalVu-PC for running tests and programming control of the RSA306, the software can be used with an included application programming interface (API) to execute its own extensive set of commands and measurements.

Also, a MATLAB driver is available for the SignalVu-PC API. As a result, the RSA306 can be operated with the MATLAB mathematical analysis software, as well as the Instrument



**3. With its light weight and low power consumption, the RSA306 and the SignalVu-PC software can tackle a wide range of in-the-field measurements to 6.2 GHz.**

Control Toolbox, both developed by The MathWorks ([www.mathworks.com](http://www.mathworks.com)).

By leveraging the SignalVu-PC software, the RSA306 can perform many measurements beyond a traditional spectrum analyzer. The basic software provides spectrum-analyzer functionality with three signal traces and a spectrogram trace, along with five markers with power, relative power, integrated power, and other functions.

The software also supports basic vector analysis functions—amplitude, frequency, and phase versus time, as well as I and Q versus time. The software enables AM/FM radio monitoring and measurements, multichannel power measurements, adjacent-channel leakage ratio (ACLR) measurements, and use of the

complementary cumulative distribution function (CCDF) to plot statistical variations in signal levels.

On top of that, the software can be used for spectrum mask testing with the RSA306, to simplify signal monitoring of a portion of spectrum of interest. Mask testing helps find intermittent interference or other types of spectrum violations. The software can be used to color-code signals of interest, using a mask to identify a particular portion of spectrum. When equipped with option SVP for the SignalVu-PV software, the compact RSA306 spectrum analyzer can even make pulsed signal measurements.

The SignalVu-PC MAP option allows the RSA306 to perform interference hunting and signal-strength analysis. This software can create a geographical map on the PC screen, showing different sources of interference received by the RSA306. This software option makes it possible to draw a line or an arrow on a mapped measurement to indicate the direction the measurement antenna was pointing.

Other SignalVu-PC software options cover various WLAN 802.11 testing capabilities, orthogonal frequency-division-multiplexing (OFDM) analysis, general-purpose modulation analysis, audio analysis, and settling-time (frequency and phase) measurements. Option SVM supports analysis of a wide variety of digital modulation formats.

Though compact and light in weight, the RSA306 is rugged enough for continuous field use, meeting MIL-STD-28800 Class-2 environmental requirements for shock and vibration. It can very much be thought of as a wideband radio module, working with software-defined-radio (SDR) architectures (*Fig. 3*).

The RSA306 should be given a warmup time of about 30 minutes after connecting it to a PC. P&A: \$3490; stock. **ttv**

TEKTRONIX, INC., 14200 SW Karl Braun Dr., P.O. Box 500, Beaverton, OR 97077; (877) 977-0425; [www.tektronix.com](http://www.tektronix.com)



# USB & Ethernet **SIGNAL GENERATORS**

*That fit your budget.*



from **\$1995** ea.

*Control your test setup via Ethernet or USB with a synthesized signal generator to meet your needs and fit your budget!*

Mini-Circuits' SSG-6400HS, SSG-6000RC, and the new SSG-6001RC feature both USB and Ethernet connections, giving you more choices and more freedom.

Small enough to fit in your laptop case, all models provide sweep and hopping capabilities over frequencies and power levels and are designed for easy integration with other test equipment using trigger and reference ports. They even feature built-in automatic calibration scheduling based on actual usage!

Our user-friendly GUI software, DLLs and programming instructions are all included so you can control your SSG through our software or yours! Visit [minicircuits.com](http://minicircuits.com) today to find the right model for your application!

Bands as wide as **0.25 to 6400 MHz**

#### Models Available from Stock at Low Prices!

**SSG-6400HS** \$4,995

- 0.25 to 6400 MHz
- -75 to +10 dBm P<sub>out</sub>
- AM, PM, FM, and pulse modulation
- USB and Ethernet control

**New**

**SSG-6001RC** \$3,495

- 1 to 6000 MHz
- -60 to +15 dBm P<sub>out</sub>
- Pulse modulation
- USB and Ethernet control

**SSG-6000RC** \$2,795

- 25 to 6000 MHz
- -65 to +14 dBm P<sub>out</sub>
- Pulse modulation
- USB and Ethernet control

**SSG-4000LH** \$2,395

- 250 to 4000 MHz
- -60 to +10 dBm P<sub>out</sub>
- Pulse modulation
- Low harmonics (-66 dBc)
- USB control

**SSG-4000HP** \$1,995

- 250 to 4000 MHz
- High power, -50 to +20 dBm
- Pulse modulation
- USB control



2U 19" Rack-Mount Option Available



# Exceptional companies have superior labs.

**1. Test port cable assemblies & metrology adapters** - the industry's best VSWR spec!

**2. Turnkey in-fixture characterization** of non-50Ω load pull, noise parameters & s-parameters up to 110 GHz.

**3. Phase Stable & Amplitude Stable cable assemblies** for all VNA applications. Maury's *Stability™* - phase stability at its best!

**4. Pulsed IV/RF solutions** for model development & validation - essential for GaN R&D!

**5. World's Fastest Active Load Pull System** - Maury's MT2000 is the only solution to control wideband impedances for modulated signals!

**6. Turnkey on-wafer characterization systems** built by Maury for non-50Ω load pull, noise parameters & s-parameters up to 110 GHz.

**7. Torque wrenches & connector gages** - for guaranteed interconnections!

**8. The industry's best price/performance** - Maury's *Utility™* cable assemblies are ideal for everyday lab applications.

**9. Lab adapters for everyday use** - Maury's *Test Essentials™* offer the excellent performance at the right price.

**10. Coaxial & waveguide calibration kits** for all VNAs - when only mechanical calibrations will do!

**11. Color-Coded precision adapters** - use Maury's *ColorConnect™* adapters to avoid expensive mismatch mistakes!



## Complete your lab with Maury Microwave.



**MAURYMW.COM**

MAURY MICROWAVE CORPORATION

2900 Inland Empire Blvd., Ontario, California, USA 91764

Tel: 909-987-4715 • FAX: 909-987-1112 • Email: [maury@maurymw.com](mailto:maury@maurymw.com)



*Your Calibration, Measurement & Modeling Solutions Partner!*



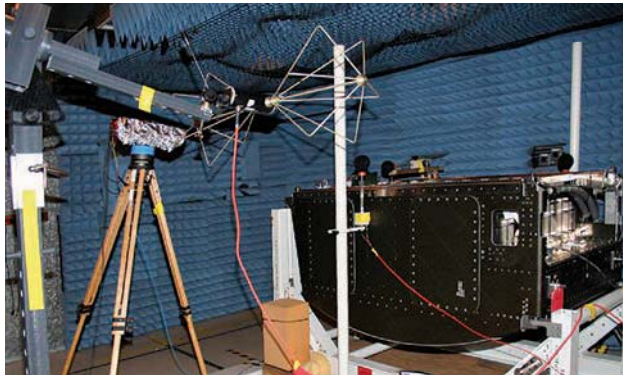
# Raise EMI/EMC Testing Speed, Cut Size and Cost

**With more and more devices coming to market, EMI/EMC testing must become faster and less burdensome while avoiding any certification shortcuts.**

**FOR THOUSANDS OF** electronic device manufacturers, electro-magnetic interference and compliance (EMI/EMC) testing has grown very complex and difficult. This necessary design step has traditionally been fraught with time-consuming and costly testing rounds, which use large and expensive setups (Fig. 1). EMI/EMC testing demands have also increased because virtually all markets require more electronic devices.

According to a report by Frost & Sullivan, many companies are looking for alternative approaches to costly EMI/EMC testing—especially since 2008’s economic downturn continues to affect many companies’ ability to purchase capital equipment. These factors have inspired a large number of these firms to design creative solutions to common EMI/EMC testing challenges. In doing so, they are making EMI/EMC testing more cost-effective and better suited to the size of the application, and at the same time lessening its impact on today’s rapid-paced design cycles.

Among the issues that need to be overcome is the large bottleneck caused by compliance testing in the rollout of the latest electronics. For EMC testing in particular, one of the most challenging aspects is tracking down its failure mode. To address a radiator or cause of RF leakage, the exact location on a device needs to be known. This demand is difficult to meet with remote or chamber-based testing. Yet this problem is becoming more significant with the increasingly common multi-domain printed circuit boards (PCBs)



**1. Traditional EMI/EMC testing is done in large RF-interference-shielded chambers with emission-absorbing walls.** (Courtesy of NASA)

used in the latest devices. Common methods of hand-probing are also prone to error and high costs while consuming a lot of time.

As mentioned, creative solutions are being developed. For example, EMscan designed products to aid designers rapidly troubleshoot and achieve pre-compliance EMC testing in a low-cost, small tabletop footprint without the need for an anechoic chamber.

The EMxpert near-field scanner consists of an array of magnetic field (H) probes, which connect to a switch array with a built-in spectrum analyzer. That analyzer passively couples with the near-field (NF) emissions of a device placed on the device-under-test (DUT) surface above the probe array. Insertion loss and antenna factor compensation are applied to each individual probe to lower sensing error.

In addition, interpolation algorithms are applied on the array of 1218 probes to artificially increase the real-time resolution of the scanner down to 3.75 mm. Using a Gorilla glass plate for the DUT to rest on, X/Y-axis stepper motors can precisely adjust

the device to move among four positions. This motion effectively increases the number of test points to 4096 while bringing resolution as low as 0.12 mm.

Because the NF magnetic probe array and algorithms mitigate the effective interference and noise from outside radiators, an anechoic chamber is largely unnecessary. Additionally, the PC-driven EMC scanner software can be used to pinpoint the exact location of



**2. This probe head promises to enable long, low-cost, and lightweight cable that is immune to RFI. It also does not degrade signal quality as significantly as long coaxial cabling.** (Courtesy of Wavecontrol)



## EMI/EMC Testing

a troubled area with a schematic or device drawing overlaying the emissions mapping. Alternatively, the system can be incorporated into an automated testing scheme powered by the PC.

Because the EMscan instrument offers enhanced scan resolution and scanner speed, large device manufacturers are using these scanners to speed their design process without suffering from any cost implications. Given the decreases in military/defense spending and the tightening cost savings with commercial device manufacturers, testing that offers performance in small, fast, and cost-effective packages is becoming increasingly valuable.

Another creative response to this trend is the interference and compatibility evaluation system (ICEy) by Speag. The ICEy greatly resembles a 3D printer with its precision position electronics and computer interface. The PC-driven, active 3D probing solution uses time-domain-sensor (TDS) probes with active sensor electronics in their tip and fiber-optic data transmission to the PC. The resulting small floating probe limits the perturbations of the DUT while increasing sensitivity for sensing the full electromagnetic phasor in vector form.



**3. Using a machine-vision feedback network can increase the resolution of 3D positioning.** (Courtesy of Speag)

The TDS probes connect to a National Instruments vector signal analyzer through an 18-slot PXI-based platform. ICEy is enclosed in its own anechoic chamber, allowing for scan areas to  $450 \times 450 \times 115 \text{ mm}^3$  with probe accuracy of  $\pm 25 \mu\text{m}$ . In addition, it has a built-in 3D scanning system and mapper.

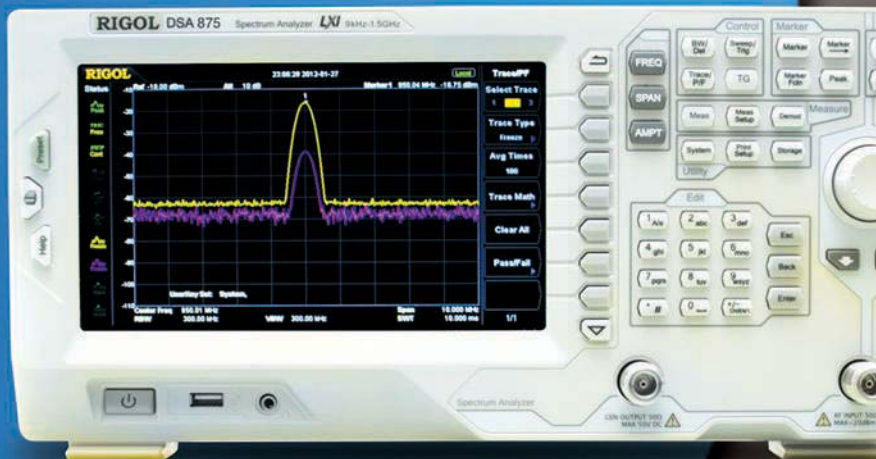
A sophisticated and compact measurement and control platform is tightly coupled to the ICEy system's advanced computational platform. This platform can be traced to international calibration standards. Furthermore, the configuration enables real-time detection of EMI/EMC issues with visual confirmation. Because the ICEy system is produced as a single product, consistency and calibration reliability are much easier to maintain than a traditional anechoic chamber.

Beyond testing for interference and compatibility, manufacturers are consistently calling for shorter design and production cycles. If large industrial equipment or devices are involved in the design or production process, the time delay for testing increases dramatically. Another issue is the need for on-site testing systems to be delivered at high cost and with long lead times. To offer an alternative approach, TÜV Rheinland developed an

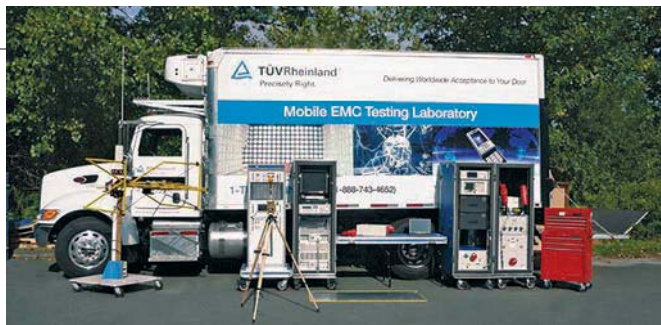
## DSA800 Series Spectrum Analyzer

### Ideal for WiFi & 2.4 GHz Apps

- 3 Models with Frequencies to 1.5 GHz, 3.2 GHz & 7.5 GHz
- DANL of -161dBm (typ) Normalized to 1 Hz
- Available Tracking Generator
- EMI and VSWR Packages
- View 3rd Harmonic of 2.4 GHz Wireless Signals
- Models Starting at \$1,295



Visit [RigolRF.com](http://RigolRF.com) or call 877-4-RIGOL-1



**4. Special care must be taken when transporting EMI/EMC test equipment, as its calibration and accuracy can be damaged as a result of temperature shifts, vibration, and pressure.** (Courtesy of TUV Rheinland)

in-situ EMC testing system on a mobile platform that operates as a dedicated mobile lab. These mobile labs have equipment specifically prepared for indoor, outdoor, and factory-floor testing, including a complete report. TUV Rheinland advertises that testing can be done within three days of arrival.

The mobile labs reside in a box truck that is specifically designed to transport sensitive test equipment while maintaining its calibration standards with both temperature/humidity control and a vibration-reducing, air-based suspension. For EMI/EMC testing in particular, having high-quality and traceable calibrations and standards is necessary.

Another way to reduce the reliance on expensive and dedicated test facilities is to automate a PC-driven testing environ-

ment with highly configurable and adaptable software. ETS-Lindgren and DARE!! have provided and advanced such software environments with the integrated laboratory environments, TILE! and RadiMation, respectively. The goal of both software systems is to provide EMC-accredited-level automated testing and report generation that is compatible with a variety of test instruments and systems.

As enterprising companies like the ones mentioned here have cut costs, increased accessibility, and enhanced the performance of EMI/EMC testing systems, they also have provided value to other engineering industries. For example, having low-cost and rapid testing available within reach in easy-to-use PC-driven systems is a practical response to the growth of EMI/EMC testing, thanks to the increase in wireless and small electronic devices.

As industrial equipment and large devices increasingly embrace more components, more mobile and rapid on-site in-situ testing also is necessary. As the volume and complexity of all testing systems continues to rise, using automated software systems with PC-driven test hardware is becoming necessary to reduce errors and increase testing speed. Meanwhile, regulatory bodies continue to demand higher-quality standards and more rigorous testing, making the use of higher-performing EMI/EMC equipment and systems inevitable. **mtw**

# Uncompromised Performance... Unprecedented Value

- Full RF Portfolio
- Spectrum Analyzers, RF Signal Generators & Application Software
- Lower Your Cost of Test

**RIGOL**  
Beyond Measure

**TRY RISK FREE  
for 30 days**



DSG3000 RF Signal Generator

**Oscilloscopes • MSOs • Waveform Generators  
RF Test • Precision Measurement**



# Touchscreens Simplify Oscilloscopes to 1 GHz

These “general-purpose” DSOs and MSOs offer as many as four analog and 16 digital input channels with touchscreens, zone triggering, and 3-dB bandwidths to 1 GHz.

**MAINSTREAM MEASUREMENTS SEEM** to grow in complexity, as evidenced by more and more functions being packed into electronic products. As a result, workhorse instruments such as oscilloscopes must do more across their measurement ranges. Thus, the challenge for instrument developers is to provide the enhanced capability without added complexity.

The answer, courtesy of Keysight Technologies ([www.keysight.com](http://www.keysight.com)), is the InfiniiVision 3000T X-Series of portable digital storage oscilloscopes (DSOs) and mixed-signal oscilloscopes (MSOs). Available with upgradable 3-dB measurement bandwidths from 100 MHz to 1 GHz, these instruments provide a capacitive touchscreen for ease of use.

The InfiniiVision 3000T X-Series of portable oscilloscopes (see figure) are versatile instruments suitable for research, education, and general-purpose testing. They are available in DSO models with two or four analog input channels and MSO models with two or four analog channels (each with 16 digital channels). As examples, Model DSOX3102T is a DSO with two input channels and a 3-dB measurement bandwidth of 1 GHz; the model DSOX3104T provides the same measurement bandwidth with four analog input channels. Model MSOX3102T is an MSO with a 3-dB measurement bandwidth of 1 GHz across two ana-

log input channels and 16 digital input channels, while model MSOX3104T is an MSO with 1-GHz bandwidth, four analog input channels, and 16 digital input channels.

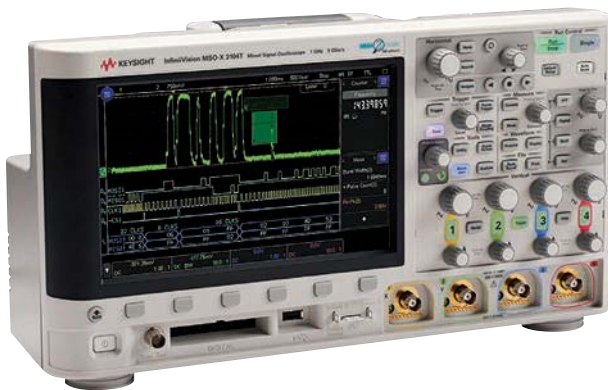
For those in need of less test bandwidth, the model DSOX3012T DSO offers a 100-MHz, 3-dB measurement bandwidth for two analog input channels, while the model DSOX3014T DSO features the same bandwidth for four analog input channels. For those requiring the digital input channels as well, the models MSOX3012T and MSOX3014T MSOs each provide 16 digital input channels with two and four analog input channels, respectively.

Each of the oscilloscopes incorporates 4 Mpoints of memory. The normal (default) waveform update rate of the InfiniiVision 3000T X-Series instruments is better than 1 million/s; it does not require any special setup requirements. The powerful signal-processing circuitry within these scopes captures signals at sampling rates to 5.0 Gsamples/s when applied to one-half the measurement channels and 2.5 Gsamples/s when applied to all.

Not to be overshadowed by all of this power is the ease of use of these machines, aided by an 8.5-in. capacitive touchscreen. The touchscreen interface is designed to simplify setting up measurements and boost measurement productivity; it also helps with collecting documentation for different test projects.

The InfiniiVision 3000T X-Series instruments are actually much more than just oscilloscopes, with a total of six instrument functions packed into the portable housing: oscilloscope, logic analyzer, protocol analyzer, 20-MHz arbitrary waveform generator (AWG), 3-digit digital voltmeter (DVM), and 8-digit time/frequency counter. The oscilloscopes are designed around a standard three-year calibration cycle.

The scopes are available with support for the N7020A power rail for power integrity measurements, with large offset range of  $\pm 24$  VDC and large active signal range of  $\pm 850$  mV. And, of course, these new oscilloscopes can be used with the firm's free BenchVue test and measurement software (see p. 96). [mww](http://mww)



The InfiniiVision 3000T X-Series oscilloscopes are available as DSOs and MSOs with two or four analog input channels at bandwidths to 1 GHz.

KEYSIGHT TECHNOLOGIES, INC., 1400 Fountaingrove Pkwy., Santa Rosa, CA 95403; (707) 577-2663, [www.keysight.com](http://www.keysight.com)





# MODULAR TEST SYSTEMS

***Built Your Way and Delivered within 2 Weeks!***

*Signal Routing & Attenuation Control for Production Test, R&D and More!*

Mini-Circuits' new ZTM-Series RF test systems dramatically accelerate custom solutions for a wide range of applications in test environments. Choose from our lineup of extra-long-life SP4T, SPDT and transfer switches, and programmable attenuators with attenuation ranges of 0 to 30, 60, or 90 dB. We'll build and ship a solution tailored to your exact requirements *within just 2 weeks!*

It's that simple! Give us a call and talk to our engineers about how Mini-Circuits' ZTM-Series custom rack mount test solutions can improve efficiency, increase throughput, and save cost in your business!

## Features

- Rugged 19" Rack Mountable Chassis
- Customizable Front Panel Layout
- Light Weight
- USB and Ethernet Control
- User-friendly GUI and DLLs Included
- Qualified to 100 Million Switch Cycles
- Affordable Cost
- ***Delivery within 2 Weeks!***

*Choose from hundreds of possible configurations!*



SPDT Switches  
DC – 18 GHz



SP4T Switches  
DC – 18 GHz



Transfer Switches  
DC – 18 GHz



0 – 30, 60, or 90 dB  
Programmable Attenuators  
1 MHz – 6 GHz



# Software Simplifies Microwave Testing

The second major release of Keysight's BenchVue software provides flexible data logging, along with the capability to combine functionalities of different measurement equipment.

**MEASUREMENTS PROVIDE WINDOWS** into performance, but RF/microwave measurements have grown in complexity in recent years as test equipment continues to gain in functionality and power. Fortunately, a personal computer (PC) with the right software can coordinate and simplify those measurements, and that software may just be Release 2 of the BenchVue software from Keysight Technologies.

This offering supports simplified connectivity among different types of test equipment, including oscilloscopes, power sensors, function generators, digital multimeters, power supplies, and spectrum analyzers. The software for the PC makes it easier to operate the many different instruments that it supports. And best of all—it is free of charge.

The BenchVue PC test software is extremely easy to use, with simple point-and-click data capture and the ability to manipulate test results on a PC. BenchVue now supports seven instrument types: oscilloscopes, power supplies, spectrum analyzers, digital multimeters, function generators, power sensors, and data-acquisition units.

This latest version of the BenchVue software delivers more functionality with spectrum analyzers, such as screen image capture, screen image logging, trace logging, and deep data

capture of advanced signal information. Furthermore, it features expanded oscilloscope capabilities.

The test software allows a user to show information from different connected test gear simultaneously (*Fig. 1*), and enables closer views of data on a single screen (*Fig. 2*). The test data can be manipulated into different file formats.

To use the software, a user plugs an instrument into a PC running BenchVue by means of a general-purpose interface bus (GPIB), Universal Serial Bus (USB), or local area network (LAN) connector. A compatible instrument is automatically configured for use in BenchVue; no separate instrument drivers are needed. Measurement data can be captured with just a few mouse clicks.

The software can be loaded free of charge from [www.keysight.com/find/benchvue](http://www.keysight.com/find/benchvue). Upgrades for all instrument types are available at moderate cost, ranging from \$150 to \$750. Despite their price tags, these “Pro” versions feature enviable functionality. For instance, a mobile application enables remote monitoring and response to testbenches via a smartphone or tablet. BenchVue software supports more than 200 instrument models. [mww](http://mww)

KEYSIGHT TECHNOLOGIES, INC., 1400 Fountaingrove Pkwy., Santa Rosa, CA 95403; (707) 577-2663, [www.keysight.com](http://www.keysight.com)



1. Using the measurement view, BenchVue can be used to correlate results from different measurements in one PC.



2. The software provides extensive data trace and logging capabilities to analyze data from different instruments.



# USB & Ethernet Programmable ATTENUATORS

0–30, 60, or 90 dB 1 MHz to 6 GHz from **\$395**

Mini-Circuits programmable attenuators give you more options and more freedom with both USB and Ethernet control. Available in versions with maximum attenuation of 30, 60, and 90 dB with 0.25 dB attenuation steps, all models provide precise level control with accurate, repeatable performance for a wide range of test applications. Our unique designs

maintain linear attenuation change per dB over the entire range of attenuation settings. Supplied with user-friendly GUI control software and everything you need for immediate use out-of-the-box, Mini-Circuits programmable attenuators offer a range of solutions to meet your needs and fit your budget. Visit [minicircuits.com](http://minicircuits.com) for detailed performance specs, great prices, and off-the-shelf availability!

 RoHS compliant

Models	Attenuation Range	Attenuation Accuracy	Step Size	USB Control	Ethernet Control	RS232 Control	Price \$ ea.
RUDAT-6000-30	0 – 30 dB	±0.5 dB	0.25 dB	✓	-	✓	\$395
<b>NEW</b> RCDAT-6000-30	0 – 30 dB	±0.5 dB	0.25 dB	✓	✓	-	\$495
RUDAT-6000-60	0 – 60 dB	±0.8 dB	0.25 dB	✓	-	✓	\$625
RUDAT-6000-90	0 – 90 dB	±0.9 dB	0.25 dB	✓	-	✓	\$695
<b>NEW</b> RCDAT-6000-60	0 – 60 dB	±0.8 dB	0.25 dB	✓	✓	-	\$725
<b>NEW</b> RCDAT-6000-90	0 – 90 dB	±0.9 dB	0.25 dB	✓	✓	-	\$795





## GENERATOR Spans 25 to 6000 MHz

**FOR THOSE IN** need of a simple source of test signals to 6 GHz, the model SG6000L from DS Instruments is a compact test signal generator capable of generating clean sine-wave output signals from 25 MHz to 6 GHz. It can be operated by a rudimentary front panel using several pushbutton controls or by a host PC and its Universal Serial Bus connection. For those in need of higher frequencies, the frequency synthesizer is available with an optional doubler to provide output signals to 12 GHz.

The SG6000L (see figure) is very compact, measuring just 2.75 x 6.00 x 1.13 in. Nonetheless, it provides robust output signals at levels from +6 to +11 dBm through 6 GHz, with a typical output level of +8 dBm. When equipped with the optional frequency doubler, the output power ranges from +9 to +14 dBm, with a typical frequency-doubled output-power level of +11 dBm. The output-power flatness for both fundamental-frequency and doubled outputs is typically  $\pm 2$  dB. For a low-cost source, output signals are relatively clean, with single-sideband (SSB) phase noise of typically -80 dBc/Hz offset 10 kHz from a 6-GHz carrier.

This is a test signal source that provides basic output signals with little fuss or complexity, showing output frequency on an organic light-emitting-diode (OLED) display and controlled by just a few buttons for power and frequency up or down. It can also be controlled by a host computer with a USB port running the supplied software. The signal source runs with industry-standard Standard Commands for Programmable Instruments commands to change frequency and output-power level. Depending on the band of operation, the signal source can tune frequencies in steps of 20 Hz or less to a maximum step size of 3 kHz. The OLED display enables operators to see command frequencies from the USB interface or from the front-panel frequency up/down buttons.

The synthesized SG6000L signal source can operate with its internal 10-MHz reference source or, as an option, with an external 10-MHz reference source. The signal generator includes an autodetect function to switch to the external reference source when it is connected.

**DS INSTRUMENTS**, San Luis Obispo, CA 93401; (805) 242-6685, [whsamuels@dsinstruments.com](mailto:whsamuels@dsinstruments.com), [www.dsinstruments.com](http://www.dsinstruments.com)



**Model SG6000L is a compact test signal generator capable of fundamental-frequency outputs to 6 GHz and doubled-frequency outputs to 12 GHz.**

## TEST SET HANDLES BLE Extended Data

**THE MODEL MT8852B** Bluetooth test set has been upgraded to handle measurements of the Data Length Extension associated with the latest Bluetooth Core Specification version 4.2, in particular for Bluetooth Low Energy (BLE) equipment and systems. The MT8852B is essentially a complete portable measurement system that includes a low-noise signal generator, measurement receiver, microprocessor, and software to perform key measurements on the latest Bluetooth BLE gear. The MT8852B can be used to conduct radio-layer tests on Bluetooth Smart and Bluetooth Smart Ready devices according to the new Bluetooth 4.2 standard.

The MT8852B (see figure) features a built-in signal generator with a frequency range of 2.40 to 2.50 GHz and 1-kHz frequency resolution. The test signal source offers an amplitude range of 0 to -90 dBm with an amplitude accuracy of  $\pm 1$  dB and amplitude resolution of  $\pm 0.1$  dB. The Bluetooth test set includes a measurement receiver that can gauge average and peak power levels over an average-power range of -50 to +22 dBm with 0.1-dB resolution and  $\pm 1.5$ -dB worst-case accuracy. It can measure frequency over an error range of 0 Hz to  $\pm 150$  kHz with 1-kHz resolution.

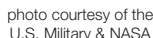


**This integrated test set includes a receiver and test signal generator for performing all of the latest Bluetooth measurements.**

It allows new test cases in the Data Length Extension option to be run as part of a test script to simplify generation of test programs.

The MT8852B can be used as a control panel to perform BLE measurements. The test set controls a device under test (DUT) in Direct Test Mode (DTM) by means of USB connection and RS-232 HCI, two-wire, or USB-to-serial-adaptor control interfaces. The test set's Data Length Extension option is also supplied with a PC application that eases the development of test programs on a remote PC. The application enables creation of graphical data as well as clear pass/fail notices following any supported measurements. The Data Length Extension option supports a number of Bluetooth EDR transmitter and receiver test cases.

**ANRITSU CO.**, 490 Jarvis Dr., Morgan Hill, CA 95037-2809; (408) 778-2000, Fax: (408) 776-1744, [www.anritsu.com](http://www.anritsu.com)



*Low NF 0.5 dB    High IP3 up to 38 dBm    Low DC current 65 mA*    **\$4<sup>95</sup>**  
ea. (qty 20)

**Robust performance across wide bandwidths** makes them ideal for instrumentation, or anywhere long-term reliability adds bottom-line value. Go to [minicircuits.com](http://minicircuits.com) for all the details today, and get them in your hands as soon as tomorrow!

### Electrical Specifications (-55 to +105°C)



3 x 3 x 1.14 mm

Model	Freq. (GHz)	Gain (dB)	P <sub>OUT</sub> (dBm)	IP3 (dBm)	NF (dB)	DC (V)	Price \$ea. (qty 20)
CMA-62+	0.01-6	15	19	33	5	5	4.95
CMA-63+	0.01-6	20	18	32	4	5	4.95
CMA-545+	0.05-6	15	20	37	1	3	4.95
<b>NEW</b> CMA-5043+	0.05-4	18	20	33	0.8	5	4.95
<b>NEW</b> CMA-545G1+	0.4-2.2	32	23	36	0.9	5	5.45
<b>NEW</b> CMA-162LN+	0.7-1.6	23	19	30	0.5	4	4.95
<b>NEW</b> CMA-252LN+	1.5-2.5	17	18	30	1	4	4.95

 RoHS compliant



ADVERTISER	PAGE
<b>A</b>	
AEROFLEX / INMET, INC. ....	55
	<a href="http://www.cobham.com/Inmet">www.cobham.com/Inmet</a>
AEROFLEX / WEINSCHEL, INC. ....	61
	<a href="http://www.cobham.com/Weinschel">www.cobham.com/Weinschel</a>
ANRITSU CORPORATION .....	C1
	<a href="http://www.anritsu.com">www.anritsu.com</a>
ARRA .....	C3
	<a href="http://www.arra.com">www.arra.com</a>
<b>C</b>	
CALIFORNIA EASTERN LAB .....	8
	<a href="http://www.cel.com/TK-MWRF">www.cel.com/TK-MWRF</a>
CIAO WIRELESS INC .....	17
	<a href="http://www.ciaowireless.com">www.ciaowireless.com</a>
CML MICROCIRCUITS (UK) LTD .....	60
	<a href="http://www.cmlmicro.com">www.cmlmicro.com</a>
COILCRAFT .....	10
	<a href="http://www.coilcraft.com">www.coilcraft.com</a>
CST OF AMERICA INC .....	2
	<a href="http://www.cst.com/antenna">www.cst.com/antenna</a>
<b>D</b>	
DBM CORP .....	26
	<a href="http://www.dbmcorp.com">www.dbmcorp.com</a>
<b>E</b>	
ECLIPSE MICROWAVE .....	64
	<a href="http://www.eclipsemdi.com">www.eclipsemdi.com</a>
EMPOWER RF SYSTEMS INC. ....	47
	<a href="http://www.EmpowerRF.com">www.EmpowerRF.com</a>
<b>F</b>	
FAIRVIEW MICROWAVE .....	27
	<a href="http://www.fairviewmicrowave.com">www.fairviewmicrowave.com</a>
<b>H</b>	
HEROTEK INC .....	13
	<a href="http://www.herotek.com">www.herotek.com</a>
<b>J</b>	
JFW INDUSTRIES INC .....	42
	<a href="http://www.jfwindustries.com">www.jfwindustries.com</a>
<b>K</b>	
KEYSIGHT TECHNOLOGIES - USA .....	20-21
	<a href="http://www.keysight.com/find/LTE-A-Insight">www.keysight.com/find/LTE-A-Insight</a>
KEYSIGHT TECHNOLOGIES - USA .....	39
	<a href="http://www.keysight.com/find/newUXA">www.keysight.com/find/newUXA</a>
KEYSIGHT TECHNOLOGIES - USA .....	53
	<a href="http://www.keysight.com/find/rfpowertips">www.keysight.com/find/rfpowertips</a>
KRYTAR INC .....	44
	<a href="http://www.krytar.com">www.krytar.com</a>

ADVERTISER	PAGE
<b>L</b>	
LINEAR TECHNOLOGY CORPORATION .....	19
	<a href="http://www.linear.com/product/LTC5599">www.linear.com/product/LTC5599</a>
<b>M</b>	
M/A COM TECHNOLOGY SOLUTIONS, INC .....	C2
	<a href="http://www.macom.com/gan">www.macom.com/gan</a>
MAURY MICROWAVE INC .....	90
	<a href="http://www.maurymw.com">www.maurymw.com</a>
MECA ELECTRONICS INC .....	9
	<a href="http://www.e-MECA.com">www.e-MECA.com</a>
MICRO LAMBDA WIRELESS, INC .....	45
	<a href="http://www.microlambdawireless.com">www.microlambdawireless.com</a>
MINI-CIRCUITS/SCI COMPONENTS ...	12, 14-15, 25, 30-31, 33, 37, 43, 59, 73, 77, 85, 89, 95, 97, 99, 103
	<a href="http://www.minicircuits.com">www.minicircuits.com</a>
<b>N</b>	
NARDA DIV OF L-3 COMMUNICATIONS .....	3
	<a href="http://www.nardamicrowave.com">www.nardamicrowave.com</a>
NATIONAL INSTRUMENTS .....	29
	<a href="http://www.ni.com/define">www.ni.com/define</a>
NI AWR .....	4
	<a href="http://www.ni.com/awr">www.ni.com/awr</a>
NI MICROWAVE COMPONENTS .....	24
	<a href="http://www.ni-microwavecomponents.com">www.ni-microwavecomponents.com</a>
<b>P</b>	
PLANAR MONOLITHICS INDUSTRIES .....	1
	<a href="http://www.pmi-rf.com">www.pmi-rf.com</a>
<b>R</b>	
RIGOL USA .....	92-93
	<a href="http://www.RigolRF.com">www.RigolRF.com</a>
<b>S</b>	
SAN-TRON INC .....	C4
	<a href="http://www.santron.com">www.santron.com</a>
SKYWORKS SOLUTIONS INC .....	6-7
	<a href="http://www.skyworksin.com">www.skyworksin.com</a>
STANFORD RESEARCH SYSTEMS (SRS) .....	70-71
	<a href="http://www.thinkSRS.com">www.thinkSRS.com</a>
SYNERGY MICROWAVE .....	51, 65
	<a href="http://www.synergymwave.com">www.synergymwave.com</a>
<b>W</b>	
W.L. GORE & ASSOCIATES INC .....	79
	<a href="http://www.gore.com/test">www.gore.com/test</a>
WAVELINE INC .....	58
	<a href="http://www.wavelineinc.com">www.wavelineinc.com</a>

This index is provided as an additional service by the publisher, who assumes no responsibility for errors or omissions.

## Subscription Assistance and Information:

(ISSN 0745-2993)

*Microwaves & RF* is published monthly. **Microwaves & RF** is sent free to individuals actively engaged in high-frequency electronics engineering. In addition, paid subscriptions are available. Subscription rates for U.S. are \$95 for 1 year (\$120 in Canada, \$150 for International). Published by Penton Media, Inc., 9800 Metcalfe Ave., Overland Park, KS 66212-2216. Periodicals Postage Paid at Shawnee Mission, KS and at additional mailing offices.

**POSTMASTER:** Send change of address to *Microwaves & RF*, Penton Media Inc., P.O. Box 2095, Skokie, IL 60076-7995. For paid subscription requests, please contact: Penton Media Inc., P.O. Box 2100, Skokie, IL 60076-7800. Canadian Post Publications Mail agreement No. 40612608. Canadian GST# R126431964. Canada return address: IMEX Global Solutions, P.O. Box 25542, London, ON N6C6B2.

Back issues of **MicroWaves** and **Microwaves & RF** are available on microfilm and can be purchased from National Archive Publishing Company (NAPC). For more information, call NAPC at 734-302-6500 or 800-420-NAPC (6272) x 6578. Copying: Permission is granted to users registered with the Copyright Clearance Center, Inc. (CCC) to photocopy any article, with the exception of those for which separate copyright ownership is indicated on the first page of the article, provided that a base fee of \$1.25 per copy of the article plus 60 cents per page is paid directly to the CCC, 222 Rosewood Dr., Danvers, MA 01923. (Code 0745-2993/02 \$1.25 +.60) Copying done for other than personal or internal reference use without the expressed permission of Penton Media, Inc., is prohibited. Requests for special permission or bulk orders should be addressed in writing to the publisher.

Copyright 2014 • Penton • All rights reserved. Printed in the U.S.



**APPLICATIONS ENGINEER:** Required by RF Micro Devices for position in Greensboro NC. Responsible for the documentation and marketing tools necessary to bring products into the market place including working with Design Engineers during IC development and supporting customers during design cycles and into production. Enable company's products to achieve the desired performance on the customer reference design which is supplied to potential end customers by providing the required marketing support, design support and customer support. Responsible for working on end customer reference designs and tune RFMD products to produce desired performance using RFMD's lab or by traveling to customer sites. Provide customers, both internal and external to RFMD, with RF technical product support at the RF system and component level which typically requires extensive travel. Perform detailed circuit design tuning of RF amplifiers, front-end modules (FEMs), LNAs, and switches for RF applications. Create and update product data sheets to include RF parameters, schematics, tunings and application information. Participate with new standard and custom RFIC product development efforts. Perform testing and debugging of product evaluation boards and customer reference design boards, making improvements as necessary and follow up with training material as needed. Knowledge in RF systems design and with direct Wi-Fi. Possess full knowledge of RF test equipment such as spectrum analyzers, network analyzers, etc. Knowledge of ADS simulation. MSEE and 1 year experience in RF circuit design, filter design, impedance matching, and board layout tools. Qualified candidates send resumes to [employment@rfmd.com](mailto:employment@rfmd.com) and refer to Job Code: **JLSHI**

**APPLICATIONS ENGINEER:** Required by RF Micro Devices for position in Greensboro NC. Responsible for the documentation and marketing tools necessary for the bringing of new products into the marketplace including working with Design Engineers during IC development and supporting customers during design cycles and into production. Provide customers, both internal and external to RFMD, with RF technical product support at the RF system and component level. Perform detailed circuit design of RF amplifiers, mixers, VCO's and power amplifiers for RF applications. Create and update data sheets to include RF parameters, schematics, tunings, and application information. Participate with new standard and custom RFIC product development efforts. Perform testing and debugging of product evaluation boards, making improvements as necessary.

Knowledge of RF systems design. Expertise in cellular standards is required such as WCDMA, LTE, TD-LTE and TDSCDMA. BSEE (or foreign equivalent) and 2 years of experience in RF Engineering System Design and Optimization. Qualified candidates send resumes to [employment@rfmd.com](mailto:employment@rfmd.com) and refer to Job Code: **JLBAI**

### TO ADVERTISE IN DIRECT CONNECTION, CONTACT:

Brand Director, S. California - Tracy Smith: [tracy.smith@penton.com](mailto:tracy.smith@penton.com)

Brand Champion, Northeast/Eastern Canada

David Madonia: [dave.madonia@penton.com](mailto:dave.madonia@penton.com)

Northwest/Northern CA/Western Canada

Jamie Allen: [jamie.allen@penton.com](mailto:jamie.allen@penton.com)

South - Bill Yarborough: [bill.yarborough@penton.com](mailto:bill.yarborough@penton.com)

Mid-Atlantic/Midwest - Stephanie Campana: [stephanie.campana@penton.com](mailto:stephanie.campana@penton.com)

Europe - Mark Durham: [mark.durham@penton.com](mailto:mark.durham@penton.com)

## New Products

### Phase Shifter Tunes

#### 150 to 300 MHz

**MODEL SF29A7** is a voltage-controlled phase shifter for applications from 150 to 300 MHz. It provides continuous phase adjustment range of 0 to 360 deg. with tuning voltages of 0 to +20 VDC, featuring maximum VSWR



of 1.90:1 and maximum insertion loss of 4 dB across the operating frequency range. Available in surface-mount housings and packages with coaxial connectors, the component is part of a full family of phase shifters spanning 1 to 2500 MHz. Among these is model SF31A7, which provides a full 360-deg. control range from 1800 to 2000 MHz via control voltages from 0 to +20 VDC. It offers maximum VSWR of 1.90:1 and maximum insertion loss of 4.4 dB across its operating bandwidth. The firm also offers octave-band phase shifters with 180-deg. control ranges.

#### **SIGATEK MICROWAVE LLC,**

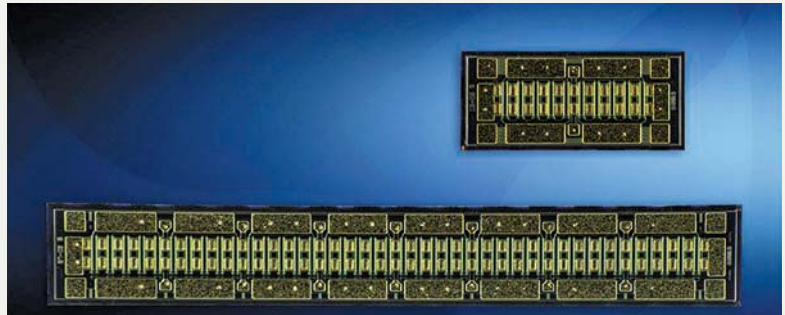
423 Black Oak Ridge Rd., Wayne, NJ 07470; (973) 706-8475, FAX: (973) 832-4435, e-mail: sales@sigatek.com, [www.sigatek.com](http://www.sigatek.com)

### VCO Cuts Phase Noise at 2.5 GHz

**MODEL CVCO33CC-2500-2500** is a voltage-controlled oscillator (VCO) for use at 2.5 GHz. It typically draws 20 mA from a +3.3-VDC supply and tunes (minimally) across a range of 0 to +3.3 VDC with typical tuning sensitivity of 10 MHz/V. It provides at

### GaN Transistors Pass 300 W through 4 GHz

**DESIGNERS OF** high-power RF/microwave amplifiers now have additional options when using +50-VDC discrete gallium-nitride (GaN) power transistors, with a trio of bare GaN high-electron-mobility-transistor (HEMT) die providing power levels as high as 320 W through 4 GHz. The three discrete transistor die include a device capable of 20-W output power through



6 GHz, a device capable of 75-W output power through 6 GHz, and one that's capable of 320-W output power through 4 GHz. The GaN HEMT die exhibit 17-dB typical small-signal gain and 60% typical power-added efficiency (PAE) at 6 GHz and 18-dB typical small-signal gain and 65% typical PAE at 4 GHz. They are well suited for applications in cellular infrastructure, two-way radios, satellite-communications (satcom) systems, and test instrumentation.

**CREE, INC.,** 4600 Silicon Dr., Durham, NC 27703; (919) 313-5300, (800) 533-2583, FAX: (919) 313-5558, [www.cree.com](http://www.cree.com)



least +5-dBm output power, usually pushing of 1 MHz/V. The VCO exhibits typical spurious content of -20 dBc with typical phase noise of -105 dBc/Hz offset 10 kHz from the carrier and -145 dBc/Hz offset 1 MHz from the carrier. It is supplied in a surface-mount package measuring 0.300 x 0.300 x 0.175 in. and designed for operating temperatures from -20 to +70°C.

**CRYSTEK CORP.,** 12730 Commonwealth Dr., Fort Myers, FL 33913; (239) 561-3311, (800) 237-3061, FAX: (239) 561-1025, [www.crystek.com](http://www.crystek.com)

### PIN Diode Switches Tackle 200 W to 1 GHz

**SUITABLE FOR** land, sea, and air applications in commercial, industrial, and military systems, a new pair of PIN diode switches can handle as much as 200 W CW incident power from 50 MHz to 1 GHz with low loss and high isolation. Models MASW-011040 and MASW-011041 are single-pole, four-throw (SP4T) and single-pole, three-throw (SP3T) switches supplied in surface-mount housings. They can be used for either pulsed or CW signals, and both switches exhibit



# DC-12 GHz 1W Attenuators

**\$18<sup>95</sup>**  
only ea. qty. 1-9

## Accurate attenuation over ultra-wide frequency range at low cost!

Mini-Circuits' new FW-series fixed SMA attenuators cover your applications from DC – 12 GHz with a wide selection of attenuation values to meet your needs. All models offer excellent attenuation flatness versus frequency, low VSWR, and 1W input power handling, making them ideal, cost-saving solutions for impedance matching and signal level adjustment in a broad range of systems.

Built using Mini-Circuits rugged unibody construction with SMA(M) to SMA (F) connectors, FW-Series attenuators provide outstanding reliability in tough operating conditions. Just go to [minicircuits.com](http://minicircuits.com) for full specs and see how these attenuators can add performance and value to your design! They're available off the shelf for immediate shipment. Order today, and have them in hand as soon as tomorrow!

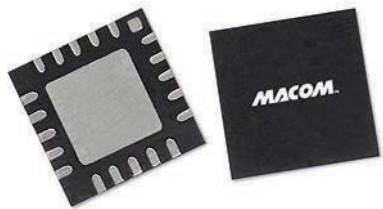
Model	ATTENUATION		VSWR (:1) Midband Typ.	Power (W)
	Nominal (dB)	Flatness (dB)		
FW-1+	1	±0.15	1.15	1.0
FW-2+	2	±0.15	1.15	1.0
FW-3+	3	±0.20	1.15	1.0
FW-4+	4	±0.20	1.15	1.0
FW-5+	5	±0.20	1.15	1.0
FW-6+	6	±0.25	1.15	1.0
FW-7+	7	±0.25	1.15	1.0
FW-8+	8	±0.30	1.15	1.0
FW-9+	9	±0.30	1.15	1.0
FW-10+	10	±0.30	1.15	1.0
FW-12+	12	±0.30	1.20	1.0
FW-15+	15	±0.35	1.20	1.0
FW-20+	20	±0.50	1.20	1.0

 RoHS compliant.



[www.minicircuits.com](http://www.minicircuits.com) P.O. Box 350166, Brooklyn, NY 11235-0003 (718) 934-4500 [sales@minicircuits.com](mailto:sales@minicircuits.com)





less than 0.5-dB insertion loss and more than 40-dB isolation between ports across their full frequency ranges. Harmonics are controlled to better than -70 dBc. The switches are manufactured in the firm's proven hybrid manufacturing process and housed in 9-mm HQFN 20-lead plastic packages.

**MACOM TECHNOLOGY SOLUTIONS, INC.**, 100 Chelmsford St., Lowell, MA 01851; (800) 366-2266, (978) 656-2896, [www.macom.com](http://www.macom.com)

### Low-Pass Filters Run 30 MHz to 3 GHz

**NINE-POLE LOW-PASS** Chebyshev filters in the LC9S series are available in nine models with different 1-dB passbands, from 30 MHz to 3 GHz. The maximum passband insertion loss is 1 dB with stopband attenuation of



-40 dBc at a 1.50:1 ratio (rejection frequency to passband frequency) and -60 dBc at a 2.0:1 ratio. Employing SMA female connectors, these RoHS-compliant filters can handle power levels from 5 to 10 W. They are designed for operating temperatures from 0 to +70°C.

**TTE FILTERS, LLC**, 11652 West Olympic Blvd., Los Angeles, CA 90064-1400; (310) 478-8224, FAX: (310) 445-2791, e-mail: [tte@tte.com](mailto:tte@tte.com), [www.tte.com](http://www.tte.com)

### Low-Noise Amplifier Gains Ka-Band Range

**MODEL AMF-6F-27003100-22-13P** is a low-noise amplifier (LNA) developed for use from 27 to 31 GHz. Over that range, it exhibits maximum noise figure of 2.2 dB, with a typical noise figure of 2.0 dB. The gain is 40 dBm with worst-case gain flatness of  $\pm 1$  dB. The RoHS-compliant LNA delivers +13-dBm output power at 1-dB com-



pression with a third-order intercept point of typically +21 dBm. It typically draws 275 mA from a +15-VDC supply and is supplied in a housing measuring 0.38 x 0.75 in. (excluding the 2.92-mm coaxial connectors). It has an operating temperature range of -40 to +75°C and is available in a hermetic version.

**MITEQ, INC.**, 100 Davids Dr., Hauppauge, NY 11788; (631) 436-7400, FAX: (631) 436-7430, [www.miteq.com](http://www.miteq.com)

### Amplifier Boosts L-Band Applications

**MODEL 13G05A** is a power amplifier developed for applications from 800 to 2000 MHz. It provides at least 35-W



output power across that frequency range when fed with a nominal drive level of 0 dBm. It boasts better than 40% module efficiency and more than 45-dB small-signal gain. The amplifier is supplied in an aluminum chassis for effective dissipation of heat; it measures just 4.50 x 3.50 x 0.61 in. It is a candidate for a wide range of applications on the ground and in the air, from communications systems and electronic-warfare (EW) systems to test systems.

**NUWAVES LTD.**, 132 Edison Dr., Middletown, OH 45044-3269; (513) 360-0800, FAX: (513) 539-8782, [www.nuwaves.com](http://www.nuwaves.com)

### Broadband Connectors Provide Extra Protection

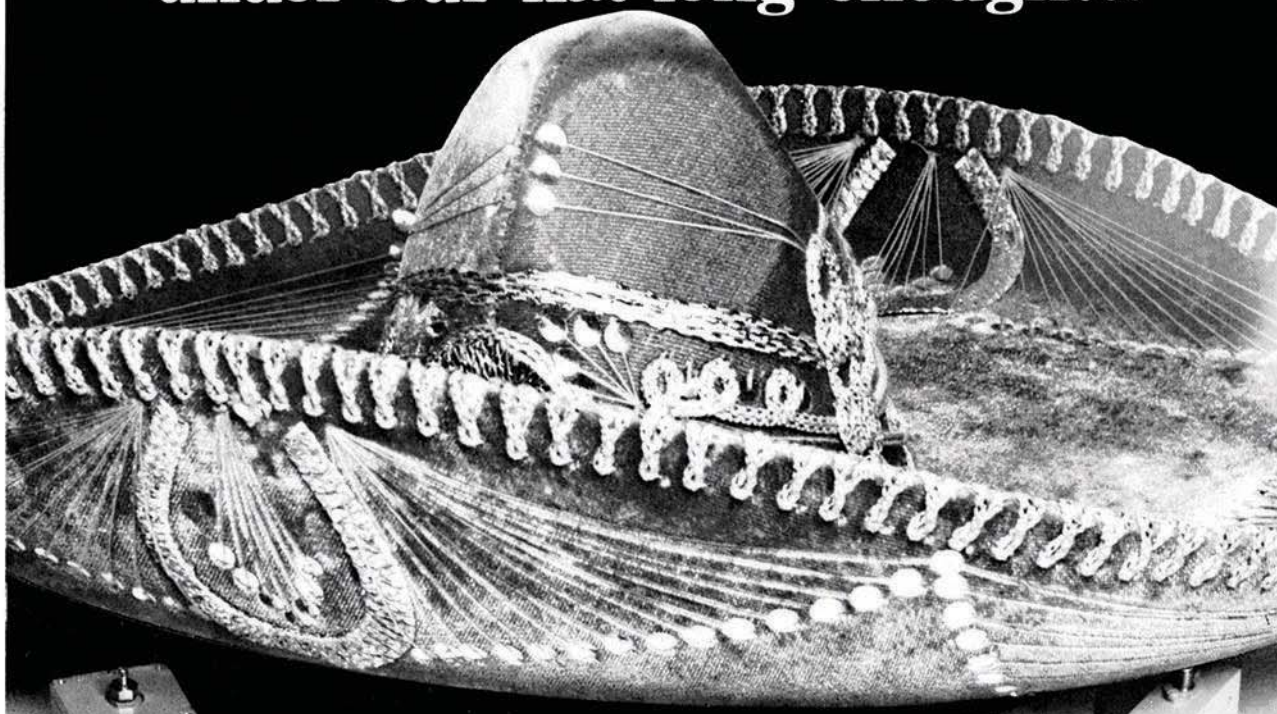
**THE LP-18-240** and LP-18-195 surge-protector connectors have been added to the Times-Protect series of in-line broadband DC pass connectors as additions to the LP-18-400 line. The design, which uses and the firm's EZ Advantage X-series crimp-style connector interface unit, provides



effective lightning protection for applications from DC through 6 GHz. This combination eliminates the cable connector needed with conventional lightning protection with a low-return-loss unit that meets the IP-67 standard for outdoor as well as indoor use. The DC-pass connectors are constructed of solid brass and attach directly to the firm's LMR-400, LMR-240, and LMR-195 cables.

**TIMES MICROWAVE SYSTEMS**, 358 Hall Ave., Wallingford, CT 06492; (800) 867-2629, (203) 949-8429, FAX: (203) 949-8423, [www.timesmicro.com](http://www.timesmicro.com)

# We've kept these ARRA Attenuators under our hat long enough...



## Low Freq. Variable Attenuators

*The "no-nonsense" attenuator...*  
For Audio, IF, and VHF.  
Simple, straight forward, no frills. Not bad when this economy model performs in the same classy manner as other ARRA high precision units.

- SMA connectors, others available
- Off-the-shelf delivery
- 50 ohm impedance, 75 ohms available
- Specs that beat the competition's

### Directly calibrated models

Freq Range (MHz)	Atten Range (dB)	Atten vs Freq (dB)	Model No.
DC-60	40	$\pm 1.0$	0682-40F
DC-100	15	$\pm 0.3$	0682-15F
DC-100	30	$\pm 0.5$	0682-30F
DC-250	10	$\pm 0.5$	0682-10F

### Uncalibrated models

DC-60	40	$\pm 1.0$	0682-40
DC-100	20	$\pm 0.6$	0682-20
DC-100	30	$\pm 0.5$	0682-30
DC-200	30	$\pm 2.0$	0682-30A
DC-250	15	$\pm 1.2$	0682-15
DC-500	10	$\pm 0.25$	0682-10

Visit our website at [www.arra.com](http://www.arra.com)

## Phaseless Variable Attenuators

*The "incredible" attenuator...*  
Elegant, classic, exceptional. With all the extras you'd expect at the top of the ARRA line. So uniquely new in its approach, it's one of a kind. Nothing else like it on the market. It's got everything...

- Low phase
- High RF Power
- Low VSWR & Insertion loss
- Extremely flat frequency response
- 0-3 dB & high attenuation models
- Bands from 350-5000 MHz

... the last word in variable attenuators

# ARRA INC.

15 Harold Court • Bay Shore NY 11706-2296

Tel 631-231-8400

Fax 631-434-1116

E-Mail: [sales@arra.com](mailto:sales@arra.com)





Patent Pending

## The perfect PIM cable assembly. For the not-so-perfect world.

Achieving low PIM performance in a lab is hard enough. But in the real world, where shock and vibration are present, keeping PIM at bay can be challenging. Until now. SRX™ cable assemblies and adapters are the proven solutions being deployed in the toughest environments around the world.

Visit **Santron.com** to learn more and request pricing.



*Always Thinking*



**Download the  
SRX brochure at  
[Santron.com/SRX](http://Santron.com/SRX)**

A full line of low PIM solutions are detailed including flexible assemblies with innovative SRX-141 cable, jumpers and long haul assemblies, and several within- and between-series adapters.

